

Chemical Characterization of Mineral Aerosols: Sources, Transport and Atmospheric Transformations

A THESIS

submitted for the Award of Ph. D. degree of

MOHANLAL SUKHADIA UNIVERSITY

in the

Faculty of Science

By

Ashwini Kumar



Under the Supervision of

PROFESSOR M. M. Sarin

SENIOR PROFESSOR

**Physical Research Laboratory,
Ahmedabad-380 009, India.**

**MOHANLAL SUKHADIA UNIVERSITY
UDAIPUR**

2010

DECLARATION

I Mr. **Ashwini Kumar**, S/o: Mr. Lalit Kumar Jha, resident of C-3, PDF Qtrs, PRL residences, Navrangpura, Ahmedabad – 380009, hereby declare that the research work incorporated in the present thesis entitled “**Chemical Characterization of Mineral Aerosols: Sources, Transport and Atmospheric Transformations**” is my own work and is original. This work (in part or in full) has not been submitted to any University for the award of a Degree or a Diploma. I have properly acknowledged the material collected from secondary sources wherever required. I solely own the responsibility for the originality of the entire content.

Date:

(Ashwini Kumar)

C E R T I F I C A T E

I feel great pleasure in certifying the thesis entitled “*Chemical Characterization of Mineral Aerosols: Sources, Transport and Atmospheric Transformations*” by **Ashwini Kumar** under my guidance. He has completed the following requirements as per Ph.D. regulations of the University

- (a) Course work as per the university rules.
- (b) Residential requirements of the university
- (c) Regularly submitted six monthly progress report
- (d) Presented his work in the departmental committee
- (e) Published/accepted minimum of one research paper in a referred research journal.

I am satisfied with the analysis of data, interpretation of results and conclusions drawn.

I recommend the submission of thesis.

Date:

Name and Designation of Supervisor

*Countersigned by
Head of the Department*

Dedicated to my
“Ma and Papa”

ABSTRACT:

With the natural variability in emissions, atmospheric circulation patterns and the current changes brought about by the anthropogenic activities, the distribution and chemical properties of mineral aerosols and their direct/indirect effects on climate are the focus of present-day scientific issues. This thesis study presents a first comprehensive data set on the chemical composition of size-segregated aerosols (PM_{10} and $PM_{2.5}$) collected from a high-altitude site located in a high-dust semi-arid region (Mt. Abu, 24.6 °N, 72.7 °E, 1680 m asl) of western India. The principle objective is to assess the temporal variability in the atmospheric abundance of mineral dust, its chemical composition and to assess the chemical transformation processes occurring during the long-range transport from source regions. The chemical data reveals a uniform and dominant contribution (60 – 80 %) of mineral dust in the coarse mode ($PM_{10-2.5}$) over the annual seasonal cycle. During summertime (March-June), the Fe/Al weight ratio averages around 0.5, quite similar to their ratio in the crustal material. However, enriched Ca/Al and Mg/Al ratios suggest significant contribution from carbonate minerals in the coarse fraction. The impact of anthropogenic sources is significantly pronounced in the fine mode ($PM_{2.5}$), during wintertime (Nov-Feb), as evident from the increase in concentrations of $nss-SO_4^{2-}$ and NH_4^+ as well as high enrichment factors of Cd and Pb. A significant increase in the fractional solubility of aerosol iron with a concomitant decrease in the mass fraction of mineral dust further suggest the dominant role of combustion products (emissions from biomass burning and fossil-fuel). The water-soluble ionic composition (WSIC) constitutes 50 % of the $PM_{2.5}$ mass with a dominant contribution from SO_4^{2-} and NH_4^+ . In the coarse mode, contribution of WSIC is consistently low (average ~ 20 %) with predominance of Ca^{2+} and HCO_3^- . The neutralizing capacity of mineral dust for acidic species (SO_4^{2-} and NO_3^-) is near quantitative (95 %) in the coarse mode; whereas NH_4^+ is a major neutralizing constituent in the $PM_{2.5}$.

To sum up, this thesis study provides useful parameters on the atmospheric transport of mineral dust and chemical transformation in order to validate regional models for forecasting climate-state and climate-change.

(Keywords: Aerosol Chemistry, Mineral dust, Acid uptake, Aerosol iron solubility, Deposition fluxes, Marine atmosphere)

ACKNOWLEDGEMENTS

This thesis is the result of a very nice and instructive research time during 2005-2010 at Physical Research Laboratory (PRL), Ahmedabad. It gives me a great pleasure to acknowledge all those who supported me directly or indirectly and made this thesis possible.

First and foremost, I wish to express my sincere thanks to my supervisor and mentor, Prof. Manmohan Sarin, for giving me the opportunity and the resources to conduct my doctoral research programme at PRL. I owe my deep sense of gratitude to him for the constant guidance he has provided through out my research endeavour. He directed my study to large extent from sampling preparation to analysis of aerosol samples as well as from independent thinking to scientific writing. His persistent support, farsighted guidance and broad scientific experience made my research work possible. It is a great privilege for me to get a committed companionship with him during my adolescent research period.

My sincere appreciation and thanks are due to Sudheer for giving constant help in maintaining various instruments during my experimental activities. I am highly indebted to his support during the field campaigns over remote locations (at high altitude sites and marine region), which gave me enough confidence to go ahead at later stage of my research.

I am highly obliged to Prof. S. Krishnaswamy for his suggestions and comments which helped me to improve my scientific outcome. The fruitful discussions with him always helped me to develop scientific aptitude and think in newer directions. A big thank you goes to all people at the chemistry lab (CHEM-GANG) who made the time here enjoyable. Discussion on fundamentals of atmospheric science with Renga Ji and Sudheer was always enjoyable and fruitful. I acknowledge my sincere thanks to Dr. Ravi Bhushan and Dr. Sunil K. Singh for their concern and support. My special thanks go to Bhavsar Bhai who was always available to help me in Lab activities. I am thankful to all my colleagues (Vineet, Srinivas, Waliur, Kirpa, Timmy, Gyana, Satinder, Jayati, Prashant) and staffs (Sneha and Shanta Ben) at Chemistry Lab, for being friendly and co-operative during this research journey. I feel privileged to be a part of the chemistry family.

I thank Profs. S. D. Rindani, Utpal Sarkar, R. Ramesh, Dr. J. S. Ray (subject expert in Synopsis review) and all other members of academic committee for providing critical assessment of my work and valuable suggestion at various stages of my research. I am also thankful to Profs. S. V. S. Murthy, A. K. Singhvi, J. N. Goswami, and faculty members (including scientists) for their interest in my work and interactions during the area seminars. I would like to thank Profs. S. K. Bhattacharya and R. Ramesh for teaching the course of Mathematical and

Statistical Methods during my course work at PRL which turned out to be very useful during data analysis at later stage of my research work.

The support and help from staff members of Mt Abu Observatory (Rajesh Sir, Mathur Ji, Jain Ji, Purohit Ji, Peetambar Ji, Kothari Ji, Raghuvver and Raghunath) during setting up of samplers and sample collection are duly acknowledged. I also thank staff members of Computer Centre, Library, Workshop, Maintenance and Administration for their timely help.

I wish to thank Drs. K. Krisnmoorthy and C.B.S. Dutt for their critical role in organizing the Indian National Programme on Integrated Campaign on Aerosols Trace gases and Radiation Budget (ICARB) and help in logistic onboard ORV SagarKanya. The high volume sampler provided by Dr. S. K. Satheesh for sample collection during SK-223B is thankfully acknowledged. I would also like to thank Captain and crew member of ORV SagarKanya (SK-223B) for their help during cruise period.

I take this opportunity to thank my senior colleague Dr. Neeraj Rastogi, who introduced me the world of Atmospheric chemistry and paved a smooth way for further research in this arena. Sincere discussion with him and 'not' giving ready made answers helped me a lot to spread my wings to larger extent. I was highly motivated by the working culture maintained by Dr. Santosh Rai in the lab during initial days. The three basic pillars (qualities) viz. Passion, Patience and Perseverance required for high quality research was induced to me by having interactions with these senior colleagues. Thank you Sir.

This acknowledgement section remains incomplete if there is no mention of my wonderful friends who were always there to support and help at my stay in Hostel (Main and Thaltej) and PRL campus. The CHAT GROUP (Jhajee, Arvind, Pankaj, Vineet, Bhas, Sandeep, Billu, Ketan, Patra, Sumon, Amzad, Ashok, Srikanth, Shukla jee) deserve a special recognition for numerous stress buster sessions during weekends as well as Tea-sessions on weekdays which keep recharging and refreshing me 24x7. In addition, I express my sincere thanks to my dear friends Sumita, Naveen, Tyagijee, Sumanto, Rabiul, Devagnik, Raju, and several others who made my stay in PRL pleasant and a wonderful experience.

My deepest thanks goes to my parents, bhैया-bhabhi and Anshu, for all their love, understanding and unconditional support through the good and bad times. I owe special thanks to my wife 'Kalyani' for providing moral support and encouragement during the last months of this work.

CONTENTS

Abstract		v
<i>Acknowledgements</i>		vi
List of Tables		x
List of Figures		xi
Chapter 1	Introduction	1-10
1.1	Introduction	1
1.1.1	Chemical composition of atmospheric mineral dust	2
1.1.2	Evolution of dust, transport and deposition	3
1.1.3	Impact of dust on regional environment and climate	4
1.1.3.1	Earth's radiation budget	4
1.1.3.2	Atmospheric Chemistry	5
1.1.3.3	Atmospheric deposition and marine biogeochemical cycle	7
1.2	Objective of present study	9
1.3	Thesis outline	9
Chapter 2	Materials and Methods	11-37
2.1	Introduction	11
2.2	Site description and meteorological parameter	11
2.2.1	Mt. Abu	11
2.2.2	Arabian Sea	13
2.3	Aerosol sampling	14
2.4	Analytical techniques	17
2.4.1	Aerosol mass concentration	18
2.4.2	Sample preparation	19
2.4.3	Sample analysis	22
2.4.3.1	Water-soluble ions	22
2.4.3.2	Charge balance between cations and anions	25
2.4.3.3	Crustal constituents	27
2.4.3.4	Water-soluble Fe and trace elements	34
Chapter 3	Elemental characteristics of mineral dust	38-54
3.1	Introduction	38
3.2	Results and discussion	39
3.2.1	Temporal variability in fine and coarse mode aerosol mass concentrations	39
3.2.2	Temporal variability of mineral dust over western India	41
3.2.3	Elemental composition of atmospheric mineral dust over western India	45
3.2.3.1	Iron	46
3.2.3.2	Abundances of calcium and magnesium in mineral dust	47
3.2.4	Inter-annual variability of elemental ratios	48

3.2.5	Comparison of elemental ratios in mineral dust	52
3.3	Summary and conclusions	54
Chapter 4	Chemical characteristics of mineral dust	55-82
4.1	Introduction	55
4.2	Results and discussion	57
4.2.1	Temporal variation in Water-soluble ionic composition	57
4.2.1.1	Sea-salts (Na ⁺ and Cl ⁻)	58
4.2.1.2	Anthropogenic components (NO ₃ ⁻ , SO ₄ ²⁻ and NH ₄ ⁺)	63
4.2.1.3	Biomass burning component (K ⁺)	65
4.2.1.4	Dust components (Ca ²⁺ , Mg ²⁺ and HCO ₃ ⁻)	65
4.2.2	Inter-relationship among water-soluble ionic constituents	68
4.2.3	Inter-annual variability of various ionic ratios	73
4.2.4	Interaction between mineral dust and anthropogenic components	76
4.3	Summary and conclusions	78
Chapter 5	Mineral aerosols over Arabian Sea	83-101
5.1	Introduction	83
5.2	Results and discussions	84
5.2.1	Air-mass back trajectory analysis	84
5.2.2	Total suspended particulate (TSP) concentrations	85
5.2.3	Water-Soluble constituents	86
5.2.4	Mineral aerosols over Arabian Sea	94
5.2.5	Carbonaceous aerosols over Arabian Sea	97
5.2.6	Deposition Fluxes	99
5.3	Summary and Conclusions	100
Chapter 6	Aerosol iron solubility in a semi-arid region: Temporal trend and anthropogenic sources	102-114
6.1	Introduction	102
6.2	Results and discussion	104
6.2.1	Chemical characteristics of fine mode aerosols and temporal variability	104
6.2.2	Temporal variability of aerosol iron (Fe _A) and water-soluble iron (WS-Fe)	106
6.2.3	Solubility of aerosol iron and role of anthropogenic sources	109
6.3	Conclusions and implications	113
Chapter 7	Synthesis and future direction	115-121
7.1	Synthesis	115
7.2	Scope of future research	118
	References	122-137
	List of publications	138-140

List of Tables

Tables	Content	Page
2.1	Details of sample collection over Mt. Abu during 2006 and 2007	17
2.2	Filter blanks for water-soluble ionic species	24
2.3	Optical resolution on ICP-AES	31
2.4	Filter blanks for acid-soluble species	31
2.5	Analytical conditions for the analysis of elements in GF-AAS.	35
3.1	Minimum, maximum, mean and median concentrations of crustal elements in fine and coarse mode aerosols	43
3.2	Average elemental ratios observed over different geographical locations.	53
4.1	Minimum, maximum and average concentration of water-soluble ionic constituents in fine and coarse mode aerosols	60
5.1	Concentrations of chemical species in the Arabian sea-atmospheric boundary layer	88

List of figures

Figures	Content	Page
2.1	Map showing the sampling sites of present study	13
2.2	Monthly average temperature, RH, wind speed and wind direction over Mt. Abu	15
2.3	Monthly average wind patterns over India	16
2.4	ICARB cruise track over Arabian Sea	18
2.5	Analytical scheme for sampling and analysis for bulk-aerosol sample collected over Arabian Sea.	20
2.6	Analytical scheme for the sampling and analysis for size-segregated aerosol samples collected over Mt. Abu.	21
2.7	Repeat measurements of the mass concentration of aerosols (gravimetrically; μg) on Tissuquartz filters	21
2.8	Typical chromatogram obtained for separation of anions and cations in water-soluble extract of aerosol samples	23
2.9	Repeat measurements of the chemical species in water-extract of aerosol samples	24
2.10	Charge balance between $\Sigma\text{Cations}$ and ΣAnions in the $\text{PM}_{2.5}$ and PM_{10}	26
2.11	(a) Emission intensities observed for Al and Fe	29
	(b) Emission intensities observed for Ca and Mg	30
2.12	(a) Calibration plot between emission intensity and concentrations for Al and Ca	32
	(b) Calibration plot between emission intensity and concentrations for Fe and Mg	33
2.13	Repeat measurements of the crustal component in complete digested (acid soluble) aerosol samples	34
2.14	A graphite furnace typical temperature programme	36
2.15	Standard addition method to check the matrix effect on the concentrations of Pb and Cd on GF-AAS	37
3.1	Temporal variability of aerosol mass concentration in coarse and fine mode	42
3.2	Monthly average mass concentration of $\text{PM}_{2.5}$ and $\text{PM}_{10-2.5}$ during 2007 and Dust contribution in coarse and fine mode	44
3.3	Temporal variation of Al content	44
3.4	Scatter plot of concentration of crustal elements	49
3.5	Scatter plot of different elemental ratio against estimated dust	50
3.6	Annual variability of elemental ratios in PM_{10}	51
4.1	Scatter plot among PM_{10} and $\text{PM}_{2.5}$ for WSIC, Ca^{2+} and SO_4^{2-}	59
4.2	Fractional contribution (%) of individual ionic species to the total WSIC in the coarse and fine mode aerosols	62
4.3	Temporal variation of (a) NO_3^- , (b) nss-SO_4^{2-} , (c) NH_4^+ , (d) nss-K^+ and (e) $\text{NH}_4^+/\text{nss-SO}_4^{2-}$ in the two size fractions	66

4.4	Temporal variation of nss-Ca^{2+} , HCO_3^- and nss-Mg^{2+} in the coarse and fine aerosols	67
4.5	Scatter plot for water-soluble Mg^{2+} and Na^+ to assess the source of Mg^{2+}	69
4.6	A linear relationship between abundances (in equivalent units) of nss-SO_4^{2-} and NH_4^+ in the fine ($\text{PM}_{2.5}$) aerosols	69
4.7	Scatter plot between NO_3^- and SO_4^{2-} in PM_{10}	71
4.8	Linear regression plot between nss-Ca^{2+} and HCO_3^- in the fine and coarse mode aerosols	72
4.9	Scatter plot between sea-salt corrected water-soluble Mg^{2+} and Ca^{2+}	73
4.10	Annual variability of ionic ratios in high and low dust season	74
4.11	Scatter plot between total acid (TA) and $(\text{NH}_4^+ + \text{nss-K}^+)$ for (a) fine and (b) coarse aerosols	79
4.12	Scatter plot between $(\text{nss-Ca}^{2+} + \text{nss-Mg}^{2+})$ and HCO_3^-	80
4.13	Scatter plot between “excess acid” (EA) and HCO_3^- (normalized to the abundances of Ca^{2+} and Mg^{2+})	81
5.1	Average wind pattern during ICARB in Arabian Sea	86
5.2	Typical 7-day air-mass back trajectories at three (50, 100, 500 m) arrival heights representing different air-parcels for five different dates during the cruise period	89
5.3	Air-mass back trajectories showing northward progression of ITCZ during the inter-monsoon period	90
5.4	(a) Average abundances and spatial variation of aerosol components ($\mu\text{g m}^{-3}$) in the three Regions (A, B, and C) identified based on wind regimes. (b) Percent mass fraction of mineral dust, sea-salts and nss-SO_4^{2-} to TSP	91
5.5	Spatial variations in water-soluble components (a) cations, dominated by Ca^{2+} and Na^+ and (b) anions, dominated by SO_4^{2-} followed by Cl^-	92
5.6	Scatter plot for Na^+ and Cl^- ; all data points falling below the sea-water line imply large scale depletion of Cl^- from NaCl occurring in the AABL	93
5.7	(a) Scatter plot of Al with crustal components (Fe and Ca) (b) Linear regression of Al with TSP	95
5.8	Scatter plot among total Ca and water-soluble Ca^{2+}	96
5.9	Average compositions of aerosols in the Arabian Sea during inter-monsoon season	98
5.10	Dry-deposition fluxes of Fe and Al to the Arabian Sea during the inter-monsoon are compared with the corresponding fluxes at other oceanic sites	100
6.1	Map showing sampling site (Mt. Abu) and important source regions influencing the transport of aerosols. Typical 7-day air mass back trajectories at the study site	106
6.2	Temporal variability during winter and summer seasons in 2007 at a high altitude station (Mt. Abu), for (a) $\text{PM}_{2.5}$ aerosol mass, (b) mass fraction of estimated dust, (c) Fe_A/Al weight ratio (d) concentrations of NH_4^+ , (e) NO_3^- (f) nss-SO_4^{2-}	107

6.3	Temporal variability of (a) total aerosol iron (Fe_A) concentration and (b) water-soluble fraction of iron [WS-Fe (%)], (c) concentration of Cd and (d) Pb	109
6.4	(a) Large scatter between WS-Fe (%) and nss-SO_4^{2-} suggests that chemical processing during aerosol transport is of minor significance for soluble iron fraction at the study site. (b) Linear relationship among abundances (in equivalent units) of nss-SO_4^{2-} and NH_4^+ in the fine ($\text{PM}_{2.5}$) aerosols during summer and winter seasons	111
6.5	(a) Fe_A/Al (b) Cd/Al , (c) Pb/Al ratios are plotted against total aerosol iron concentration. A sharp increase in Cd/Al and Pb/Al ratio at lower Fe_A concentration is observed for winter month samples	112
6.6	Relationship between WS-Fe (%) and Fe_A for Mt. Abu samples along with the FeATMISS data from Sargasso Sea	113

Chapter-1

INTRODUCTION

1.1 Introduction:

Aerosols play an important role in various physico-chemical processes occurring in the atmosphere by scattering and absorbing incoming solar radiation. They also provide active sites for the uptake of several chemical species and trace gases, thereby undergoing phase changes and hence modify the chemical, optical and atmospheric radiative properties (Twomey, 1977, Charlson et al, 1991, Ramanathan et.al., 2001a, 2001b). The atmospheric mineral dust, representing largest component of continental aerosols by mass (1000 - 2150 Tg yr⁻¹; accounts for nearly 35% of the global emissions) (Zender, 2004), has potential to impact atmospheric chemistry, cloud properties and precipitation development (Dentener et al, 1996; Levin et al, 1996; Tegen et al, 1996, Arimoto, 2001; Tang et al, 2004a, b; Rastogi and Sarin, 2005a; Rastogi and Sarin, 2006). The mineral aerosols derived from disturbed soils encompass wide range of sizes and shapes, ranging from less than 0.1 μm to 100 μm diameter (Seinfeld and Pandis, 1998). The environmental consequences of this mineral dust have been found not only in their source areas but also in the downwind regions as well as across the marine atmospheric boundary layer through the long-range transport (Matsumoto et al, 2004; Kumar et al, 2008a, b). A unique feature of mineral dust particles is reflected from their ability to link land, atmosphere and ocean, the three fundamental domain of the Earth climate system. In comparison to other types of tropospheric aerosols, these particles originate over land, entrained into the atmosphere and finally get deposited over the ocean. The atmospheric significance and related properties of mineral aerosols are summarized in this Chapter.

1.1.1 Chemical composition of atmospheric mineral dust

The mineral dust, also referred as 'mineral aerosols', derived from surface soils get mobilized by the action of strong winds and get entrained into the atmosphere. In their pristine phase (in the vicinity of source region), chemical composition of mineral aerosols is similar to that of the soil from the source region. The soil particles are mainly dominated by silicon and aluminium oxides (McLennan, 2001), and hence similar abundance ratio is observed in the mineral aerosols. Approximately, 60 % SiO_2 and 10-15 % Al_2O_3 , have been reported in the literature (Goudie and Middleton, 2001) from various location around the world based on the elemental composition of windblown dust. In general, mineral aerosols comprise of quartz, feldspar, micas, illite, smectite, calcite, dolomite, gypsum, haematite among the most common minerals. Quartz is one of the most abundant mineral in the atmospheric aerosols owing to large occurrence of SiO_2 in the continental rocks. The mineralogical composition is also dependent on the size fraction of the mineral aerosols. For example, coarser particles are typically composed of quartz, feldspar and carbonates, whereas, fine particles usually consist of clays and micas. As a result, overall composition of mineral dust gets enriched in clays during long-range transport via gravitational settling of coarser particles. These mineral aerosols are expected to have differences in the mineral content at a regional scale in comparison to the source region.

Mineral dust derived from the Asian region will have different elemental composition from that originating from northern Africa (Sahara Desert). These differences have been also observed based on the physical appearance (colour) of the collected dust particles. Asian dust is observed more greyish in contrast to the more brown, yellow and red colour is observed for the dust coming from African regions (Sokolik and Toon, 1999). The pronounced regional variation in mineralogy as a function of latitude is observed within North Africa (Chester et al, 1972). The concentrations of crustal elements (e.g. Al, Fe, Ca, Mg, Sc and Si) have a general limitation to resolve the source regions of atmospheric mineral dust as none of the elements serve as a unique diagnostic tracer for a specific region; however, ratios of elements are more appropriate in decoupling the source regions. Thus, elemental ratios can be used for the characterization of mineral dust as well as to decipher the temporal variability in the source region. A similar

approach has been used for the characterization of source regions of dust in Africa (Chiapello et al, 1997) and in Asia (Zhang et al, 1996).

1.1.2 Evolution of dust, transport and deposition

The entrainment of dust into the atmosphere is one of the complex processes regulated by various environmental factors. This causes high variability of dust emission on temporal as well as spatial scale. Various factors which decide injection of dust in the atmosphere includes wind velocity, physical properties of the regional soil i.e. soil moisture content, particle cohesiveness as well as particle size distribution, and the morphology of the surface (e.g. surface roughness and vegetation coverage). By the action of strong wind, particles start moving and gain kinetic energy, however, because of large size, they bounce back and dislodge smaller particle ($\sim 10\text{-}20\ \mu\text{m}$ diameter) which can be lifted in the air parcel (Usher et al, 2003).

The dust events predominantly originate in arid and semi-arid regions, which accounts for $\sim 33\%$ of total world land area. The northern hemisphere generates c.a. 90% of the global mineral dust, where it is also deposited (Duce, 1995). These dust events are quite large and reduces visibility to a large extent. These (dust events) are populated in the tropical region starting on the west coast of North Africa and extend through the Middle East and Central Asia. One of the most prominent features of these dust events is the transport of suspended dust particles to the remote locations. This extensive transport often occurs in horizontally layered plumes and can persist for days to a week over thousands of kilometres. Saharan dust has been transported in extreme westerly, northerly, and easterly directions and detected in south America (Formenti et al, 2001), northern Europe (Franzen et al, 1994) and the Middle East (Alpert and Ganor, 2001) respectively. The transport of Saharan dust to North America via Atlantic Ocean is one of the well known phenomena and documented in the literature (Perry et al, 1997; Prospero, 1999; Prospero et al, 2001). In addition, evidences have been found for the transport of Asian dust to the continental North America (Jaffe et al, 1999; Husar et al, 2001; McKendry et al, 2001; Jaffe et al, 2003) and Hawaii (Parrington et al, 1983; Holmes and Zoller, 1996; Perry et al, 1999; Kurtz et al, 2001). The long-range transport of dust particles have been also observed in the

downwind regions as well as across the marine atmospheric boundary layer of Arabian Sea and Bay of Bengal (Kumar et al, 2008a, b).

The atmospheric lifetime of dust ranges from a few hours (for particles larger than 10 μm) to several weeks (for sub-micrometer sized particles). The lifetime of dust particles depends on the precipitation efficiency, vertical distribution of dust and particle properties (hydrophilic or hydrophobic) which may change during long-range transport. The two major pathways of dust removal are (1) dry deposition and (2) wet deposition. The first one relates to the deposition of dust under the influence of gravitational force. In this process, large particles are removed more quickly than the smaller particle, which leads to the shift in particle size distribution towards smaller size during transport. The dry deposition is the dominant deposition mechanism near the source region. The latter mechanism links to the removal of dust via precipitation. In general, aerosol-cloud interaction is not well understood and hence different assumptions are considered for cloud-dust interactions. Mineral aerosols, being hydrophilic in nature, have led many researchers to assume that dust do not interact with clouds directly, however, they are scavenged via sub-cloud removal mechanisms. A large uncertainty in the wet removal process further leads to discrepancies in the life-time of mineral aerosols. Recent observations have suggested that wet deposition is more important than dry deposition over oceanic region (Rastogi and Sarin, 2006a; Hand et al, 2004).

1.1.3 Impact of dust on regional environment and climate

The influx of mineral dust, from the dust events and long-range transport from arid and semi-arid region, into the troposphere suggests that mineral aerosol interact with many atmospheric, terrestrial and marine environments. The potential role played by mineral aerosols in the Earth's climate system has been discussed in the following sections.

1.1.3.1 Earth's radiation budget:

Similar to the other atmospheric aerosols, mineral aerosols have a potential to affect the regional and global climate through the absorption and scattering of solar radiation (Sokolik and Toon, 1996; Tegen et al, 1996;

Haywood and Boucher, 2000; Satheesh and Ramanathan, 2000; Sokolik et al, 2001; Satheesh and Krishnamoorthy, 2005). The radiative forcing [Def: the change in net (down minus up) irradiance (solar plus longwave; in $W m^{-2}$) at the tropopause after allowing for stratospheric temperatures to readjust to radiative equilibrium, but with surface and tropospheric temperatures and state held fixed at the unperturbed values] is termed as direct when aerosol particles absorb and scatter radiation themselves, whereas if the particles influence the optical properties of cloud, then it is termed as indirect. Positive forcing result in warming effect and conversely, negative forcing has cooling effect. Dust aerosols contribute significantly to radiative warming below 500 mb due to shortwave absorption (Miller and Tegen, 1999; Prospero et al, 2002; Prospero and Lamb, 2003). Typically it (mineral dust) doubles (approximately) the shortwave radiation absorbance under clear sky condition (Tegen and Miller, 1998; Tanare et al, 2003). It has been shown by Tegen and Fung (1994) that dust causes net cooling at the surface along with an increase in atmospheric heating. This effect has been found pronounced over the desert region (Mohalfi et al, 1998; Haywood et al, 2001, 2003; Tanare et al, 2003; Zhang and Christopher, 2003). Recently Intergovernmental Panel on Climate Change (IPCC, 2007) has reported a “low level of scientific understanding” about the effect that mineral aerosol particles have on the radiative fluxes within the atmosphere (range: $+0.09$ to $-0.46 Wm^{-2}$; Haywood and Boucher, 2000). Such large uncertainty arising from dust aerosols is mainly attributed to the lack of understanding of varying nature of dust from one region to another, the transport and removal processes and the chemical and physical properties of particles (Sokolik et al, 2001). It has been shown in recent studies that the global radiative flux are significantly linked to the cloud microphysical processes and subsequently related to the earth climate system (Baker et al, 1997).

1.1.3.2 Atmospheric chemistry

Over the last one decade there has been growing interest in heterogeneous and multiphase chemistry (i.e. reactions that are mediated by liquid and solid aerosol particles) of atmospheric aerosols which can substantially perturb the composition of atmosphere (Molina et al, 1996; Ravishankar, 1997; Grassian,

2001; Usher et al, 2003; Abbatt, 2003; Cwiertny et al, 2009). Mineral dust, one of the most abundant components in the troposphere, provides a surface with reactive site on which reaction can occur. Consequently, these particles (mineral dust) may act as one of the important sink for various atmospheric chemical species as well as sources of others. These dust particles can undergo long-range transport during which they encounter reactive gas-phase species (including ozone, nitrogen oxides, sulphur dioxides and organics) and react with these trace species. As a result of these surface reactions, they have potential to change the gas-phase concentration of important atmospheric constituents and subsequently change the physico-chemical properties of the aerosols. Such type of changes in aerosol particle properties e.g. size, shape, composition and hygroscopicity, will alter aerosol optical properties and can impact both the direct and indirect climate forcing of mineral dust (Dentener et al, 1996; Levin et al, 1996; Tegen et al, 1996, Arimoto, 2001; Kruger et al, 2003; Tang et al, 2004a, b; Laskin, 2005; Rastogi and Sarin, 2005a; Rastogi and Sarin, 2006).

The south Asian region is currently undergoing rapid industrialization, thus, making this region a hot spot for anthropogenic emissions (Arimoto et al, 1996; Streets et al, 2003). Moreover, mineral aerosols produced from land-use changes and disturbed soils are the important constituents of the atmosphere, especially those originating from the arid and semi-arid region of Asia (Dentener et al, 1996; Song and Carmichael, 2001; Rastogi and Sarin, 2006). The atmospheric mineral dust plays a vital role in the removal of anthropogenically derived acidic gases (e.g. SO₂ and NO_x); in addition to their removal mechanism via interaction with NH₃ (Zhuang et al, 1999; Jordan et al, 2003; Krueger et al, 2003; Bates et al, 2004; Tang et al, 2004a, b; Arimoto et al, 2004, Maxwell-Meier et al, 2004; Ooki and Uematsu, 2005; Rastogi and Sarin, 2005 a, b; 2006). A modelling study conducted for the east-Asian region had reported that natural aerosols (e.g. mineral dust and sea-salts) play an important role in the abundance pattern and size-distribution of inorganic constituents (Song and Charmichael, 2001). Furthermore, they have potential to alter the size distribution of particulate SO₄²⁻ and NO₃⁻ shifting their atmospheric distribution from fine to coarse size particles (Dentener et al., 1996; Rastogi and Sarin, 2006).

The abundances and atmospheric reactivity of acidic components (e.g. nitrate and sulphate); as well as their wet and dry removal processes depend critically on the composition of mineral aerosols (e.g., carbonate versus silicate content) and their size dependent distribution (Sullivan et al, 2007). Thus, one of the major limitations of current models relate to the lack of real-time data on size dependent chemical composition of atmospheric mineral dust at regional scale. In addition, owing to their relatively short lifetime, concentration and composition of aerosols vary on a regional scale. It is thus, essential to have long term regional scale studies as well as observational campaign pertaining to the aerosol composition which provides most comprehensive and direct information about aerosol characteristics and regional scale changes. Moreover, studies near to the source regions of mineral dust (originating from arid and semi-arid regions) are required to constrain and test the models.

1.1.3.3 Atmospheric deposition and marine biogeochemical cycle

In addition to the direct and indirect effects of mineral dust on atmospheric processes and climate, they can impact on biogeochemical cycles via global transport and deposition to the ocean surface. The atmospheric transport and deposition of mineral dust is considered as one of the major sources by which iron is supplied to the ocean surface (Duce and Tindale, 1991; Fung et al., 2000; Mahowald et al, 2005, 2009; Jickells et al, 2005). Also, iron is hypothesized as a limiting factor in controlling the phytoplankton production in the high nutrient low chlorophyll (HNLC) regions (Martin et al, 1991). These are recognized as potential regions in modulating the CO₂ uptake due to the increase in phytoplankton productivity and thus, affecting the global carbon cycle and climate (Jickell et al, 2005; Meskhidze et al, 2003; Solmon et al, 2009). On average, dust aerosols contain 3.5% of iron mainly existing in the form of aluminosilicate (Duce and Tindale, 1991; Zhu et al, 1997). The aerosol Fe associated with mineral dust remains insoluble at pH conditions typical of sea-water (Stumm and Morgan, 1981; Zhu et al, 1997). However, a finite fraction of the aerosol Fe [referred as dissolved iron], is used by phytoplanktons. Several field based studies, incorporating different analytical techniques, have documented large variability (0.01 to 80 %) in the water-soluble fraction of aerosol iron and continues to

remain a major source of uncertainty in assessing the impact of atmospheric supply of iron to the marine ecosystem and the biogeochemical cycle (Hand et al, 2004; Chen and Siefert, 2004; Mahowald et al, 2005; Baker et al, 2006).

One of the proposed mechanisms for the enhanced solubility of iron is the chemical processing of aerosol particles, during long-range transport, mediated by the presence of acidic components (e.g. SO₂ and its oxidation products) and sunlight (Zhuang et al, 1992; Johansen et al, 2000; Meskhidze et al, 2003). On the contrary, some of the field experiments have indicated that the soluble iron can be enriched as a result of direct emission from fossil-fuel combustion and biomass burning (Chuang et al, 2005; Sedwick et al, 2007; Sholkovitz et al, 2009). Baker and Jickells, (2006), have argued that the increase in aerosol iron solubility is influenced by the decrease in particle size (i.e. increase in surface area to volume ratio) during atmospheric transport rather than differences in the composition of aerosols. On the contrary, Buck et al, (2008) have demonstrated that there is no such obvious correlation and that aerosol composition from the source region is a dominant factor in controlling the iron solubility.

It, thus, emerges from the above discussion that long-term regional studies of chemical composition of mineral dust are essential to assess their impact on regional climatology. It is also important to understand the atmospheric transport as well as transformation processes caused by the interaction with anthropogenically derived chemical species (SO₂, NO_x, organics and their derivatives) over arid and semi-arid regions (source region of dust aerosols) as well as over marine regions. Also, the measurements based on bulk-aerosols are inadequate to constrain the model scenario made in recent years. In this context, the present study on the chemical composition of fine (PM_{2.5}; particles less than 2.5 μm) and coarse (PM_{10-2.5}; particles between 10 and 2.5 μm) mode aerosols is most relevant from a high-altitude site (Mt.Abu; 24.6 °N, 72.7 °E, 1680m asl) located in a semi-arid region (near to the Great Thar Desert in western India). The sampling strategy from a high-altitude station is advantageous to study the long-range transport of mineral dust across western India and its role in modifying the atmospheric chemistry of acidic species. In addition, the transformation of mineral dust over marine region (Arabian Sea) downwind of the source (western India),

has been also assessed based on bulk-sampling during spring-intermonsoon season.

1.2 Objectives of thesis study

A comprehensive study in improving our understanding of the regional and seasonal characteristics of the mineral aerosols and associated chemical transformation processes has been undertaken involving chemical composition of coarse ($PM_{2.5-10}$, particulate matter less than 10 and greater than 2.5 μm aerodynamic diameter) and fine mode ($PM_{2.5}$, particulate matter less than 2.5 μm aerodynamic diameter) aerosols.

The specific objectives of my thesis study are:

- 1. To characterize regional-scale mineral dust, its atmospheric transport, particle size, chemical composition & temporal variability.**
- 2. To examine & quantify uptake of acidic species (SO_4^{2-} and NO_3^-) on mineral aerosols (chemical transformation) in high-dust regions.**
- 3. To characterize & quantify solubility of iron ($\text{Fe}^{3+} \longrightarrow \text{Fe}^{2+}$) from mineral dust vis-à-vis anthropogenic sources.**

These regional scale studies of atmospheric aerosols are important in understanding several atmospheric processes as well as effect of aerosols on climate. In the present study from high-altitude remote site and marine atmospheric boundary layer of Arabian Sea provide an important data set on chemical composition of aerosols. These data sets can also be used as inputs to various global and regional scale climate models. The objectives of the present study are similar to those of several international programs such as International Global Atmospheric Chemistry (IGAC), Deposition of Biogeochemically Important Trace Species (DEBITS), Surface Ocean Lower Atmosphere Study (SOLAS) and International Commission on the Atmospheric Chemistry and Global Pollution (iCACGP).

1.3 Thesis outline:

This thesis consist of seven chapters as summarized below:

- **Chapter 1** provides a brief introduction on mineral aerosols and their role in the troposphere. It also provides a review of the work done in this field; rationale and specific objectives of the study.
- **Chapter 2** describes the geographical site, sampling protocol and detailed analytical procedures adopted for the chemical analyses of coarse (PM_{10-2.5}) and fine (PM_{2.5}) mode aerosols.
- **Chapter 3:** The analytical data, results and discussions on dust composition (elemental ratios); their temporal variations and comparative characteristics of dust from other sampling locations are given in this chapter.
- **Chapter 4:** This chapter describes the temporal variability and relationships among various water-soluble ionic constituents in coarse and fine aerosols. This chapter also highlights the role of alkaline mineral dust in scavenging the acidic component in different size fraction.
- **Chapter 5:** This chapter highlights the chemical composition of aerosols over marine region adjoining Indian subcontinent. It also deals with various transformation processes occurring within marine atmospheric boundary layer.
- **Chapter 6:** This chapter deals with one of the important aspect of iron-solubility over semi-arid region (source region of dust). The factors affecting the aerosol iron solubility (atmospheric processing or direct emission from anthropogenic sources) at high-dust region will be presented in this chapter.
- **Chapter 7:** This chapter summarizes the important findings of the study and their implications in assessing the impacts of aerosols on climate as well as scope for future research.

Chapter 2

MATERIALS AND METHODS

2.1 INTRODUCTION

In order to achieve the specified objectives (Chapter 1), a systematic sampling strategy was designed for the collection of aerosol samples from a high-altitude site (Mt. Abu, 24.6 °N, 72.7 °E, 1680m above sea level) representing a very diverse meteorological conditions and the source strength of aerosols. A well conceived analytical scheme was an integral part of this study wherein aerosol samples in two size-ranges (PM_{2.5} and PM₁₀) were simultaneously collected onto tisuquartz filters using high-volume air samplers fitted with different inlets. The geographic location of the study site, in the Aravali range of mountains, is most ideal for the characterization of mineral aerosols and chemical species derived from anthropogenic emission sources. The sampling site also acts as a natural laboratory for studying the interaction between mineral dust and anthropogenic components. The sampling was also carried out in the oceanic region where we expect substantial gradient in the aerosol constituents, such as urban plume advecting into the non-polluted marine boundary layer (MBL). Towards this, a cruise was undertaken in the Arabian Sea for aerosol sample collection from MBL. Relevant details of the selected site, sampling protocols for aerosols and analytical procedures adopted for the measurements of mineral dust and chemical species in aerosol samples have been described in the following sections:

2.2. Site Description and Meteorological Parameters:

2.2.1 Mt. Abu:

The sampling site (shown in Fig. 2.1) for the synchronous collection of PM_{2.5} and PM₁₀ aerosols was located on the terrace of Aeronomy laboratory (~5m

above ground level) at Gurushikhar (commonly known as Mt Abu, 24.6 °N, 72.7 °E, 1680m asl). Gurushikhar is a highest peak in the southern end of Aravali range of mountain in the semi-arid western India. The proximity of the site to the great Thar Desert (~300 km) provides an ideal opportunity to study the long-range transport of mineral aerosols and their temporal variability over western India. The sampling location is characterized as a remote site with almost negligible movement of vehicular traffic within the immediate vicinity. The main town of Mt. Abu (about 10 km from sampling site) is situated at an altitude of 1220 m with a population of about 40,000. Therefore, the Guru Shikhar site provides an ideal setting for sampling in a relatively clean environment in a semi-arid region. A number of small scale marble quarries are located in the plain region.

The annual rainfall at Mt. Abu averages around 600-700 mm, mainly spread over the period of July-September (SW-monsoon). The site represents free-tropospheric conditions during winter months (Oct-Feb) when the boundary layer is relatively lower than the sampling altitude. The meteorological parameters (wind speed, wind direction, relative humidity, and air temperature, Fig. 2.2) were recorded by automatic weather station located close to the experimental site except for two months (Jan and Feb) when NCEP (National Centre for Environmental Prediction) reanalysis data (<http://www.cdc.noaa.gov/>) has been used. Based on the prevailing meteorology of this semi-arid region, the annual seasonal cycle has been referred as summer (Mar-Jun), monsoon (Jul-Sep) and winter (Oct-Dec; Jan and Feb). During wintertime (Oct-Feb), average daily temperature ranged from 7.3 to 20.6 °C and that during summer months (Mar-Jun) varied as 10.3 to 26.3 °C. The relative humidity was less than 40% for most time of the year except in the monsoon season when the humidity levels close to 100% were recorded when the prevailing winds (Fig. 2.2) bring substantial amount of moisture to the sampling location. The representative average wind patterns from Jan-Dec are depicted in Fig. 2.3.

A noteworthy meteorological feature of the sampling site relates to complete reversal of wind regimes, a shift from south-westerlies during summertime to north-easterly winds during winter months. The contrasting wind pattern during wintertime (Fig. 2.3), favours long-range transport of pollutants

and chemical species derived from large scale anthropogenic activities in northern India. The near surface wind speed at the sampling location were high during monsoon season (13.5 m/s). However, winds were usually weak during winter months, except for a few days in the month of Jan and Feb.



Fig. 2.1 Map of India showing the sampling site Mt. Abu located in a semi-arid region of western India. (Image taken from Google earth).

2.2.2 Arabian Sea

The Arabian Sea (Fig. 2.1) is one of the ideal locations, confined by land from three sides, to study the impact of continental aerosols transported to marine environment. This region is largely affected by the winds originating from north/north-western region of Indian subcontinent as well as from Central Asian countries (Oman, Yemen e.t.c). The aerosol sampling was carried out onboard ORV Sagar Kanya (cruise No. SK 223B) from 18th April to 11th May 2006. The

prevailing winds were north-westerly during initial days of the cruise and changed to south-westerly towards the end of the cruise. Figure 2.4, shows the cruise track during the campaign, making several transects between 9 °N to 22 °N and 58 °E to 75 °E. The meteorological parameters such as wind speed, relative humidity, air temperature were measured onboard at a height of 15 m from the sea level on hourly basis. The relative humidity varied from 59 to 95 %, with mean of about 80% during the campaign period. The prevailing winds were corrected for the ship's motion and found to vary between 0.5 to 10 ms⁻¹, whereas surface-level pressure variations were recorded in the range of 1005 to 1016 mb. The winds were generally strong (~10 m s⁻¹) during the sampling transect in the central Arabian Sea and relatively moderate (~8 m s⁻¹) in the Northern Arabian Sea. Details of meteorological parameter and boundary layer dynamics during this campaign are described in Alappattu et al., (2007).

2.3 Aerosol sampling

The aerosol samples (PM_{2.5} and PM₁₀) were collected by simultaneously operating two separate Hi-vol samplers (Thermo Andersen) fitted with inlet having 50% cutoff size for 10µm and 2.5 µm aerodynamic diameter particles. The Hi-vol samplers were equipped with volume flow controller to maintain a constant flow rate. However, periodic calibration of samplers was performed (once in every 2-3 week) to check on variation, if any, in the flow rate; typically the flow rate varied from 1.07-1.18 m³min⁻¹ with an uncertainty of 5%. Ambient aerosols were filtered through pre-combusted PALLFLEXTM tissuquartz filters (20x25 cm²). The sampling was carried out for ~ 18 months, starting from May-2006 till December-2007. The sampling was done in campaign mode during 2006, in which no samples were collected during monsoon period. However, a uniform sampling frequency was maintained throughout in year 2007, by collecting a sample every fifth day (5th, 10th, 15th, 20th, 25th and 30th of every month). On average 800 m³ of air was filtered in each case; Table 1 provides relevant details on collection dates, number of samples and the sampling frequency.

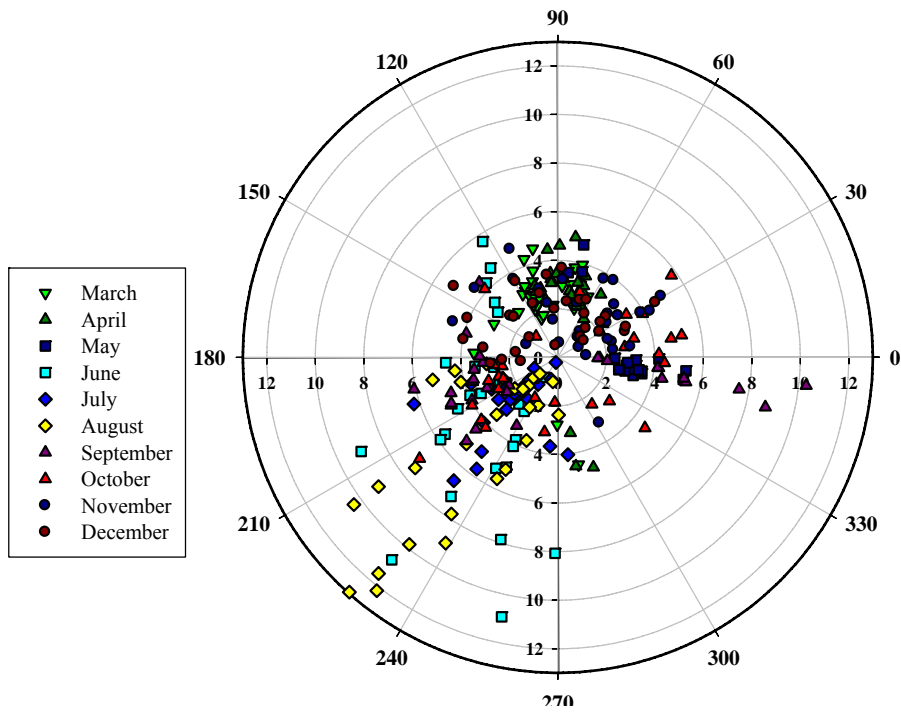
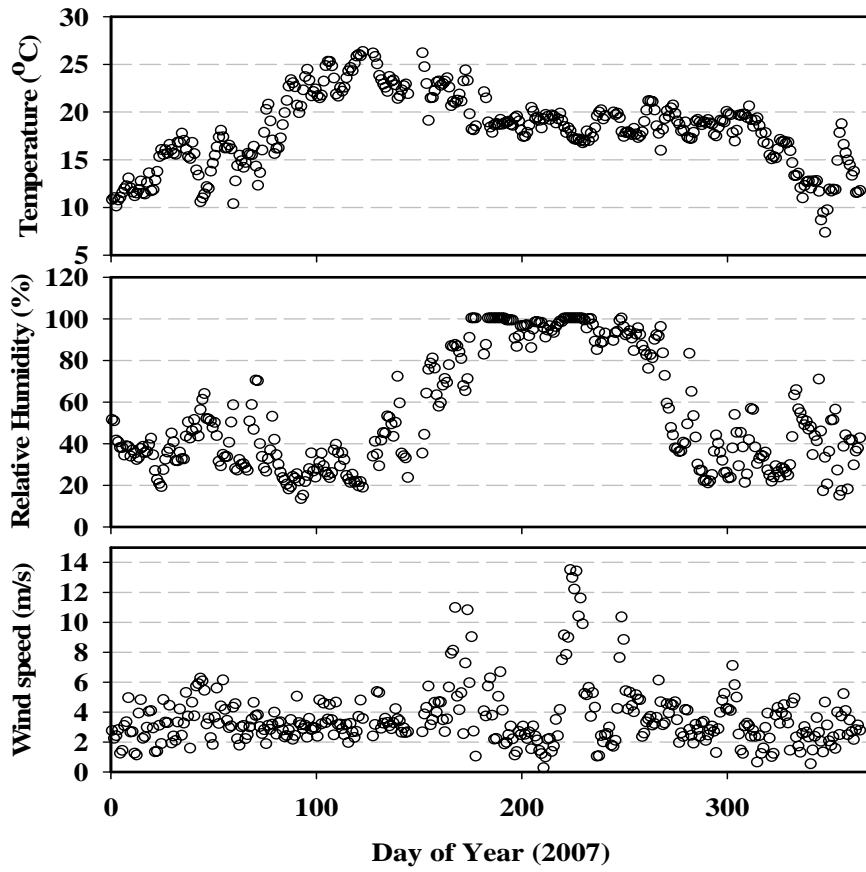


Fig. 2.2 Daily average temperature, RH, wind speed and wind direction during 2007 measured at the sampling site, Mt.Abu.

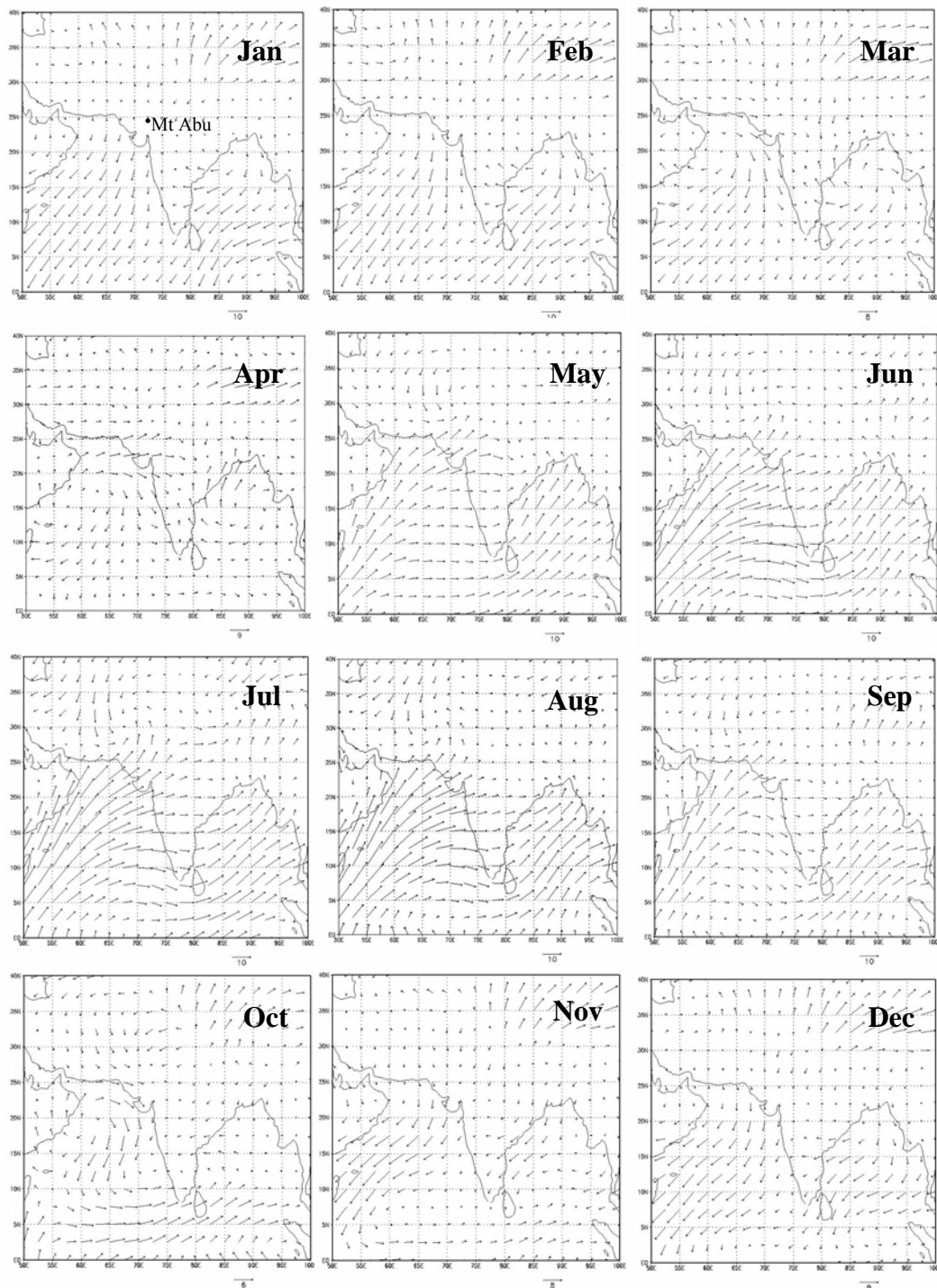


Figure 2.3 Monthly average wind patterns for the study site at Mt Abu. Southwesterly winds dominate during May-Aug while northeasterly winds prevail during Nov-Feb. During Mar-Apr and Sept-Oct, transition between the major wind patterns takes place. The length of arrows represents the magnitude ($m s^{-1}$) of wind speed (Data adopted from <http://www.arl.noaa.gov/ready>).

Table 2.1: Details of sample collected from high-altitude site (Mt.Abu) during 2006 and 2007.

Month	Sample Collected		Sampling Date
	(n)	(Day of Year-2006)	(Day of Year-2007)
Jan	9	-	3,4,7,10,11,12,16,20,29
Feb	7	-	32,39,42,47,48,57,58
Mar	5	-	64,69,74,79,84
Apr	9	-	91,95,99,102,107,111,113,115,119
May	19	121-131	123,127,131,135,137,139,144,148
Jun	12	161-166	152,156,160,165,169,172
Jul	3	-	182,205,212
Aug	3	-	232,237,240
Sep	17	256-269	255,260,268
Oct	12	300-304	276,281,286,291,296,298,301
Nov	9	305-308	306,311,314,324,331
Dec	11	344-348	337,342,347,352,357,362

In the MABL of Arabian Sea, bulk-aerosol samples were collected, onboard ORV SagarKanya, on PALLFLEX™ tissuquartz filters (200x250 mm²) by operating a high-volume sampler at a flow rate of 1.5 m³ min⁻¹. The sampler was set up on the upper deck, 15 m asl, in front of ship's navigation room. Each sample was collected over a time period ranging from 15 to 22 hrs when ship was cruising at a speed ~10 knots/hrs or above conforming to the protocol that the relative wind direction is from the bow, thus avoiding the contamination from ship's exhaust.

2.4. Analytical Techniques

All aerosol samples collected from Mt. Abu and marine atmospheric boundary layer of Arabian Sea, were analyzed for crustal constituents (Al, Fe, Ca, and Mg) and water-soluble chemical species (NH₄⁺, Na⁺, K⁺, Mg²⁺, Ca²⁺, Cl⁻,

NO_3^- , $\text{SO}_4^{=}$ and HCO_3^-). Also, carbonaceous species (EC and OC) were measured in the samples collected from MABL of Arabian Sea. In addition, trace elements (Cd and Pb) as well as water-soluble Fe (WS-Fe) have been also measured in the $\text{PM}_{2.5}$ samples collected (during winter and summer) from Mt. Abu. The sampling and analytical scheme adopted for aerosol study is outlined in Fig. 2.5 and 2.6 for Mt. Abu and Arabian Sea respectively.

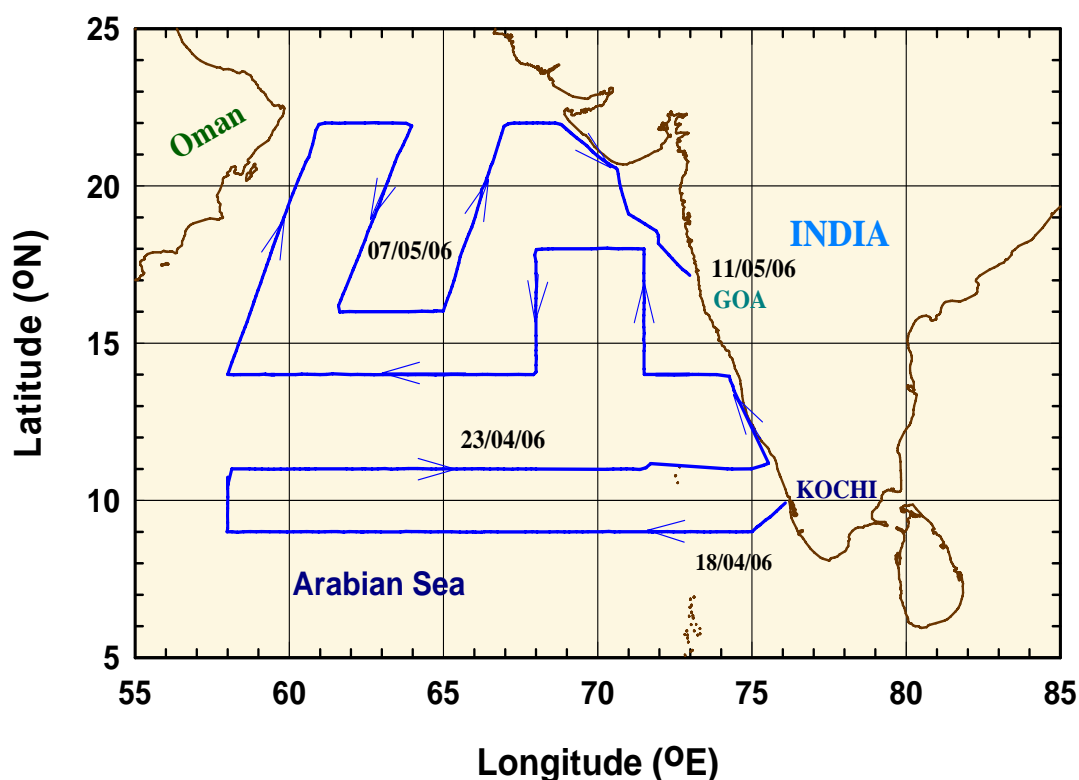


Fig. 2.4 The cruise transects carried out in the Arabian Sea for collection of bulk-aerosol samples during spring inter-monsoon (April-May'06).

2.4.1 Aerosol mass Concentration:

The aerosol mass concentrations in the $\text{PM}_{2.5}$, PM_{10} and bulk aerosols were ascertained gravimetrically (with a precision of 0.1 mg) by weighing the full filters on a large pan (pan size 8.2" x 10.4") filter balance (Sartorius, model LA130S-F) before and after the sampling. Prior to weighing, all filters were conditioned at a relative humidity of 40 ± 5 % and temperature of 22 ± 1 °C for 5-6 hrs. The repeat measurement of the filter weights provide an uncertainty of ± 1 mg

which corresponds to an overall error of ~15% in the aerosol mass concentrations. The precision of measurements for filter weights were assessed and results are shown in Fig. 2.7

2.4.2 Sample preparation:

In the laboratory, filters were cut into 1/4th section under a clean flow bench (Class 100) and were soaked in 50 ml of Milli-Q water (resistivity = 18.2 MΩ cm) for 10-12 hrs following the initial ultrasonic treatment for 15 min in teflon bombs. Subsequently, water extract was centrifuged using a centrifugation system (8000 r.p.m) and supernatant fraction was transferred to pre-cleaned polypropylene bottles (previously soaked in Milli-Q water for ~72 hrs) and analyzed for water-soluble ions (Na^+ , NH_4^+ , K^+ , Mg^{2+} , Ca^{2+} , Cl^- , NO_3^- , SO_4^{2-} , and HCO_3^-).

The concentrations of crustal elements (Al, Fe, Ca, and Mg) were analyzed using ICP-AES (JobinYovn, ULTIMA-2). In the analytical protocol used throughout this study, one-eighth portion of filter was taken in a silica crucible (pre-cleaned) heated in an oven at 400 °C for ~3 hours to decompose the organic coating (if any). Subsequently, the filter was digested in Sevillex vial (15 mL capacity) in presence of 0.5 mL HF and 3 mL HNO₃ by microwave heating (Temp = 210 °C; Pressure = 100 bars); thus ensuring complete dissolution of aerosol sample and filter. The acid-extract was finally made to 25 mL with Milli-Q water. A commercial standard (Merck[®], 23 elements) was used for the instrument calibration and making linear analytical curves between element concentrations and emission intensities measured on ICP-AES. The concentrations of crustal elements were corrected for procedural blanks (comprising of blank filters and analytical reagents). Several (n = 13) blank filters were also digested along with several batches of sample filters in order to assess the filter and procedural blank contribution to aerosol chemical data.

In the adopted analytical protocol, for measurement of water-soluble fraction of Fe, about 15 cm² section of the sample filter (equivalent to 5-circular punches area = 3.14 cm²) was treated with 10 mL Milli-Q water in a 50 mL Savilex Teflon vial followed by an ultrasonic treatment for 15 min. Subsequently,

water extract was filtered through 0.4 μm PTFE filter into a low density polyethylene vials and immediately acidified to $\text{pH} < 2$ using double distilled HNO_3 . The selection of Milli-Q water for WS-Fe, instead of seawater, is based on the rationale that Milli-Q water provides a consistent and reproducible leaching solution (Buck et al, 2006; Sedwick et al, 2007). The ultrasonic treatment during the water-extraction helps in disintegrating the aerosol particles from the filter substrate, thus achieving uniformity in the extraction procedure. The WS-Fe data reported in this study represent relative amount of soluble Fe (also referred as “operational solubility”) as compared to ‘absolute’ or ‘true’ solubility. It is rather difficult to reproduce the in-situ conditions that aerosol particles undergo subsequent to their deposition to the ocean surface.

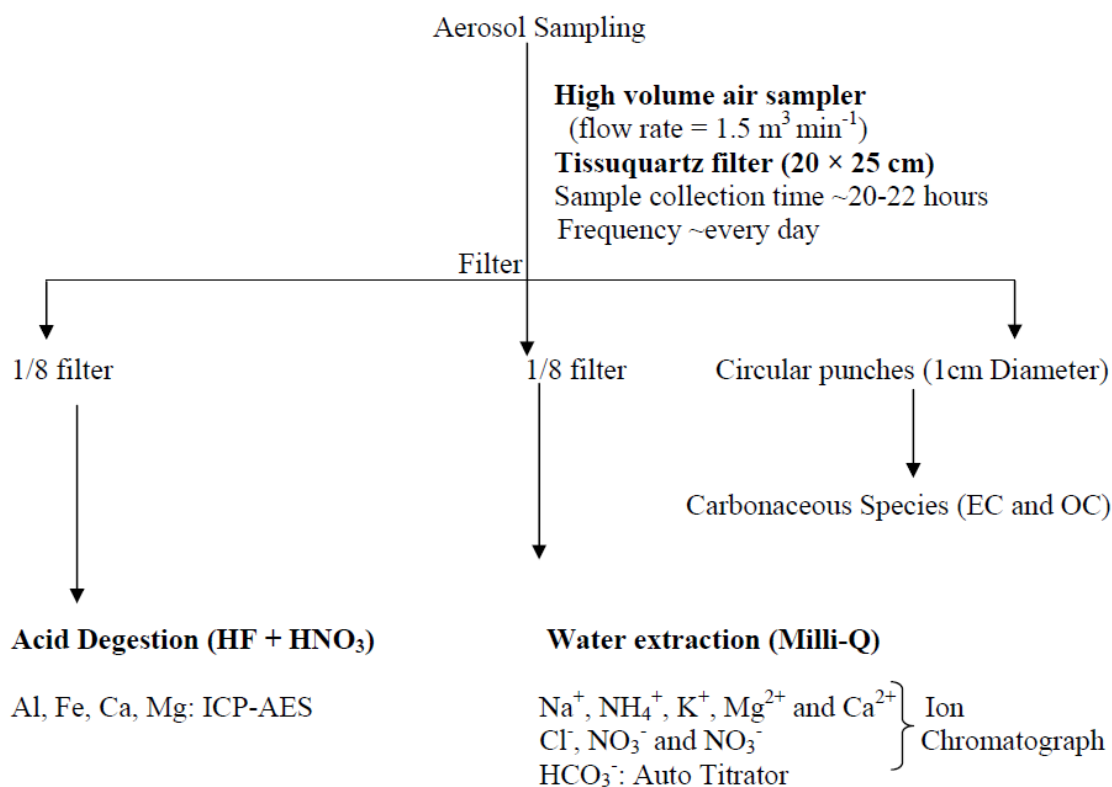


Fig. 2.5 Analytical scheme for the sampling and analysis for bulk-aerosol samples collected over Arabian Sea.

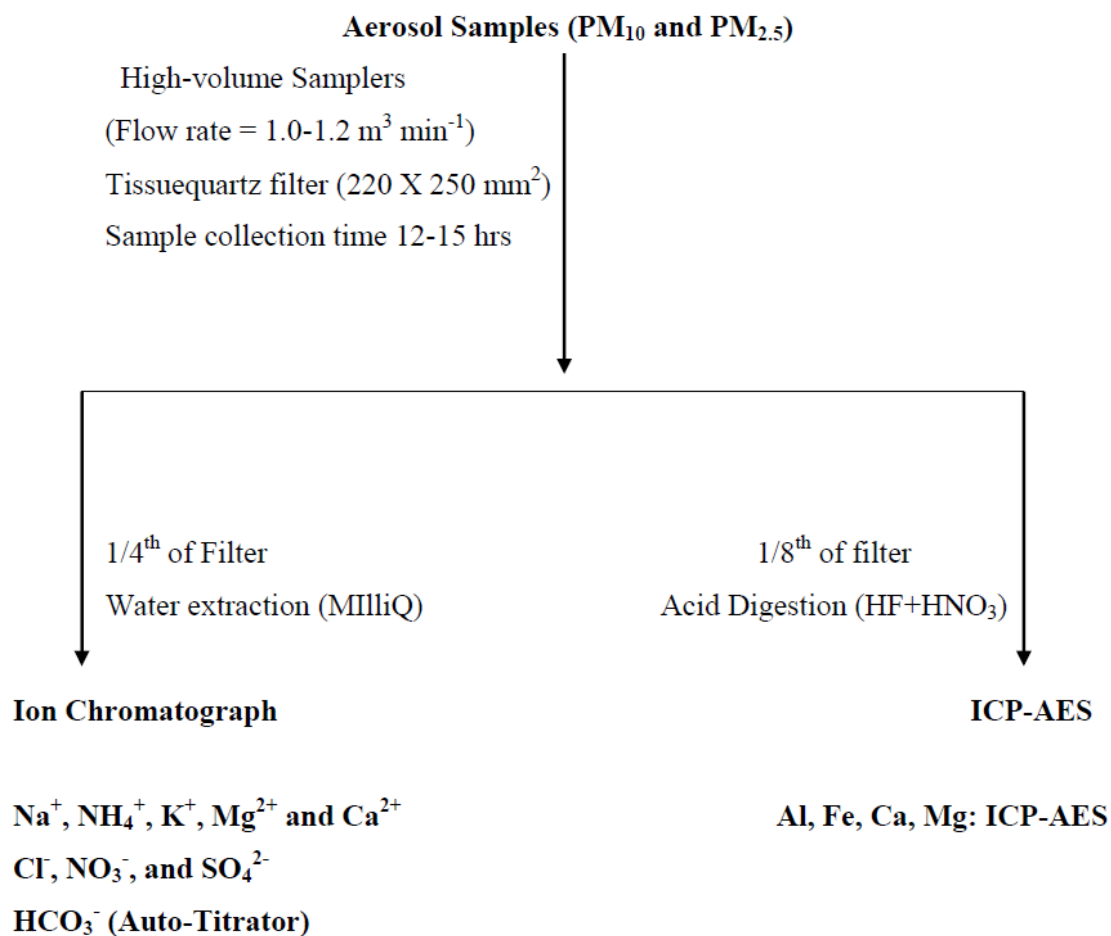


Fig. 2.6 Analytical scheme for the sampling and analysis for size-segregated aerosol samples collected over Mt. Abu.

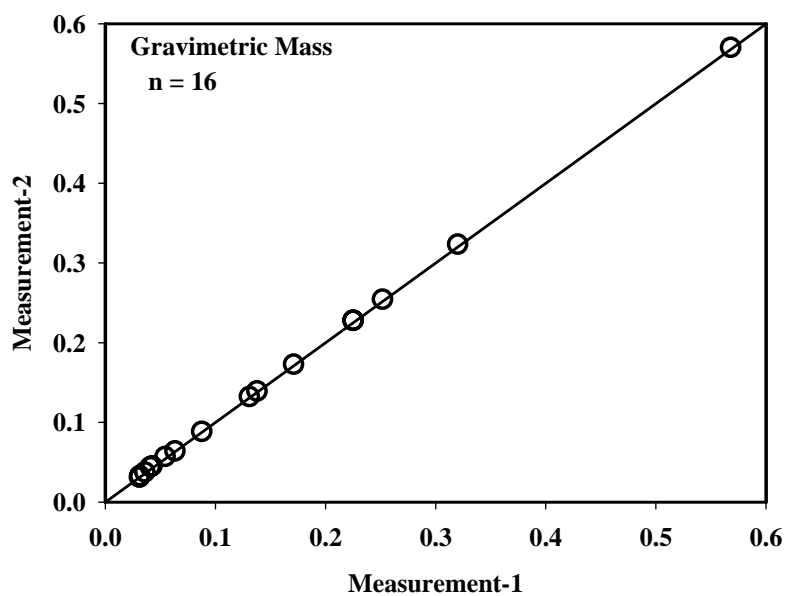


Fig. 2.7 Repeat measurements of the mass concentration of aerosols (gravimetrically; mg) on Tissuequartz filters. Solid lines represent 1:1 correspondence between the data.

In this study, Cd and Pb were also measured in the same aerosol samples in order to assess the impact of anthropogenic sources on the solubility of iron. Towards this, filter punches (ca. area = 3.14 cm²) were treated with HF and HNO₃ in Teflon vials and digested in a microwave oven (ca. 100 bar pressure and ca. 250 °C). The acid extract was made to a final volume of 15 mL and the concentration of Cd and Pb were measured on Heated-Graphite Furnace-Atomic Absorption Spectrophotometer (HG-GF-AAS).

2.4.3. Sample Analysis:

2.4.3.1 Water-Soluble ions:

The anions (Cl⁻, NO₃⁻ and SO₄²⁻) and cations (Na⁺, NH₄⁺, K⁺, Mg²⁺, and Ca²⁺) were analyzed on DIONEX[®] Ion-Chromatograph equipped with suppressed conductivity detector. The anions were separated on AS-14 analytical column and AG-14A guard column, in conjunction with an anion self-regenerating suppressor (ASRS) in recycle mode. The samples were injected through 25 µL loop and a combination of 1.8 mM Na₂CO₃ and 1.7 mM NaHCO₃ was used as an eluent maintained at a flow rate of 1.0 mL min⁻¹. The precision estimated from the standard deviation of repeat measurements of standards and samples, was better than 3% for Cl⁻, NO₃⁻ and SO₄²⁻. Analysis of cations were performed on CS-12A column, using 20 mM methanesulphonic acid as an eluent at a flow rate of 1 mL min⁻¹, coupled to a CSRS suppressor (cation self-regenerating suppressor) operated in recycle mode. In addition, field blanks (blank filters leached with Milli-Q water along with the aerosol samples) were also analyzed and concentrations of all ionic species were corrected for procedural blanks (comprising of blank filters and analytical reagents). Typical chromatograms for anions and cations are shown in Fig. 2.8. The concentrations of all anions and few cations (NH₄⁺, K⁺ and Mg²⁺) in the filter blanks were found to be below their detection limits, as given in Table 2.2. Based on blank concentrations and average volume of air filtered (~800 m³), the detection limits for the water-soluble ionic species in aerosols were ascertained (18, 8, 20, 4, 15, 15, 8 and 20 ng m⁻³ for Na⁺, NH₄⁺, K⁺, Mg²⁺, Ca²⁺, Cl⁻, NO₃⁻ and SO₄²⁻ respectively).

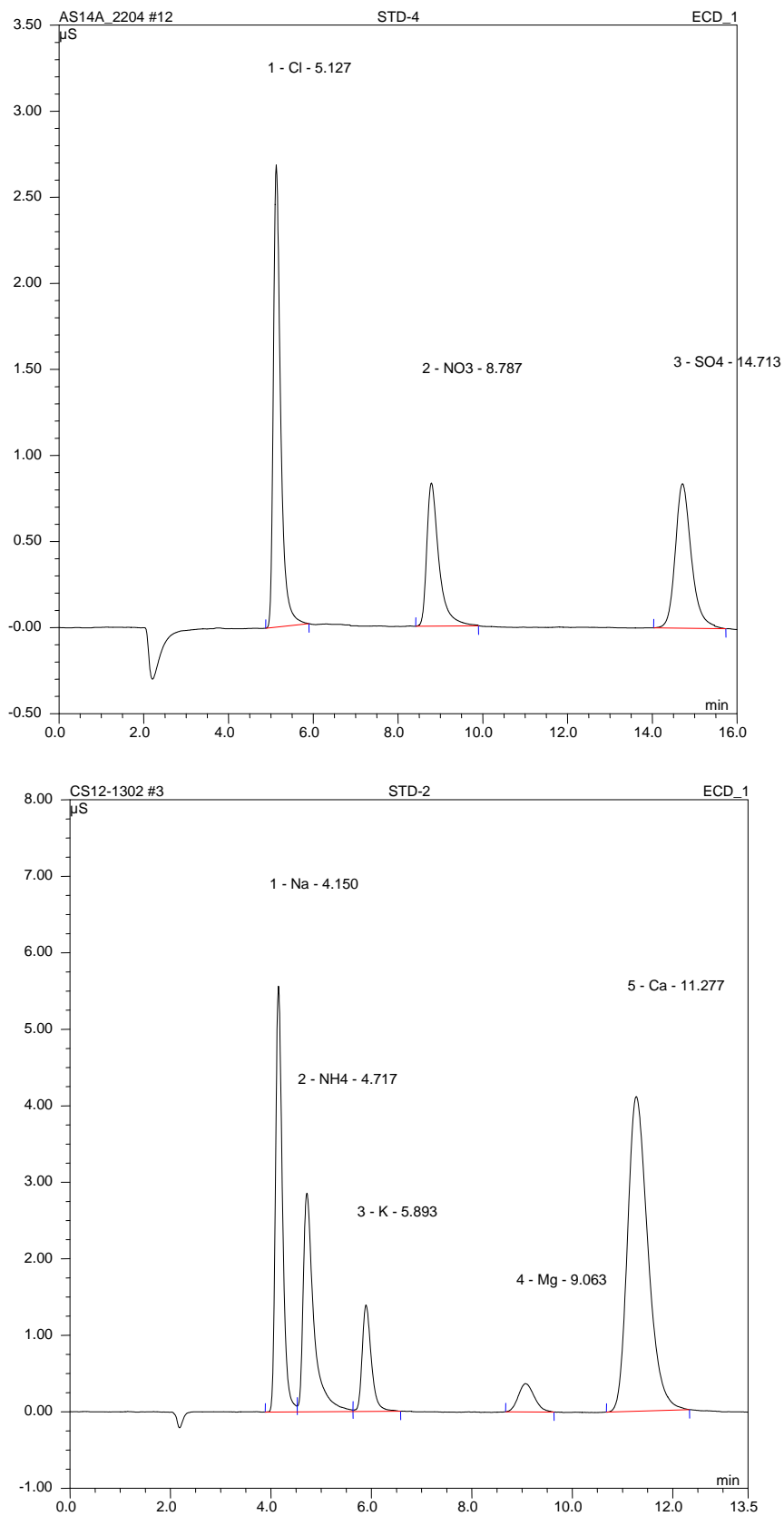


Fig. 2.8 Typical chromatogram obtained for separation of anions and cations in water-soluble extract of aerosol samples.

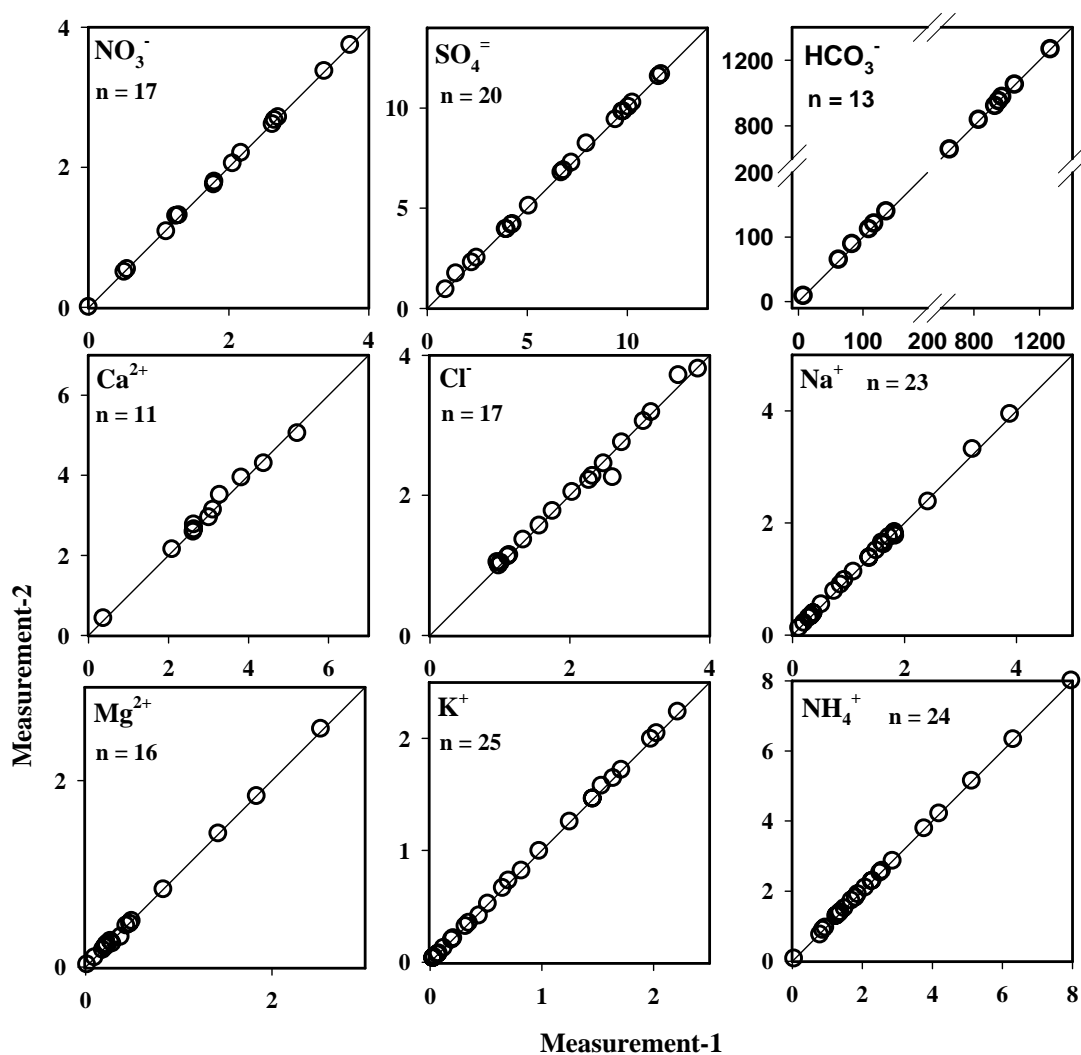


Fig 2.9 Repeat measurements of the chemical species (mg L^{-1}) in water-extract of aerosol samples. Solid lines represent 1:1 correspondence between the data.

The precision of measurements for all major ions analyzed in the water-extract of aerosol samples was assessed and results are shown in Fig. 2.9.

Table 2.2 Average concentration and standard deviation (sd) of ionic species in blank tissuquartz filter (for $n = 13$) including procedure blank.

	Na^+	NH_4^+	K^+	Mg^{2+}	Ca^{2+}	Cl^-	NO_3^-	SO_4^{2-}	HCO_3^-
Avg ($\mu\text{g}/\text{filter}$)	10.8	8.0	12.9	4.0	9.7	13.5	8.0	32.7	73.2
sd ($\mu\text{g}/\text{filter}$)	6.0	-	6.6	-	5.0	5.0	-	6.7	-

Bicarbonate (HCO_3^-) was measured by acid ($\sim 0.001 \text{ N HCl}$) titration using Auto-titrator system (Metrohm 702 SM Titrino) in combination with a glass electrode and fixed pH (4.3) end point method. Prior to measurement, the system was calibrated with freshly prepared buffer solutions of pH 4.00 ± 0.05 , 7.00 ± 0.05 and 9.20 ± 0.05 . Based on repeat analysis of a number of samples and standards, the reproducibility of bicarbonate measurements is $\sim 2\%$. The precision of measurements for HCO_3^- is shown in Fig. 2.9.

For all major ions, calibration curve was established using standard solutions prepared in the laboratory by dissolving analytical grade NH_4Cl (for NH_4^+), Na_2CO_3 (for HCO_3^-), NaCl (for Na^+ and Cl^-), KNO_3 (for NO_3^-), KCl (for K^+), Na_2SO_4 (for SO_4^{2-}) and CaCO_3 (for Ca^{2+}). Pure Mg metal was dissolved in HCl to prepare stock solution for Mg^{2+} . The stock solutions (1000 mg L^{-1}) were suitably diluted for the analysis so that concentration/absorbance was in the linear analytical range. Along with the laboratory standards, commercial standards (Merck®) were also analyzed to ascertain the accuracy of the measurements. The results showed that accuracy was better than 5% for all measured elements.

2.4.3.2 Charge balance between cations and anions:

The quality and validity of the analytical data for water-soluble ions has been ascertained based on the charge balance (in equivalent units) between the measured cations (Σ^+) and anions (Σ^-), as presented in Fig. 2.10. In the PM_{10} aerosols, ionic ratio (Σ^+ / Σ^-) varied from 0.78 to 1.22 ($A_v = 0.91$; s.d. = 0.09) and that in $\text{PM}_{2.5}$, from 0.79 to 1.10 ($A_v = 0.94$; s.d = 0.07), suggesting that maximum deviation from charge neutrality is no more than 20%. It can be argued that the observed deviation is well within the combined analytical uncertainties in taking the summation of all cations and anions. Looking from a different perspective, the anion deficiency could be attributed to the lack of consideration of water-soluble organic ions in the charge-balance. However, some of the organic acids (e.g. formic and oxalic acid), measured in the water extracts were close to the detection limits. Hence, contribution from water-soluble organic ions to the anion deficiency is expected to be insignificant. Earlier studies reporting chemical data from the Indian region have attributed the anion deficiency to the lack of

measurement of bicarbonate (HCO_3^-) ion in the chemical composition (Kulshreshtha et.al, 1998; Momin et.al, 1999; Venkatraman et.al, 2002).

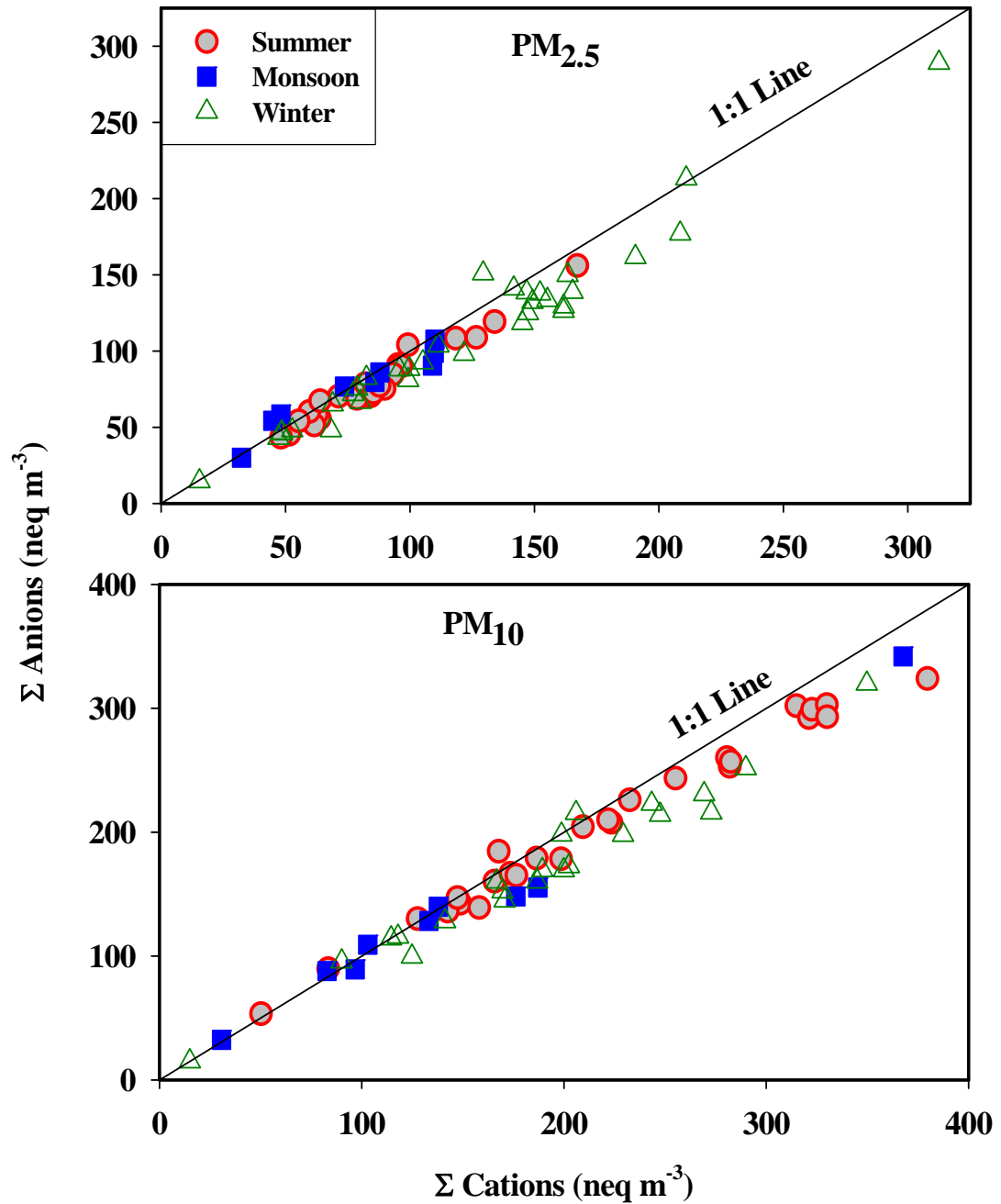


Fig. 2.10. Charge balance between $\Sigma \text{Cations}$ and ΣAnions in the $\text{PM}_{2.5}$ and PM_{10} representing the quantitative characterization of water-soluble-ionic-composition (WSIC) during the three sampling seasons

In the present study, HCO_3^- ion was independently measured in the water extracts of aerosols and included in the summation of anions for the charge balance. The measurement of HCO_3^- ion is very important for the study of aerosols collected from semi-arid region as it contributes significantly to water-soluble extract (Rastogi and Sarin, 2005b). Contributions from F^- and NO_2^- to the anion budget have been observed at few locations (Li, S.M., 1994; George et al, 2008), however their concentrations were found to be below detection limits in our analysis.

2.4.3.3. *Crustal elements:*

The concentrations of crustal elements (Al, Fe, Ca, and Mg) were analyzed using Inductively Coupled Plasma – Atomic Emission Spectroscopy (ICP-AES). The newly procured ICP-AES (JobinYovn, ULTIMA-2) was successfully installed during this thesis study. It is used for the detection of major and trace metals in environmental samples (e.g aerosols, ground water, sediments). The ICP-AES instrument consisting of a high temperature ($\sim 10,000$ K) excitation source (Ar plasma) that efficiently desolvates, vaporizes, excites and ionizes atoms generates atomic and ionic emission lines of specific wavelength. Detailed descriptions about the various components have been described in Potts, (1992). A brief description of the ICP-AES system used in this study is as under.

(a) *Torch Assembly:* The glass torch is in the form of three concentric glass tubes, upper part of which is surrounded by the radiofrequency (rf) work coil. The torch assembly is designed to deliver gases so that, a stable argon plasma is formed at the open end through which sample aerosol can be injected. Being chemically inert, Argon has been selected as plasma gas, as it suppresses the chemical interferences when sample solutions are atomized in the plasma. It is optically transparent in the uv-visible region and having low thermal conductivity ($17.72 \times 10^{-3} \text{ W} \cdot \text{m}^{-1} \cdot \text{K}^{-1}$ at 300 K) and high ionization energy (15.75 eV), makes Argon as a suitable choice to be used as a plasma source. In this study, Fassel torch has been used with outer tube having an internal diameter of 18mm. Argon is also used as a carrier gas and sample aerosols are injected into the plasma

through the intermediate tube. A small flow of argon is used (1.5 L/min) to lift the plasma off the injector, preventing overheating of the glass capillary. The Fassel torch is designed to form stable toroidal plasma through the centre of which sample aerosols can be injected.

(b) *Work coil radiofrequency*: The work coil consists of three turns of copper tube down the centre of which passes cooling water. The copper coil is wrapped around the outer tube of the torch and connected to an rf power generator. The argon gas is seeded with electrons from a Tesla coil which are subjected to intense oscillation by the radiofrequency magnetic field generated by the work coil. The free electrons collide with argon atoms causing further ionization. The charged particles under the influence of magnetic field travel in closed annular paths causing ohmic heating of the gas. Consequently, plasma temperature rises rapidly to a maximum of 10,000K. The efficiency with which power is delivered to the plasma depends on the electrical coupling between work coil and argon gas. The impedance between the two is carefully matched so that the electrical oscillator properties of plasma and work coil are tuned to ensure maximum power transfer. The radiofrequency at which the torch operates is also an important parameter in sustaining plasma operation. The instrument used in present study is equipped with crystal-controlled rf generator operating at 27.12 MHz delivering a power up to 1 KW to the plasma.

(c) *Monochromator system*: The ICP-AES ULTIMA-2 used in this study is equipped with a Czerny-Turner monochromator of 1 m focal length and 3600 grooves/mm holographic grating. The incident light from the plasma source are collimated by a concave mirror (the *collimator*), and the diffracted light is focused by a second concave mirror (the *camera*). Ideally, since the grating is planar and classical, and used in collimated incident light, no aberrations are expected to be introduced into the diffracted wavefronts. The spectrum is scanned by rotating the grating (mounted on a stepper motor). The grating is moved to normal relative to the incident and diffracted beams, which changes the wavelength diffracted toward the second mirror. As the light incident on and diffracted by the grating is collimated, the spectrum remains at focus at the exit slit for each wavelength, monitored by a photomultiplier detector.

The analyses of major crustal elements (Al, Fe, Ca and Mg) were performed by sequential scanning of the emission lines at 396.152, 240.488, 393.366 and 279.553 nm respectively. The emission signal recorded for these elements are shown in Fig. 2.11.

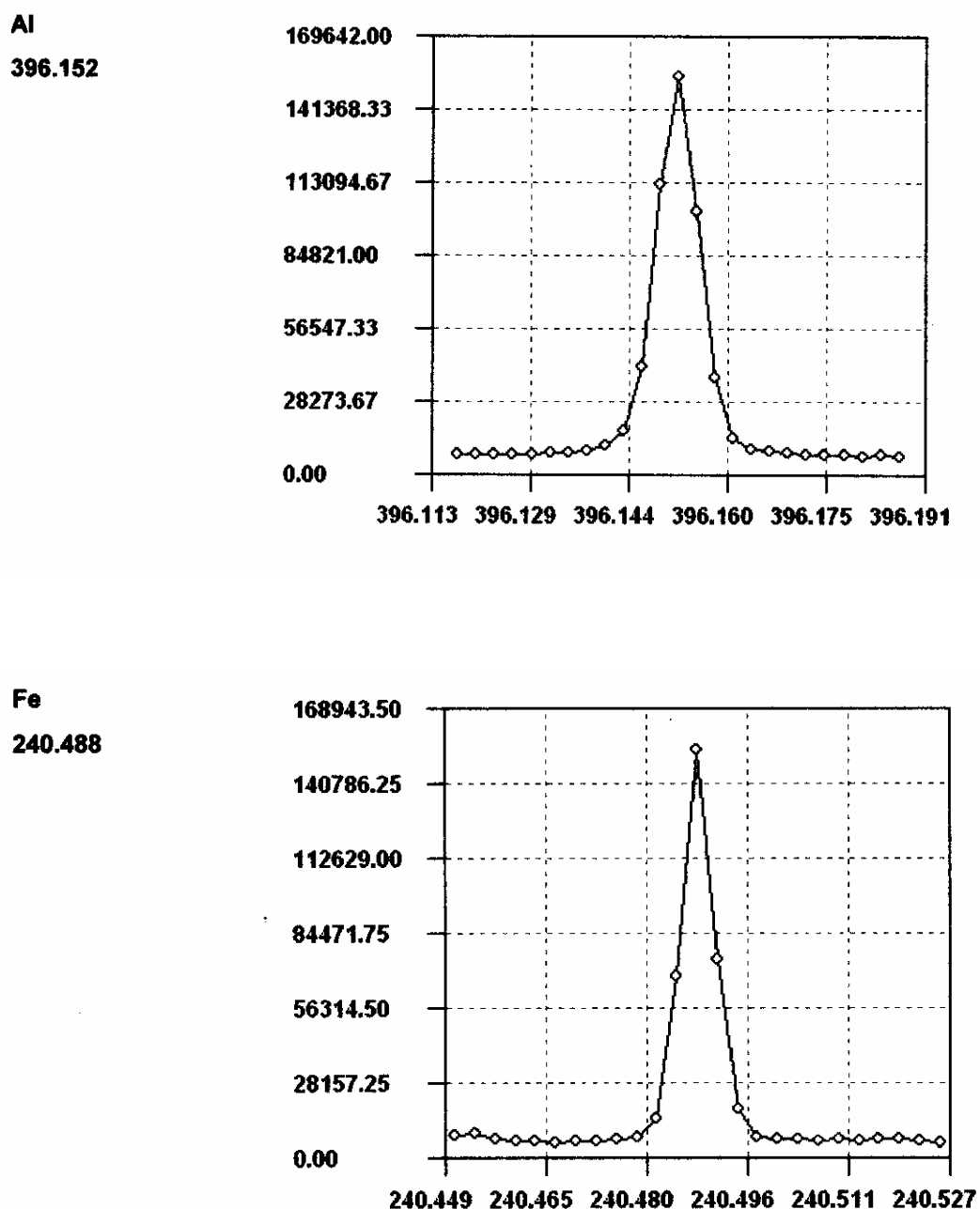


Fig. 2.11 (a) Emission intensities measured for the elements (Al and Fe) during sequential scanning of emission lines.

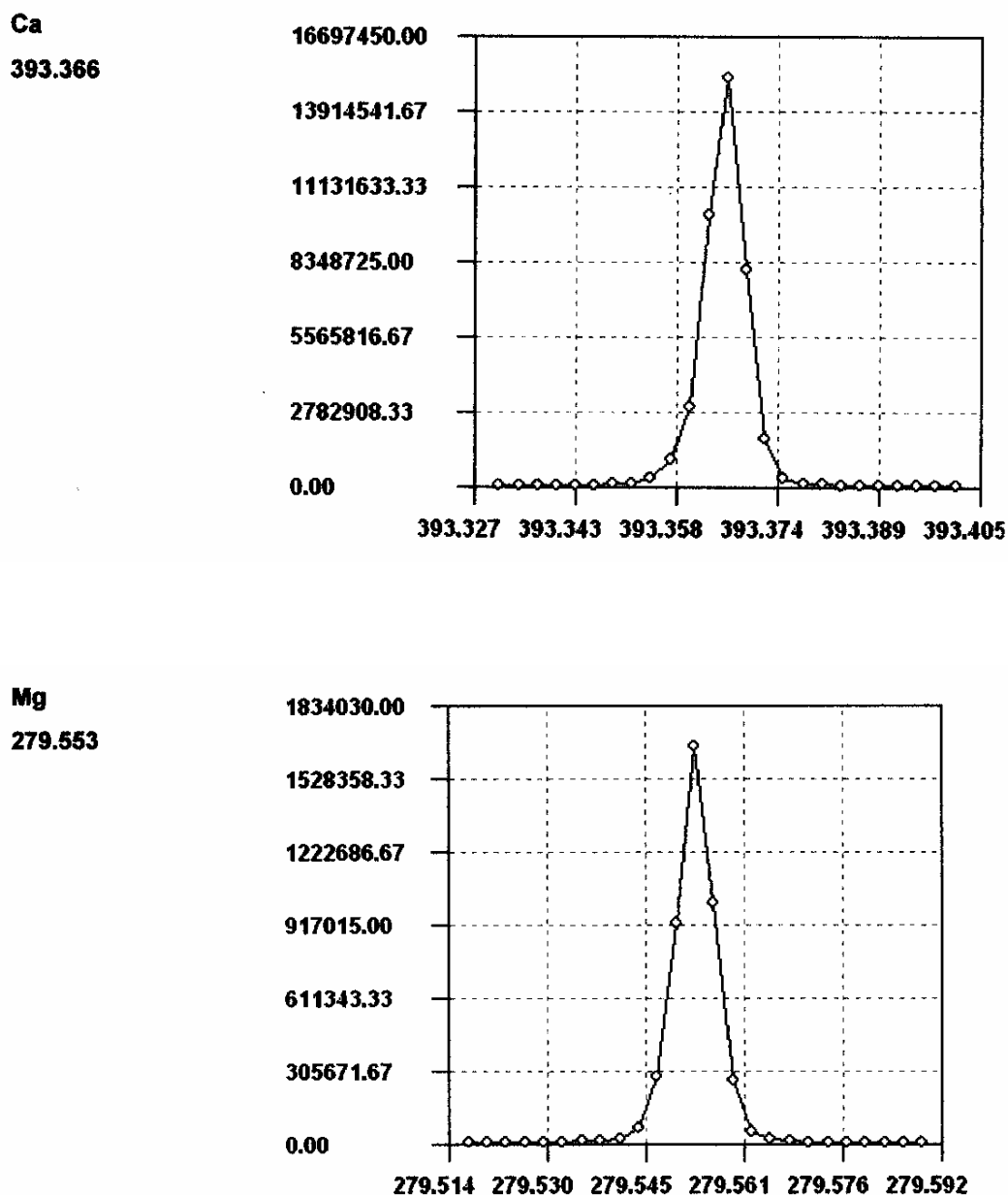


Fig. 2.11 (b) Emission intensities measured for the elements (Ca and Mg) during sequential scanning of emission lines.

The optical resolution, assessed based on full width half maximum (FWHM) of the emission spectrum of Cobalt line at 228.616 nm, was found to be less than 0.004 nm. In addition, the optical resolutions have been also calculated using the emission spectrum of four elements (Al, Fe, Ca and Mg) based on FWHM

observed for these elements as summarized in Table-2.3. The resolutions for all the elements at different wavelength are better than 0.006 nm suggesting the high sensitivity of the instrument to separate the two close-by emission lines. Independently, Mg was also measured on Flame-AAS to check the accuracy of analytical measurements with those of ICP-AES.

Table 2.3 Optical resolution of acid-soluble species on ICP-AES.

Element	Wavelength (nm)	Optical resolution*
Al	396.152	0.006
Fe	240.488	0.006
Ca	393.366	0.006
Mg	279.553	0.005

**Optical resolution is assessed based on FWHM of emission lines of each elements*

A commercial standard (Merck[®], 23 elements) was used for the instrument calibration and making linear analytical curves between element concentrations and emission intensities measured on ICP-AES (Fig. 2.12). The concentrations of crustal elements were corrected for procedural blanks (comprising of blank filters and analytical reagents; Table-2.4). Based on blank concentrations and average volume of air filtered (~800 m³), the detection limits for the elements were ascertained (90, 90, 25, and 40 ng m⁻³ for Al, Ca, Fe and Mg respectively). The reproducibility in the analytical data for the measured concentration is within 10% based on the repeat analysis of a number of samples and standards. The precision of measurements for all acid-soluble species in aerosol samples was assessed and results are shown in Fig. 2.13.

Table 2.4 Filter blanks (including procedure blanks) for acid-soluble species.

	Al	Fe	Ca	Mg	Cd	Pb
Avg (µg/filter)	653.0	113.0	210.0	98.6	17.0	0.5
sd (µg/filter)	30.0	16.2	8.3	13.3	14.0	0.1

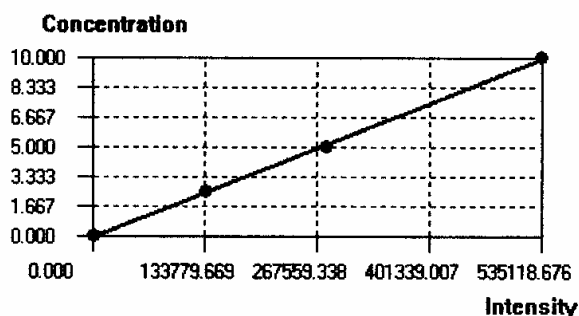
Standard	Net Intensity	RSD(%)	Conc.	Unit
std1	1805.98	85.79	0	mg/l
std2	135029.43	1.61	2.50	mg/l
std3	280035.25	0.94	5.00	mg/l
std4	535118.68	2.12	10.00	mg/l

Line: Al, 396.152 nm

Calibr. curve: $C = -0.07628 + 0.0000187 * I$

Parameters of curve

Sigma : 0.13229
 BEC : 76.3 µg/l
 LOD : ***
 Correl. : 0.99968
 Weight: 0.99968



#	Sample Name	Intensity	Chem. Conc.	Calc. Conc.	Rel. dev(%)	Valid
1.	std1	1805.98	0	-0.0425 mg/l		Yes
2.	std2	135029.43	2.50	2.45 mg/l	2.03	Yes
3.	std3	280035.25	5.00	5.16 mg/l	3.22	Yes
4.	std4	535118.68	10.00	9.93 mg/l	0.68	Yes

Line: Ca, 393.366 nm

Calibr. curve: $C = -0.06149 + 0.000000194 * I$

Parameters of curve

Sigma : 0.042963
 BEC : 61.5 µg/l
 LOD : ***
 Correl. : 0.99997
 Weight: 0.99997

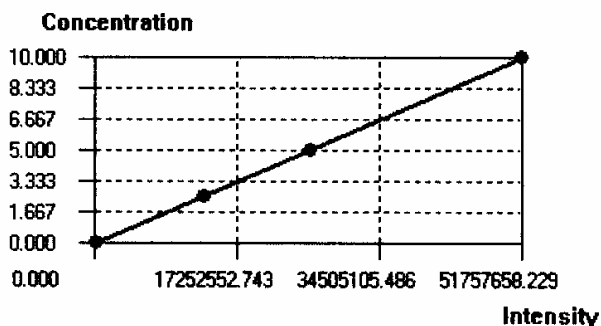


Fig. 2.12 (a) Calibration plot between emission intensities and concentrations for Al and Ca to calculate concentration of unknown samples.

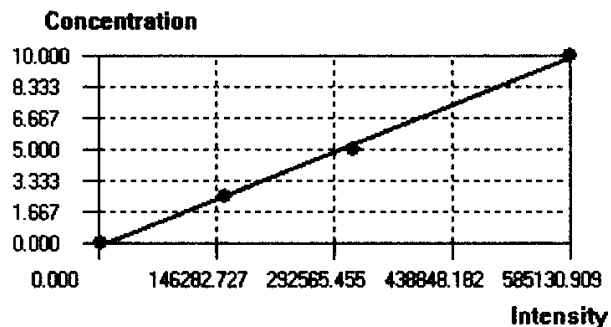
#	Sample Name	Intensity	Chem. Conc.	Calc. Conc.	Rel. dev(%)	Valid
1.	std1	127175.79	0	-0.0368 mg/l		Yes
2.	std2	13348878	2.50	2.53 mg/l	1.10	Yes
3.	std3	26263538	5.00	5.03 mg/l	0.65	Yes
4.	std4	51757658	10.00	9.98 mg/l	0.23	Yes

Line: Fe, 259.940 nm

Calibr. curve: $C = -0.1759 + 0.00001717 * I$

Parameters of curve

Sigma : 0.22302
 BEC : 176 µg/l
 LOD : ***
 Correl. : 0.99909
 Weight: 0.99909



#	Sample Name	Intensity	Chem. Conc.	Calc. Conc.	Rel. dev(%)	Valid
1.	std1	2541.15	0	-0.132 mg/l		Yes
2.	std2	156199.88	2.50	2.51 mg/l	0.24	Yes
3.	std3	316328.05	5.00	5.26 mg/l	5.11	Yes
4.	std4	585130.91	10.00	9.87 mg/l	1.29	Yes

Line: Mg, 279.553 nm

Calibr. curve: $C = 0.0426 + 0.0000001863 * I$

Parameters of curve

Sigma : 0.10544
 BEC : 42.6 µg/l
 LOD : ***
 Correl. : 0.9998
 Weight: 0.9998

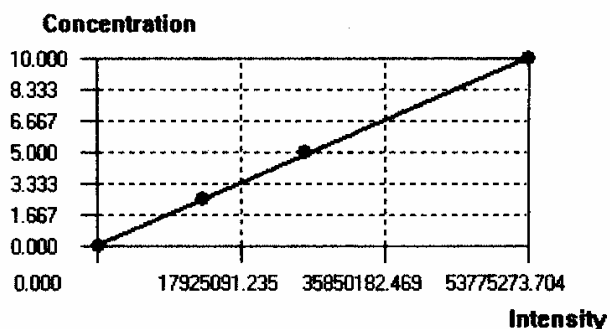


Fig. 2.12 (b) Calibration plot between emission intensities and concentrations for Fe and Mg to calculate concentration of unknown samples.

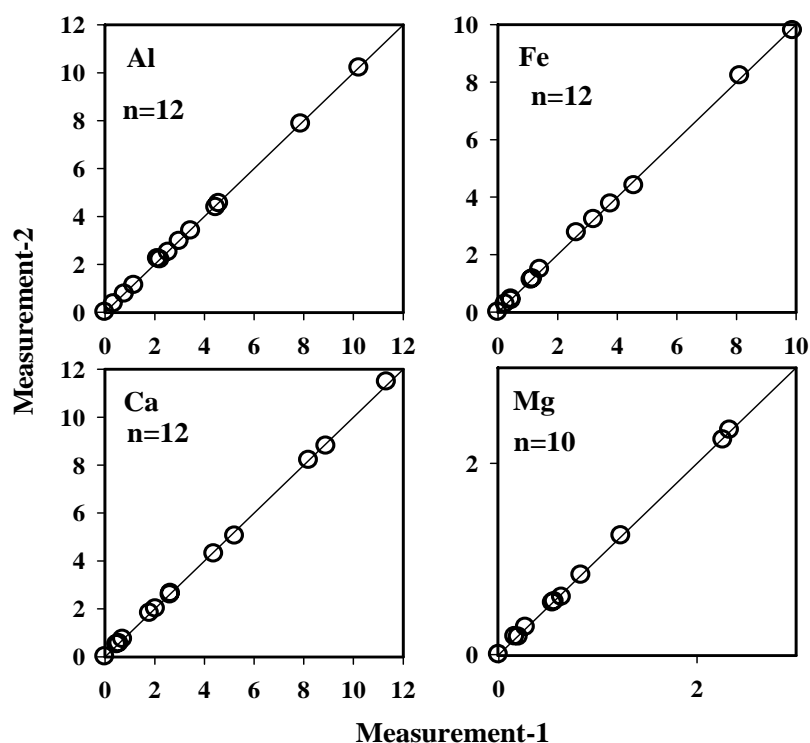


Fig 2.13 Repeat measurements of the crustal component (mg L^{-1}) in complete digested (acid soluble) aerosol samples. Solid lines represent 1:1 correspondence between the data.

2.4.3.4 Water-soluble Fe and Trace-elements:

The water-soluble iron (WS-Fe) and trace elements (Cd and Pb) were measured on Graphite Furnace-Atomic Absorption Spectrometer (GFAAS, Perkin-Elmer AAS, AAnalyst 100 coupled to a Graphite Furnace, HGA 800). The basic components of an atomic absorption spectrophotometer consist of light source, atomizer, photometer, monochromator and detector. An atom absorbs light of a specific wavelength (referred as resonance wavelength). In order to measure this narrow light absorption with maximum sensitivity, it is necessary to use a line source, which emits the specific wavelengths to be absorbed by an atom. The two most common line sources used in atomic absorption are the hollow cathode lamps (HCL) and electrodeless discharge lamps (EDL). In the present study, HCL is used as light source in GF-AAS in conjunction with a double-beam photometer configuration. In this configuration, single light beam from lamp is divided into a “sample beam” (directed through the sample cell) and

a “reference beam” (through the graphite tube). The reference beam serves as a monitor of lamp intensity and response characteristics of common electronic circuitry. Therefore, the observed absorbance, determined from a ratio of sample beam and reference beam readings, is free from effects due to drifting lamp intensities and other electronic noise. The Czerny-Turner Design is used as a standard monochromator to avoid excessive light loss. Light from the source enters the monochromator at the entrance slit and is directed to the grating where dispersion takes place. The diverging wavelength of light is then directed toward the exit slit. The high dispersion gratings are most widely used in the commercial atomic absorption instrument.

In atomic absorption graphite furnace, a small volume of sample solution is quantitatively placed into the tube, through a sample injection hole located in the centre of the tube wall. The tube is heated through a programmed temperature sequence until finally the analyte present in the sample is dissociated into atoms for the atomic absorption to occur. As atoms are created and diffuse out of the tube, the absorbance rises and falls in a peak shaped signal. The peak height or integrated peak area is used as the analytical signal for quantification. The volume of sample placed into the furnace and heating parameters can be controlled and optimized for each step. These steps include: 1) drying; 2) pyrolysis; 3) cool down; 4) atomization; 5) clean out; 6) cool down. A typical graphite furnace program is illustrated in Fig. 2.14. During the measurement of all three species (WS-Fe, Cd and Pb), recommended analytical and instrument settings were used. The detailed analytical settings and wavelength used for three elements have been tabulated in Table-2.5.

Table- 2.5: Analytical conditions for the analysis of elements in GF-AAS.

Element	Wavelength (nm)	Drying Temp (°C)	Ramp (Sec)	Charring Temp (°C)	Atomization Temp (°C)
Cd	228.8	120	120	700	1600
Pb	283.3	120	100	800	1800
Fe	248.3	120	100	1200	2300

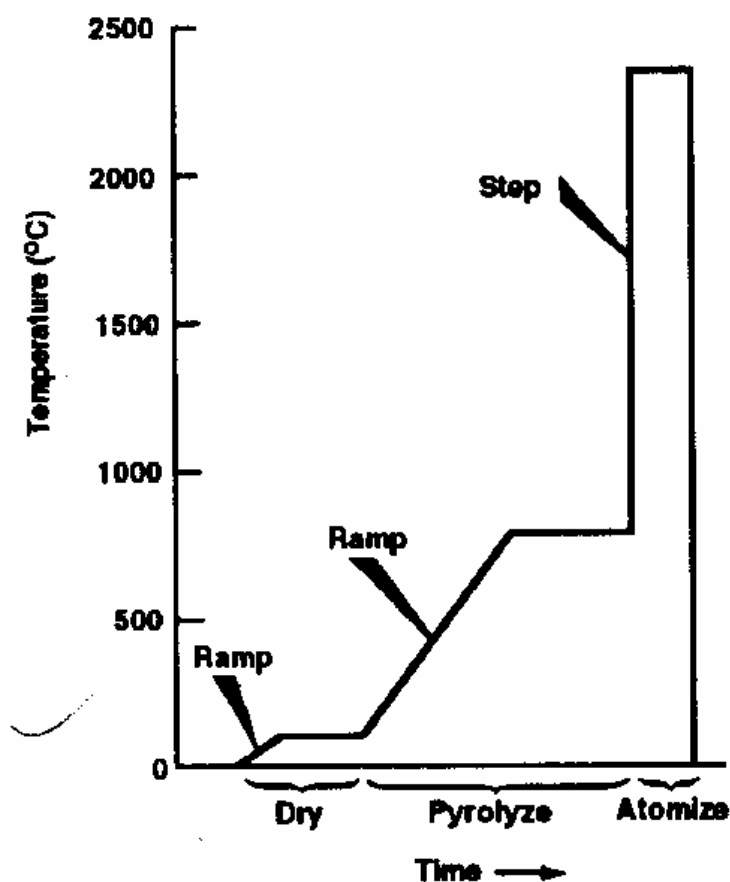


Fig. 2.14 A graphite furnace typical temperature programme.

Commercial standards (Merck®, 23 elements) were used for calibration of Fe, Cd and Pb. Based on repeated analyses of number of samples and standards, reproducibility of Fe, Cd, and Pb are 5%. In addition, standard addition method was adopted for the determination of Fe, Cd and Pb on GFAAS to further ascertain the accuracy of the measurements. The difference between the expected and measured concentrations of Cd and Pb were found to be within the analytical uncertainty limits as shown in Fig. 2.15. Filter blanks (inclusive of procedure blanks) were also ascertained for these species as tabulated in Table 2.4. These values are less than 5% of the minimum concentration collected on filters for all species. Pb concentrations in filter blank were very low ($\sim 5 \text{ ng mL}^{-1}$) or below detection limit (0.3 ng mL^{-1}).

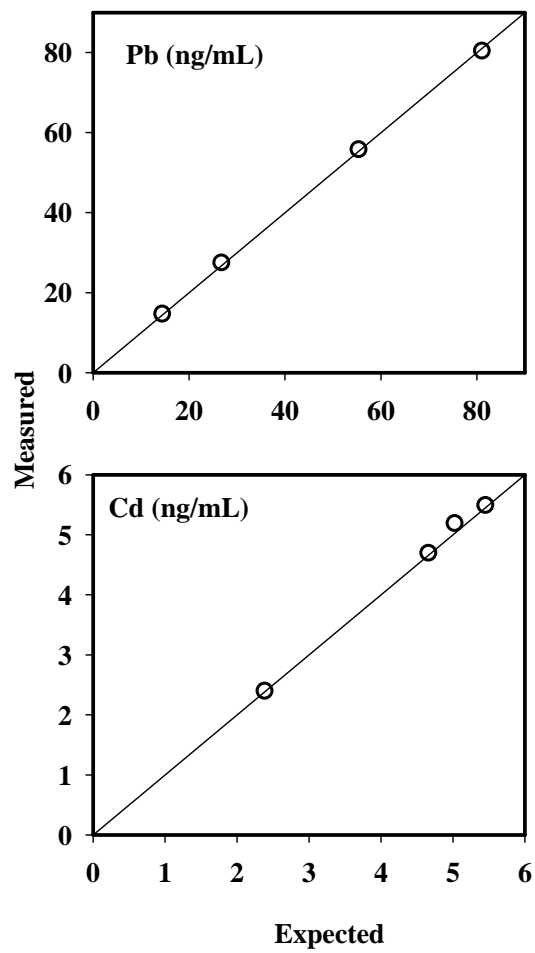


Fig 2.15 Standard addition method to check the matrix effect on the concentrations of Pb and Cd on GF-AAS.

Chapter 3

ELEMENTAL CHARACTERISTICS OF MINERAL DUST

3.1. Introduction:

The atmospheric mineral dust, representing largest component of continental aerosols by mass (1000-2150 Tg yr⁻¹) (Zender, 2004), has potential to impact global atmospheric chemistry, cloud properties and precipitation development (Dentener et al, 1996; Levin et al, 1996; Tegen et al, 1996, Arimoto, 2001; Tang et al, 2004a, b; Laskin et al, 2005; Rastogi and Sarin, 2005a; Rastogi and Sarin, 2006). The soil derived particles encompass wide range of size, ranging from less than 0.1 µm to 100 µm diameter (Prospero et al, 1983). The coarser particles get deposited near the source regions, whereas long-range transport of fine mode particles (0.1 to 10 µm) is of utmost relevance in the marine atmospheric boundary layer (Arimoto et al, 1995, Kumar et al, 2008a, b). Mineral dust is typically considered as having a “coarse mode” type of distribution, contributing significantly to the total mass of global aerosols; however, dust particles are also found in the accumulation mode (<2.5 µm) which provides conducive surface area for the heterogeneous phase atmospheric chemistry.

The fine mode dust particles on interaction with atmospheric gaseous and secondary species undergo changes in chemical composition and can, thus, alter the optical and radiative properties of aerosols. For example, alteration of calcium carbonate mineral increases the hygroscopicity of dust through chemical reactions with HNO₃ and H₂SO₄ ; subsequently enhancing its ability to act as cloud condensation nuclei (CCN) and, thus, influencing the indirect climate forcing. The atmospheric dust has potential to enhance precipitation formation over continents

by accumulating coarse CCN, forming large size droplets with high coalescence efficiency (Yin et al, 2002). On the contrary, mineral aerosols could suppress precipitation efficiency through increase in the number density of CCN, further leading to formation of small size droplets with poor coalescence efficiency (Rosenfeld et al, 2001). The mineral aerosols also exhibit large temporal and spatial variabilities in the chemical composition giving rise to varying degree of physical and chemical interactions with variety of gaseous pollutants and organic species (Usher et al, 2003). For example, the kinetics of the oxidation of SO₂ and NO₂ in the atmosphere may be enhanced by mineral surfaces mediated via coating of organic material. Recently, Sullivan et al, (2007), have reported their observation on the preferential accumulation of nitrate on calcium rich dust compared to sulphate accumulation on alumino-silicate rich dust. Furthermore, mineral dust in different size fractions has characteristically different chemical composition. The regional and temporal scale studies are, thus, essential to assess the physico-chemical properties of mineral aerosols and their potential role in atmospheric chemistry and the direct/indirect impact on climate.

In this chapter, a comprehensive data set on temporal variability of mineral dust in coarse and fine mode fractions and its elemental composition based on samples collected from a high-altitude site (Mt. Abu) located in a high-dust semi-arid region of western India has been discussed. The detailed study involving use of elemental ratios as diagnostic tracers, in conjunction with meteorological parameters, is very timely and by far such data are poorly documented in the literature, especially for south-Asian region.

3.2. Results and Discussions:

3.2.1 Temporal variability in fine and coarse mode aerosol mass concentrations:

The temporal variation in the mass concentration of coarse and fine mode aerosols is shown in Fig. 3.1(a); each data point represents the aerosol mass abundance on a particular day of sample collection. The analytical data has been split into three seasons, summer (Mar-Jun; Day of Year [DOY]: 59-181), monsoon (Jul-Sep; DOY: 182-273) and winter (Oct-Feb; DOY: 182-273, 1-58), based on the prevailing meteorological conditions over the study site. The

maximum, minimum, mean and median concentrations of aerosol mass along with elemental composition in coarse and fine mode have been summarized in Table 3.1. Over the annual seasonal cycle, concentration of coarse mass ($PM_{10-2.5}$) varied from 2.3 to $102 \mu\text{g m}^{-3}$ (Table 3.1); the relatively low concentration occurring during the winter and monsoon seasons and higher abundance in the summer months. Under the influence of moderately high winds and convective mixing during summer, mineral dust derived from the disturbed soils is lifted in the atmosphere. The sampling site, being located in a semi-arid region, the evolution of dust in the atmosphere is perennial and influences the coarse mass. The well marked transition period between north-east and south-west winds, during March and April (beginning of summer season), exhibits relatively high abundance of aerosol mass (33.1 ± 18 and $37.7 \pm 13 \mu\text{g m}^{-3}$; Fig. 3.2a). With advancement of summer, coarse mass further increases to 52.1 ± 19 and $41.4 \pm 34 \mu\text{g m}^{-3}$ (Fig. 3.2a) in May and June respectively. The back trajectory analysis suggests that winds during summer time transport dust from the Thar Desert located in the western India and as far as from coast of Oman.

The fine aerosol mass ($PM_{2.5}$) ranged from 1.6 to $46.1 \mu\text{g m}^{-3}$ over the annual seasonal cycle (Fig. 3.1a; Table 3.1). During winter months, the prevailing north-easterly winds transport anthropogenically derived chemical species from the northern India to the sampling site. A variety of small scale industries (leather, textile, and sugar mills), wide-spread biomass burning (wood fuel, cow dung and agricultural waste) and fossil fuel combustion make the northern region an important source of anthropogenic sulphate, nitrate, ammonia, soot and organics. The abundance of fine aerosol mass is relatively low compared to the coarse mass; however, somewhat comparable in winter season. During monsoon season (Jul, Aug and Sep), atmospheric aerosol abundance is influenced by the two processes: 1) wet removal, and 2) hygroscopic growth of particles in presence of high moisture conditions. The former favours the removal of coarser particles leading to enhancement of fine aerosol concentration. The second process facilitates the fine particles to grow and, thus, enhances the number density of coarse particles. The comparative mass concentrations of both fine and coarse

mode aerosols, during monsoon, could be explained in terms of these two processes.

The temporal variability in mass fractions of fine and coarse mode particles (expressed as ratio of fractional mass concentration of respective size to total PM_{10} mass) at the high altitude sampling site, together with the average wind speed on a particular sampling date, is summarized in Fig. 3.1 (b), (c). It is noteworthy that during the winter months (Jan, Feb, Nov and Dec), characterized by moderate wind speed, relative contribution of each mass fraction to the total aerosol abundance is comparable. In contrast, during summer months, contribution of coarse mass fraction is characteristically significant (Fig. 3.1 b). This is interpreted in terms of enhanced contribution of mineral dust particles from desert regions of Thar and Oman associated with favourable winds during summer. During wintertime, the long-range advective transport of aerosols from polluted regions of northern India increases the mass abundance of fine fraction ($PM_{2.5}$). In general, mass fraction of submicron aerosols shows dependence on the wind speed during wintertime (Fig. 3.1 b). These observations further support our contention that the selection of a high altitude site is advantageous to study the long-range transport of aerosols and their regional climatic impacts.

3.2.2 Temporal variability of mineral dust over western India:

The temporal changes in wind regimes (Fig 2.3; chapter 2) at the sampling site suggest the predominance of dust sources from the Thar and Arabian deserts during summer months and from the Indo-Gangetic Plain during winter months. In order to characterize and quantify the abundance of atmospheric mineral dust, we have used Al as a diagnostic tracer of crustal origin. It is implicit in such an approach that contribution of Al from anthropogenic sources (metal industries) is insignificant compared to its crustal source. The linear-regression analyses among the crustal elements (Al, Fe, Ca, and Mg) have been discussed in later section. Using abundance of Al as an index of mineral dust, its mass fraction in the ambient aerosols has been estimated (assuming 8.04 % of Al as a composition of upper continental crust; [McLennan, 2001; Rastogi and Sarin, 2006]). Fig. 3.2 (b) summarizes the results on the mass fraction of dust in the fine ($PM_{2.5}$) and coarse

(PM_{10-2.5}) mode. It is evident that coarse fraction is dominated by crustal dust through out the year; with fractional contribution varying from 60 to 80 %. The lowest value is observed during the month of June, when prevailing winds are south-westerly (maritime air-mass) leading to the increased abundance of sea-salts in the coarse mode. In contrast, abundance of dust in fine mode shows a large variation ranging from 11 to 75 %. The contribution of fine dust is maximum during April and steadily decreases through the monsoon and post-monsoon months (Sep-Dec; Fig 3.2 b).

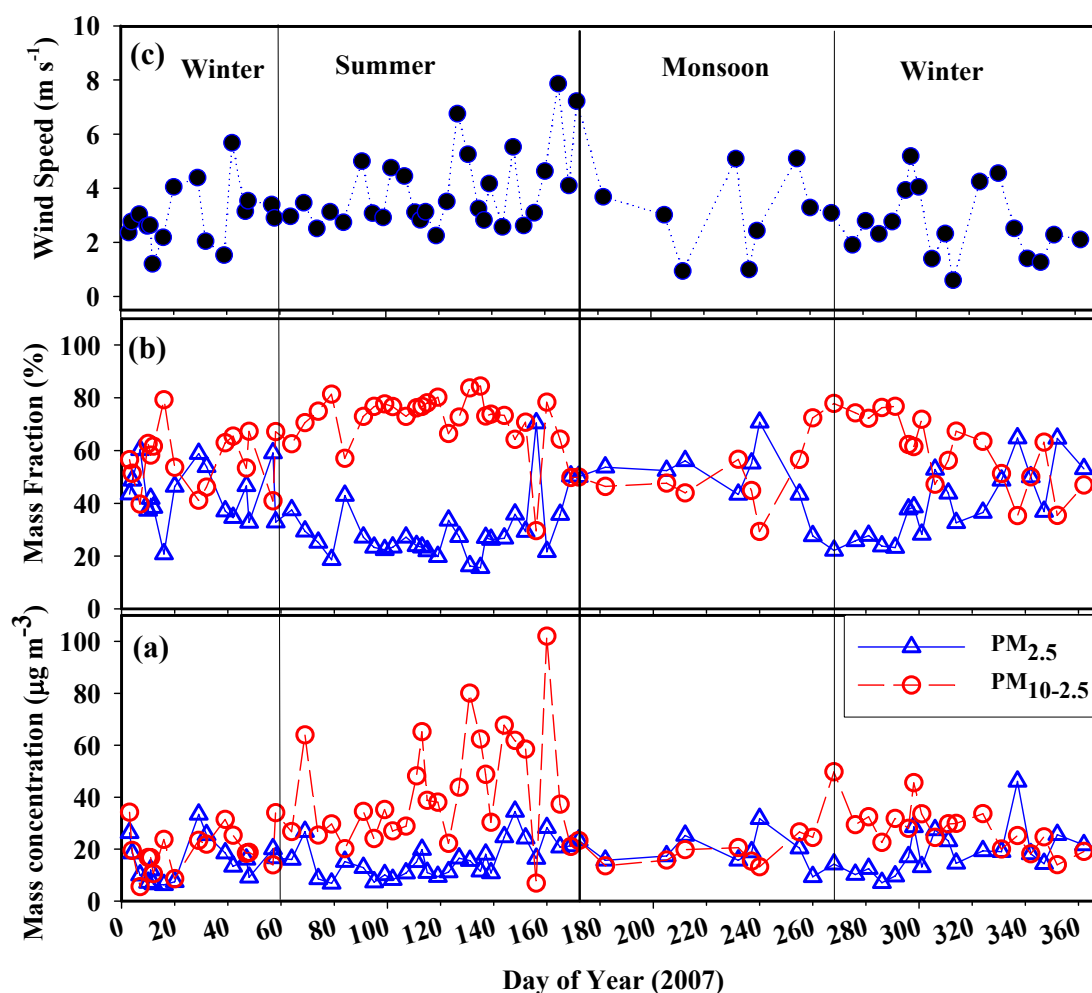


Fig. 3.1 (a) Temporal variability of aerosol mass concentration in coarse (PM_{10-2.5}) and fine mode (PM_{2.5}), (b) Contribution of coarse and fine mass to total (PM₁₀) mass loading, (c) Daily average wind speed on sampling dates.

Table 3.1: Minimum, maximum, mean and median concentrations ($\mu\text{g m}^{-3}$) of crustal elements in fine ($\text{PM}_{2.5}$) and coarse ($\text{PM}_{10-2.5}$) mode aerosols in Summer (March - June), Monsoon (July – September) and Winter (October –February) seasons in 2007.

Fine	Summer				Monsoon				Winter			
	<i>Min</i>	<i>Max</i>	<i>Mean</i>	<i>Median</i>	<i>Min</i>	<i>Max</i>	<i>Mean</i>	<i>Median</i>	<i>Min</i>	<i>Max</i>	<i>Mean</i>	<i>Median</i>
Mass	6.8	34.5	16.2	15.3	9.4	31.7	18.7	17.3	1.6	46.1	16.9	16.3
Al	<0.09*	1.45	0.61	0.53	<0.09	0.82	0.31	0.28	<0.09	0.54	23.0	0.21
Fe	<0.02	0.91	0.40	0.37	0.03	0.49	0.19	0.20	<0.02	0.40	0.16	0.15
Ca	<0.09	1.30	0.51	0.44	<0.09	0.68	0.20	0.16	<0.09	0.57	0.20	0.18
Mg	<0.04	0.52	0.21	0.16	<0.04	0.32	0.14	0.13	<0.04	0.17	0.07	0.04
Coarse												
Mass	6.9	101.9	41.8	36.2	13.1	49.7	22.1	19.7	2.3	45.5	23.0	23.5
Al	0.16	6.04	2.4	2.01	0.47	3.96	1.37	1.10	0.09	3.28	1.38	1.31
Fe	0.11	3.56	1.46	1.25	0.32	2.35	0.80	0.64	0.10	1.98	0.86	0.84
Ca	0.16	9.94	3.34	2.81	0.25	5.42	1.66	1.50	<0.09	3.29	1.59	1.55
Mg	<0.04	2.91	0.96	0.76	0.13	1.45	0.44	0.39	<0.04	0.96	0.44	0.41

*Detection limit for Al, Fe, Ca, and Mg are 0.09, 0.02, 0.09, and $0.04 \mu\text{g m}^{-3}$ respectively.

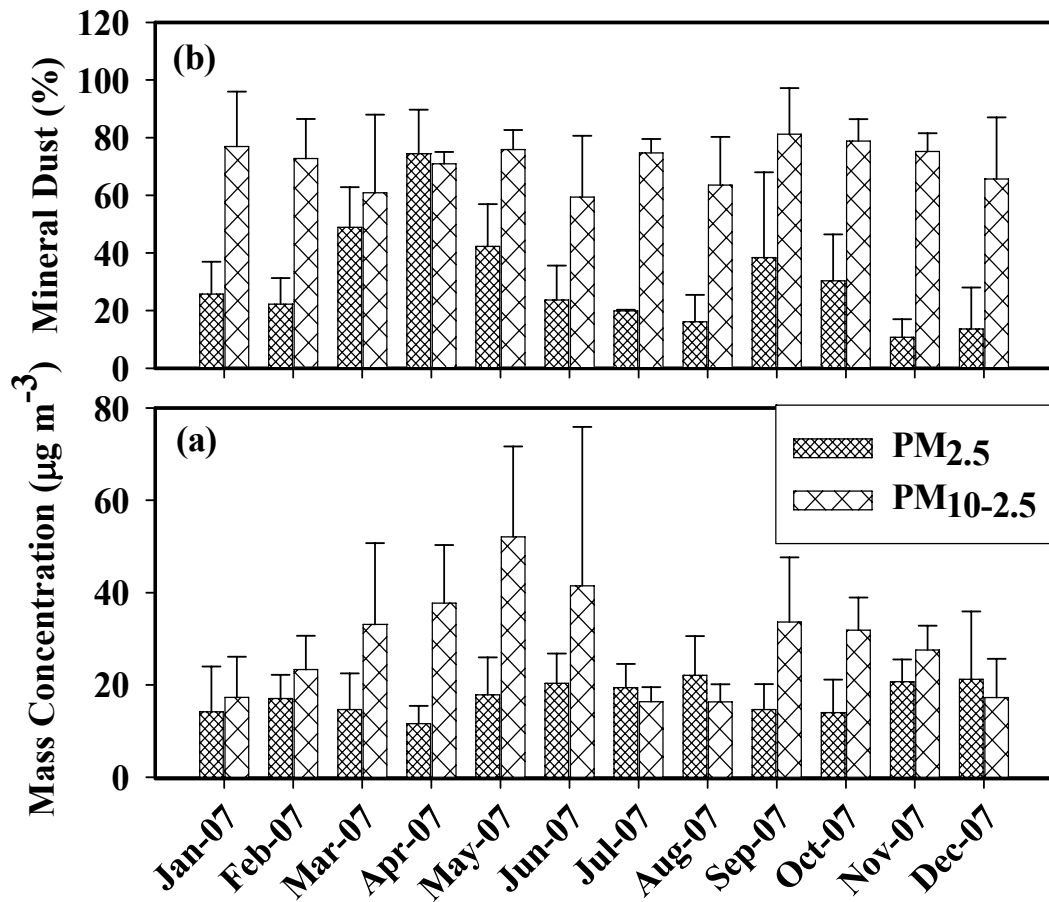


Fig. 3.2 (a) Monthly average mass concentration of PM_{2.5} and PM_{10-2.5} at sampling site during 2007. (b) Contribution of dust in coarse and fine mode indicating the dominance of dust in coarse mode throughout the year.

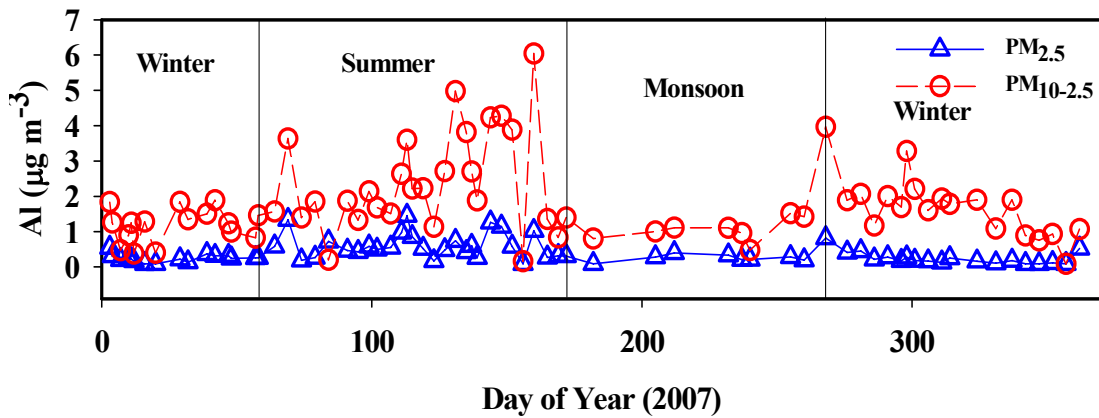


Fig. 3.3 Temporal variation of Al content (representative of dust) in PM_{2.5} and PM_{10-2.5} over the study site.

During winter months, dust contribution in the fine mode is also relatively low; indicating that ambient atmospheric aerosol loading is dominated by long-range transport of anthropogenic species under favourable NE-winds.

Rastogi and Sarin, (2006), had documented temporal variability in the abundance of dust (Range: 57 to 81 %) based on the bulk samples collected from an urban site, (Ahmedabad, 23.0 °N, 72.6 °E, 49 m asl) located in a semi-arid region of western India. A significant covariance among TSP and the abundance of dust is a conspicuous feature of the data from this urban location. However, such relationship is not observable for the size-segregated samples collected from Mt. Abu (Fig 3.2). The temporal variability in the abundance of Al in coarse mode (range: 0.09 to 6.04 $\mu\text{g m}^{-3}$) and fine mode (range: <0.09 to 1.45 $\mu\text{g m}^{-3}$) is presented in Fig. 3.3. During summer a synchronous increase or decrease is observed in the Al abundance of PM_{2.5} and PM_{10-2.5} fractions. However, during winter season (Jan, Feb, Oct-Dec); Al abundance is relatively low in both the size fractions; with concentrations approaching close to detection limit in the PM_{2.5}. In general, Al in coarse mode (Al_c) is consistently higher than that in the fine (Al_f) aerosol; except on 25th March (DOY: 84) when Al_f (0.72 $\mu\text{g m}^{-3}$) exceeds the Al_c (0.20 $\mu\text{g m}^{-3}$). The ratio of Al_f/Al_c ranged from 0.07 to 0.49 over the annual seasonal cycle (except on 25th March when the ratio = 3.56); with relatively narrow range of 0.11 to 0.40 during the summer season.

3.2.3 Elemental composition of atmospheric mineral dust over western India:

The concentrations of crustal elements (e.g. Al, Fe, Ca, Mg, Sc and Si) have general limitation to resolve the source regions of atmospheric mineral dust as none of the elements serve as a unique diagnostic tracer for a specific region; however, ratios of elements are more appropriate in decoupling the source regions. In this study, we have used a suit of crustal elements (e.g. Al, Fe, Ca and Mg) and their ratios for characterization of mineral dust as well as to decipher the temporal variability in the sources. A similar approach has been used for characterization of dust source regions in Africa (Chiapello et al, 1997) and in Asia (Zhang et al, 1996).

3.2.3.1 Iron:

On average, desert dust aerosols contain 3.5% iron (Duce and Tindale, 1991) primarily as insoluble ferric iron [Fe (III)] in the form of aluminosilicates (e.g. Zhu et al, 1997). At the sampling site, Fe concentration in the fine and coarse mode aerosols varied from 0.03 to 0.91 and 0.11 to 3.57 $\mu\text{g m}^{-3}$ (Table 3.1), respectively. The variability of Fe concentration in both the size ranges is linked to the prevailing meteorology (i.e. wind speed and direction); relatively high values occurring during summer and lower abundance in the winter season. The chemical alteration of insoluble Fe (III) to soluble Fe (II) in mineral aerosols, during long-range transport, is increasingly recognized as an important process (Jickells and Spokes, 2001; Mahowald et al, 2005; Luo et al, 2005; Fan et al, 2006). In addition to its dominant contribution from mineral dust, fossil-fuel combustion processes and biomass burning could serve as potential sources of atmospheric soluble iron (Chuang et al, 2005; Guieu et al, 2005; Luo et al, 2008).

The linear regression analyses performed on the abundances of Fe and Al in $\text{PM}_{2.5}$ and $\text{PM}_{10-2.5}$ (Fig. 3.4) reveals characteristic Fe/Al ratio in the mineral dust over western India. A significant positive correlation in the coarse ($r^2 = 0.98$) and fine ($r^2 = 0.96$) mode aerosols, during all seasons, suggest their conservative atmospheric transport. However, Fe/Al ratio varied from 0.47 to 1.21 and 0.45 to 1.13 in coarse and fine mode respectively. During their study over Canary Island, Bergametti et al, (1989), had reported an increase in Si/Al and Fe/Al ratios for the dust associated with source from Sahelian region compared to that originated from Morocco. Abundance of aerosol silica has not been measured in this study because of our choice of using tisuquartz filters for sample collection. Instead, Fe/Al ratio, derived for the annual and seasonal data provides useful information on source regions of mineral dust. The ratios of Fe/Al in $\text{PM}_{2.5}$ and $\text{PM}_{10-2.5}$ are presented in Fig. 3.5 as a scatter plot against the mass of mineral dust (derived based on Al abundance in respective size fractions). In majority of coarse mode samples ($\sim 90\%$), the Fe/Al ratio exhibit a narrow range (0.5 to 0.7) and seasonal variability is not significantly pronounced; except in few samples collected during winter months. In contrast, relatively large variation in Fe/Al (0.45 to 1.13, Fig. 3.5) ratio is observed for $\text{PM}_{2.5}$ samples. This large variability is associated with

characteristic lower abundance of dust (Fig. 3.2). Several of the PM_{2.5} samples in wintertime, under favourable north-easterly winds, exhibit higher Fe/Al ratio (greater than 0.70). These observations suggest that enriched Fe/Al ratios are characteristic of the fine mode aerosols from the source regions in northern India. The Fe/Al ratio in the surface soils of (as inferred from composition of river sediments) north Indian Plains ranges from 0.55-0.63 (Sarin et al, 1979). Such an observation suggests that contrary to the dust sources from northern India, dominant contribution of Fe from advective transport of pollutants (derived from fossil-fuel combustion processes and biomass burning) is a plausible mechanism for the relatively enriched Fe/Al ratio in PM_{2.5} during wintertime. In a recent study, Majestic et al, (2006), have indicated that combustion of fossil-fuel (in automobiles) releases iron in the fine mode (less than 1 µm; PM₁). The enriched Fe/Al mass ratio has been also reported for fuel oil fly ash and exhaust particle produced by diesel combustion (Desboeufs et al, 2005). Likewise, Chuang et al, (2005), has also demonstrated the significant contribution of particulate soluble Fe concentration from anthropogenic activity rather than atmospheric processing of aerosols during long-range transport in the East Asian outflow.

3.2.3.2 Abundances of calcium and magnesium in mineral dust:

The abundance of calcium and magnesium in mineral dust is typically represented as 2.9 and 1.3 %, respectively (Wedepohl, 1995). These elements are present as carbonate component of dust (e.g calcite (CaCO₃) and dolomite (Ca Mg (CO₃)₂)) which are relatively more reactive towards acid neutralization than alumino-silicate phase. Depending on the source region these carbonate components can comprise as much as 30% of total mineral aerosols (Claquin et al, 1999). The aerosol abundances of these two elements in the coarse and fine mode ranged as Ca: 0.11 to 10.04 and <0.09 to 1.31 µg m⁻³ and, Mg: <0.04 to 3.22 and <0.04 to 0.61 µg m⁻³ (Table 2), respectively. Their measured concentrations have been corrected for the contribution from sea-salts based on water soluble sodium abundance in the samples (Kumar et al, 2008b). The sea-salt contribution is found to be less than 5% and 15% for Ca and Mg respectively, except during monsoon seasons, when it is enhanced to 10% and 25% respectively. The linear regression

analysis of Ca and Mg, with Al in the two size fractions is shown in Fig 3.4. The Ca abundance in coarse fraction exhibits relatively high correlation ($r^2 = 0.85$) with Al than its abundance in fine fraction ($r^2 = 0.78$). Similar to abundance of Fe, a large scatter is observed in fine fraction (Fig. 3.4) due to relatively low abundance of dust during winter and monsoon seasons. Furthermore, chemical composition of aerosols shows an enrichment of calcium (Fig. 3.4) in contrast to crustal ratio of $\text{Ca/Al} = 0.38$ (Upper continental crust; McLennan, 2001). The linear regression plots of Mg with Al (Fig. 3.4) shows similar feature as Ca; with relatively high correlation with Al ($r^2 = 0.94$) in coarse mode than fine mode ($r^2 = 0.86$).

The scatter plots of Ca/Al and Mg/Al with abundance of dust (Fig. 3.5) provides further insight in to the temporal characteristics of mineral aerosols and their source regions. In coarse mode, (Ca/Al) ratio (for more than 80% of data) show significant scatters ranging from 0.6 to 1.5 (Fig. 3.5). However, in the fine mode, Ca/Al ratio is relatively low (0.38 to 1.2); and shows large scatter in samples with low abundance of dust. This comparison suggests relative enrichment of carbonate dust in coarse fraction compared to the fine mode; with higher values ($\text{Ca/Al} = 0.79$ to 2.19; Table 3.1) characteristics of summer months. Similar to Ca, enrichment of Mg is observed in the coarse fraction versus fine fraction (Fig. 3.4 and 3.5). A similar study on the enrichment of carbonates in coarse size fraction has been reported in the literature (Usher et al, 2003).

3.2.4 Inter-annual variability of elemental ratios

In the source region, intense dust storm activities are occurring and the dust particles are sustained in atmosphere for several days. This dust storm can induce significant changes in the dust characteristics and subsequently introduce large uncertainties in climate forcing (Christopher and Wang, 2004). In this section, the PM_{10} elemental ratios have been discussed in two subsequent years. A comprehensive comparison has been done for the elemental ratios during high dust (April-June) and low dust conditions (September – December). The temporal variability of crustal element ratio (Fe/Al , Ca/Al and Ca/Mg) during high and low dust condition (shaded region) is shown in Fig. 3.6. The Fe/Al ratio for PM_{10} is

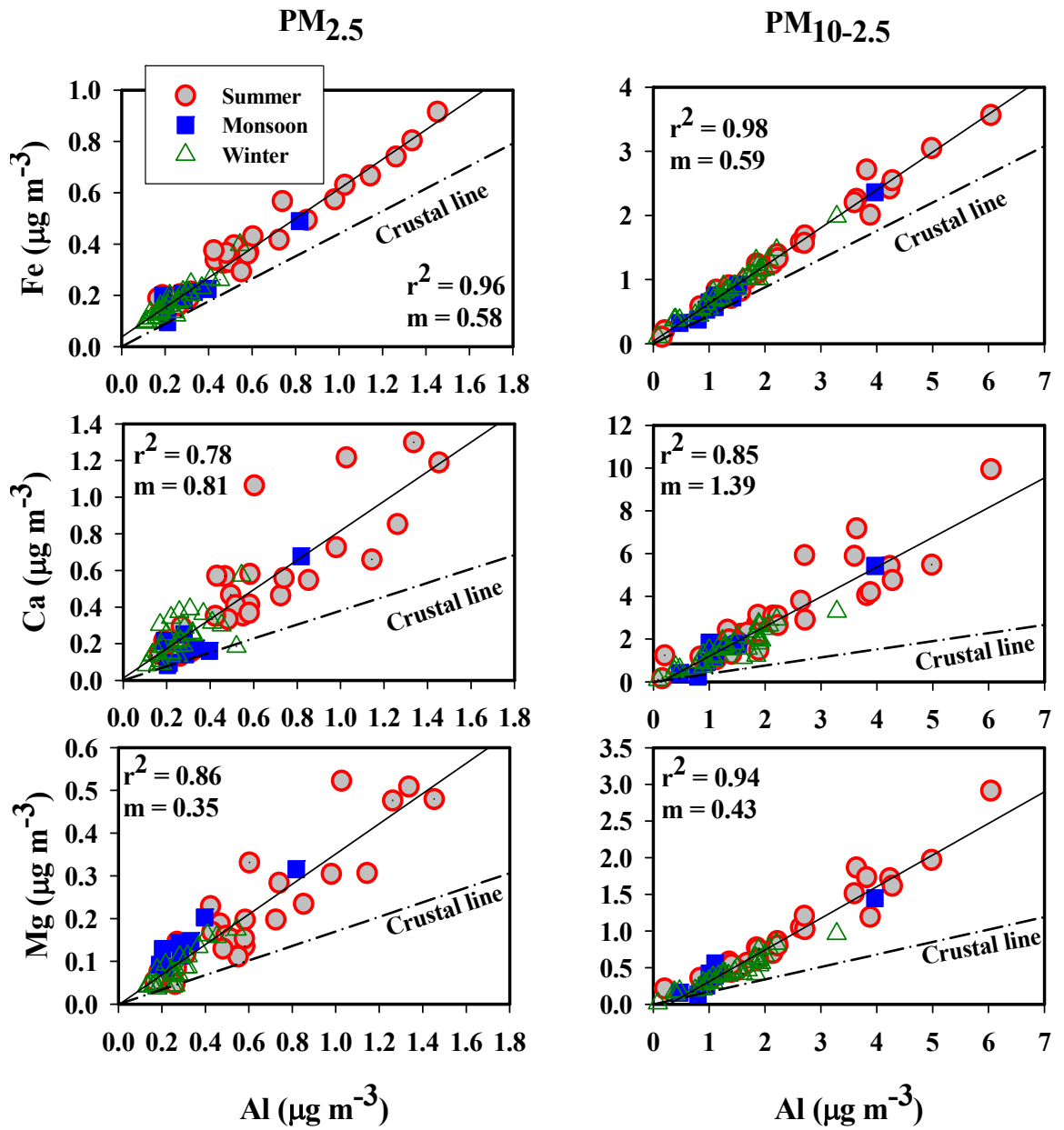


Fig. 3.4 Scatter plot of concentration of crustal elements Fe, Ca, and Mg with respect to Al in coarse and fine mode aerosol.

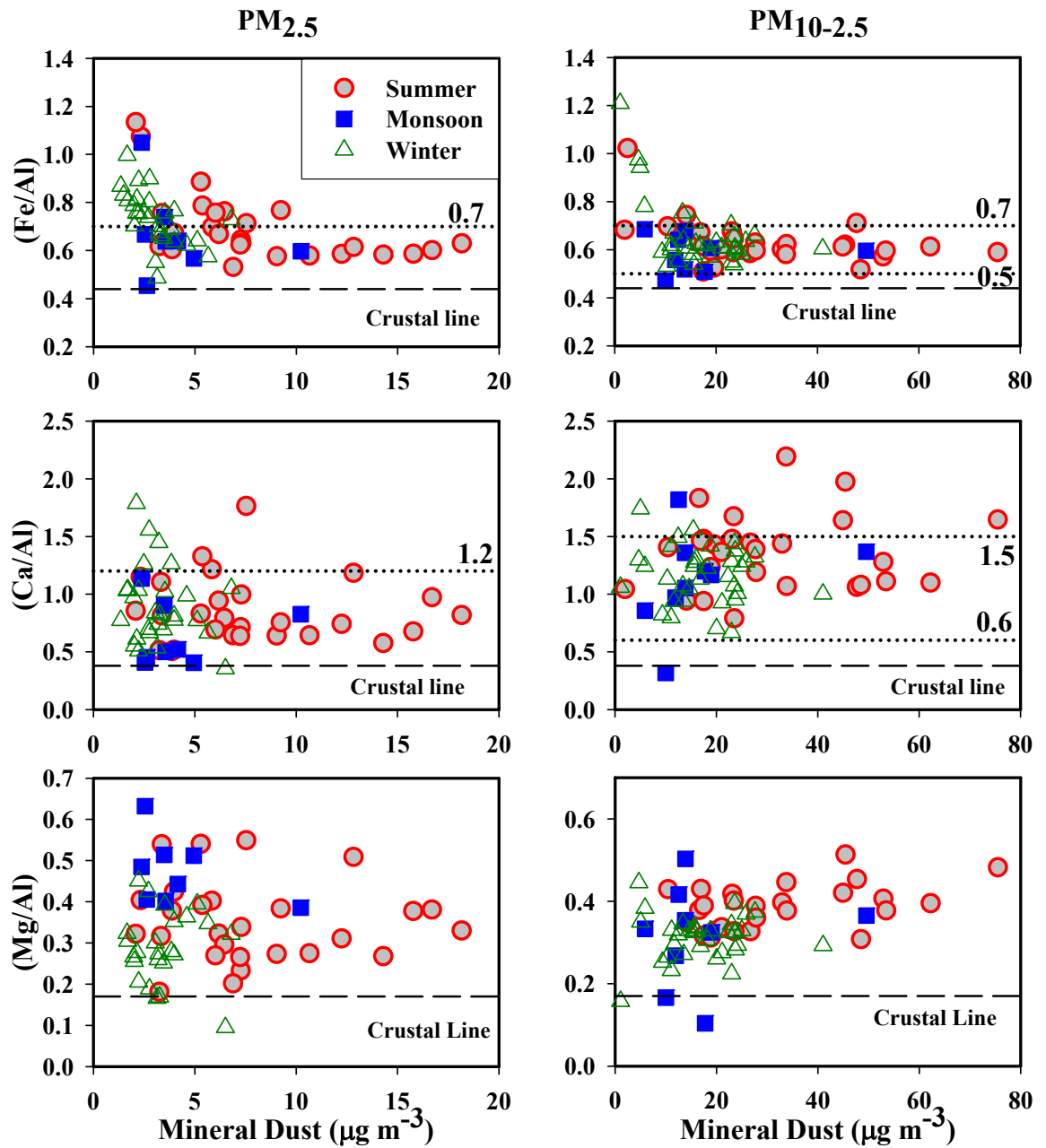


Fig. 3.5 Scatter plot of different elemental ratio against estimated dust concentration (based on Al) in fine and coarse mode.

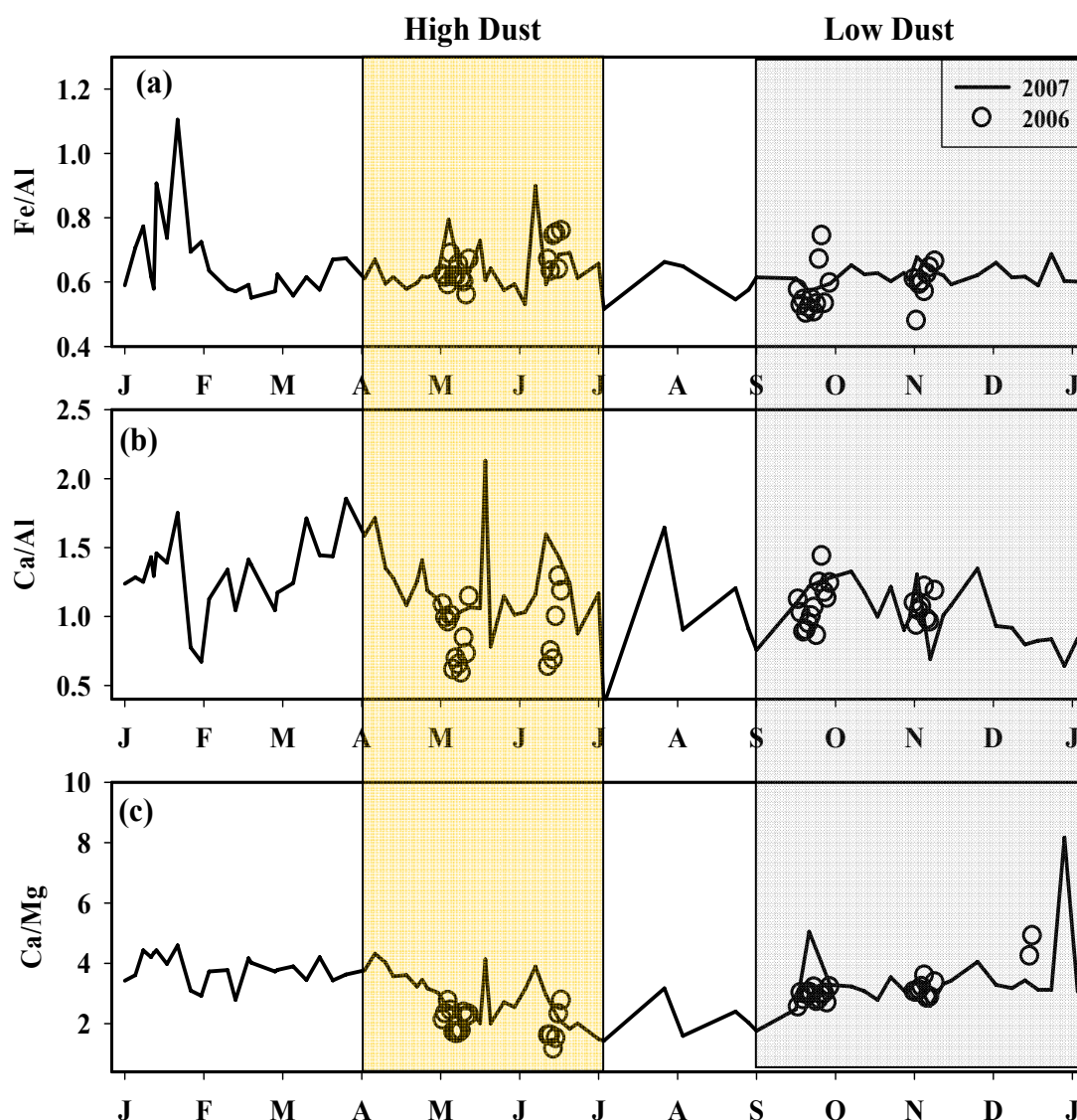


Fig. 3.6 Temporal variability of crustal element ratios in two subsequent years (2006 and 2007). The two shaded region are representative of high (April-June) and low dust condition (September-December).

found to vary in a narrow range of 0.50 to 0.70 with few outliers at ~ 0.80 in both years (2006 and 2007). The ratio is a representative of dust over western India. However, a large variability is observed in the Fe/Al ratio during wintertime. Based on the elemental ratio discussed in previous section, the enrichment of iron is observed from the contribution of Fe from anthropogenic sources. The data in 2006, during low dust period, also document higher Fe/Al ratios (Fig. 3.6a). However, the size-segregated samples give a better representation of elemental

ratio in coarse and fine dust. The Ca/Al ratio (Fig. 3.6b) show enriched values throughout the year indicating the dominance of carbonate rich dust over western India. The ratios are showing large variability in both high as well as low dust period. However, the ratios have gone as low as 0.39 during monsoon period, when the coarser dust gets efficiently removed by precipitation. It is interesting to note the relatively lower ratios were found during May-2006. Such variability in elemental ratios is driven by various meteorological parameters e.g. wind speed and directions. The Ca/Mg ratio (shown in Fig. 3.6c) observed over the sampling site found to vary between 1.14 to 4.32 in high dust and 2.47 to 5.08 in low dust condition. The ratios are by and large conservative in two different years (2006 and 2007) with few spikes observed during wintertime (low dust condition).

3.2.5 Comparison of elemental ratios in mineral dust:

The elemental ratios measured in the atmospheric aerosols from a number of locations (continental sites, marine boundary layer and coastal locations) have been reported in the literature and are summarized in Table 3.2. Although this comparison is not comprehensive, however, it illustrates the variation in crustal element ratios in different environment. The average Fe/Al ratio over the adjoining Bay of Bengal and Arabian Sea has been reported as 0.72 ± 0.37 (range: 0.47 to 2.28) and 0.51 ± 0.05 (range: 0.40 to 0.59) respectively (Kumar et al, 2008a, b). The respective Ca/Al ratio (0.81 ± 0.16) and (0.89 ± 0.27) shows enrichment of Ca by a factor of 2-3 than upper continent crust (UCC) ratio (0.38; McLennan, 2001, Kumar et al, 2008a, b). The desert regions of Thar and Oman are the potential source regions of dust which is rich in carbonate minerals reflecting a similar enrichment in aerosols collected from the sampling location (Table 3.1; Kumar et al, 2008a, b). In the present study, coarse dust shows an enrichment of calcium by a factor of 4 and 3 during summer and winter season compared to UCC value, a remarkable feature of the dust in Asian region compared to other geographical location. The ubiquitous alkaline-nature of rainwater in this high-dust semi-arid region (Rastogi and Sarin, 2005c) further provides credence to the enriched carbonate content of dust which in turn has potential to neutralize acidic species (Rastogi and Sarin, 2006).

Chapter-3

Table 3.2: Average elemental ratios observed over different geographical locations. Range of the ratio has been given for Mt.Abu (Mean \pm standard deviation of ratios are given in parentheses).

Location	Sampling Date	Type of sample	Fe/Al	Ca/Al	Mg/Al	Reference
Mt.Abu (24.7°N, 72.7°E)	Mar-Jun, 2007	#PM _{10-2.5}	0.51-1.02 (0.63 \pm 0.09)	0.79-2.19 (1.36 \pm 0.33)	0.31-1.06 (0.39 \pm 0.05)	Present study
	Jul-Sep, 2007	PM _{10-2.5}	0.47-0.68 (0.58 \pm 0.07)	0.38-1.82 (1.12 \pm 0.41)	0.17-0.50 (0.31 \pm 0.12)	Present study
	Oct-Dec;Jan-Feb, 2007	PM _{10-2.5}	0.53-1.21 (0.66 \pm 0.14)	0.67-1.74 (1.16 \pm 0.24)	0.17-0.45 (0.31 \pm 0.05)	Present study
	Mar-Jun, 2007	@PM _{2.5}	0.53-1.13 (0.69 \pm 0.14)	0.51-1.76 (0.85 \pm 0.29)	0.18-0.55 (0.35 \pm 0.1)	Present study
	Jul-Sep, 2007	PM _{2.5}	0.45-1.05 (0.67 \pm 0.17)	0.44-1.13 (0.64 \pm 0.27)	0.39-0.63 (0.47 \pm 0.08)	Present study
	Oct-Dec;Jan-Feb, 2007	PM _{2.5}	0.49-1.00 (0.72 \pm 0.13)	0.38-1.79 (0.73 \pm 0.33)	0.17-0.45 (0.30 \pm 0.08)	Present study
Arabian Sea (9-22°N, 58-77.3°E)	April-May, 2006	TSP	0.51 \pm 0.05	0.89 \pm 0.27	-	Kumar et.al, 2008a
Bay of Bengal (5.6-20.5°N, 80.4-93.4°E)	March-April, 2006	TSP	0.72 \pm 0.37	0.81 \pm 0.16	-	Kumar et.al, 2008a
Zhenbeitai (38.3°N, 109.7°E)	April, 2002	TSP	0.63 \pm 0.04	0.79 \pm 0.15	0.32 \pm 0.03	Alfaro et.al, 2003
Zhenbeitai (38.3°N, 109.7°E)	April, 2001	PM _{2.5}	0.59	1.00	0.35	Arimoto et.al, 2004
Barbados (13.2°N, 59.4°E)	August 1988-1990	TSP	0.51	0.29	0.37	Arimoto et.al, 1995
Bermuda (32.2°N, 64.9°E)	June 1988-1990	TSP	0.61	0.33	0.32	Arimoto et.al, 1995
Izana (28.3°N, 16.5°E)	April 1989-1990	TSP	0.70	0.36	0.30	Arimoto et.al, 1995
UCC	-	-	0.44	0.37	0.16	McLennan, 2001

Referred as Coarse mode based on difference in mass concentration of PM₁₀ and PM_{2.5}; @ Fine mode

It is noteworthy that iron enrichment is relatively enhanced in the fine fraction than coarse fraction (Table 3.2); significantly different than the Fe/Al ratio reported from Zenbeitai (38.3°N, 109.7°E). The enriched iron content in fine mode is attributed to the dominance of anthropogenic sources. This has implication to the chemical processing of aerosol particles during the advective transport to MABL and increased supply of dissolved iron (bio-available) to surface ocean.

3.3. Summary and conclusions:

Based on one-year record of aerosol sampling from a high-altitude site, this study represents a first comprehensive data set on the characteristics of atmospheric mineral dust and its temporal variability over western India. The important findings and conclusions are:

- 1) The mass concentration of coarse mode ($PM_{10-2.5}$) aerosols is influenced by the uniform contribution of dust (60-80%) all through the year. In contrast, dominance of anthropogenic sources in modifying the elemental composition of the fine ($PM_{2.5}$) mode particles is discernible. The enriched abundance of Fe in $PM_{2.5}$ during winter months, as evident from comparison with Fe/Al ratio of 0.44 in the upper continental crust, suggests dominant contribution of Fe from long-range down-wind transport of combustion products from fossil-fuel and biomass burning sources in the Indo-Gangetic Plain. This has implication to advective transport of pollutants from northern India to the MABL of Bay of Bengal under favourable meteorological conditions (Kumar et al, 2008a).
- 2) The Ca/Al and Mg/Al ratios exhibit enrichment of Ca and Mg in the coarse mode indicating their dominant source from carbonate minerals. A ubiquitous alkaline-nature of rainwater in this high-dust semi-arid region (Rastogi and Sarin, 2005b) further attests to the dominant role of carbonate dust in efficient neutralization of atmospheric acidic species.

To sum up, results from this study provide an important data-base especially for the regional-scale models that need to be designed for the high-dust semi-arid regions of the sub-tropics in south-Asia.

Chapter 4

CHEMICAL CHARACTERISTICS OF MINERAL DUST

4.1. Introduction:

It is well recognized that ubiquitous presence of aerosols in the atmosphere, derived from natural sources (mineral dust, sea-salts and volcanic emissions), had a pronounced impact on the global climate system in the past. With the present-day growing anthropogenic activities (contributing to sulphate, nitrate and carbonaceous species), the global mean aerosol burden of the atmosphere has been substantially altered (both in terms of physical and chemical properties of aerosols). As a result, the recent studies on direct effects of aerosols have gained significant importance in amplifying/dampening climate change on a regional to global scale. In addition, an increase in number density of sub-micron size particles and their ability to act as cloud condensation nuclei (CCN) have become the basis for studying the indirect effects of aerosols (Ramanathan et al., 2001a; 2001b). Recent studies have shown that the atmospheric radiative forcing due to anthropogenic aerosols is capable of offsetting the forcing caused by the greenhouse gases (Intergovernmental Panel on Climate Change (IPCC), 2001). However, a large degree of uncertainty in the earlier evaluation (IPCC, 2001) has been somewhat better constrained in recent years through the availability of emerging data on chemical and physical properties of aerosols (IPCC, 2007). From a different perspective, increase in the abundances of mineral and anthropogenic aerosols has potential to affect the atmospheric chemistry

as well as marine ecosystem in remote oceanic regions (Duce et al., 1991; Jickells, 1999; Arimoto et al., 2001; Jickells et al., 2005).

The south Asian region is currently undergoing rapid industrialization, thus, making this region a hot spot for anthropogenic emissions (Arimoto et al., 1996; Streets et al., 2003). Moreover, mineral aerosols produced from land-use changes and disturbed soils are the important constituents of the atmosphere, especially those originating from the arid and semi-arid region of Asia (Dentener et al., 1996; Song and Carmichael, 2001; Rastogi and Sarin, 2006). The atmospheric mineral dust plays a vital role in the removal of anthropogenically derived acidic gases (e.g. SO₂ and NO_x); in addition to their removal mechanism via interaction with NH₃ (Zhuang et al., 1999; Jordan et al., 2003; Krueger et al., 2003; Bates et al., 2004; Tang et al., 2004; Arimoto et al., 2004, Maxwell-Meier et al., 2004; Ooki and Uematsu, 2005; Rastogi and Sarin, 2005 a, b; 2006). A modeling study conducted for the east-Asian region had reported that natural aerosols (e.g. mineral dust and sea-salts) play an important role in the abundance pattern and size-distribution of inorganic constituents (Song and Charmichael, 2001). Furthermore, they have potential to alter the size distribution of particulate SO₄²⁻ and NO₃⁻, shifting their atmospheric distribution from fine to coarse size particles (Dentener et al., 1996; Rastogi and Sarin, 2006).

The abundances and atmospheric reactivity of nitrate and sulphate; as well as their wet and dry removal processes critically depend on the composition of mineral aerosols (e.g., carbonate versus silicate content) and their size dependent distribution (Sullivan et.al, 2007). Thus, one of the major limitations of current models relates to the lack of real-time data on size dependent chemical composition of atmospheric mineral dust and the associated spatial-temporal variability. The measurements based on bulk-aerosols are inadequate to constrain the model scenario made in recent years. In addition, studies near to the source regions of mineral dust (originating from arid and semi-arid regions) are required to constrain and test the models. In this context, the present study on the chemical composition of fine (PM_{2.5}; particles less than 2.5 μm) and coarse (PM_{10-2.5}; particles between 10 and 2.5 μm) mode aerosols is most relevant from a high-altitude site (Mt.Abu; 24.6 °N, 72.7 °E, 1680m asl) located in a

semi-arid region (near to the Great Thar Desert in western India). Our sampling strategy from a high-altitude station is advantageous to study the long-range transport of mineral dust across western India and its role in modifying the atmospheric chemistry of acidic species. The chemical data involving water-soluble inorganic species has been also used to document the temporal changes over the annual seasonal cycle (summer, monsoon and winter).

4.2. Results and Discussions:

Details regarding abundances the water-soluble constituents in coarse and fine fractions and temporal variability have been discussed in section 4.2.1. Section 4.2.2 describes the relationship among water-soluble constituents in order to assess their major sources. Inter-annual variability of some ionic ratios used as diagnostic tracer has been discussed in section 4.2.3. The neutralization of acidic species (SO_4^{2-} and NO_3^-) in the coarse and fine mode and role of mineral dust has been evaluated in section 4.2.4. It is relevant to state that PM_{10} aerosols also include mass of $\text{PM}_{2.5}$. In view of the synchronous operation of the two samplers and their frequent calibration, contribution of fine fraction ($\text{PM}_{2.5}$) can be subtracted from PM_{10} mass in order to assess the chemical composition of coarser ($\text{PM}_{10-2.5}$) aerosols. Such an approach will further incorporate an uncertainty of 7% in the calculation of coarse aerosol mass and its chemical composition. In this study, we have referred 'coarse' fraction as $\text{PM}_{10-2.5}$ (difference of PM_{10} and $\text{PM}_{2.5}$) and 'fine' fraction as $\text{PM}_{2.5}$. The scatter plots among $\text{PM}_{2.5}$ and PM_{10} (Fig. 4.1) suggest that coarse aerosol ($\text{PM}_{10-2.5}$) dominate the water-soluble ionic composition (WSIC) and Ca^{2+} composition of PM_{10} aerosols and that all of SO_4^{2-} abundance in PM_{10} is influenced by $\text{PM}_{2.5}$. The above reasoning forms a strong basis for subtracting the fine mass aerosols from PM_{10} for interpretation of the chemical data.

4.2.1 Temporal variation in Water-soluble ionic composition (WSIC):

The water-soluble ionic composition (WSIC) varied from 1.0 to 19.5 $\mu\text{g m}^{-3}$ in the fine ($\text{PM}_{2.5}$, Table-4.1 a) and 0.1 to 24.8 $\mu\text{g m}^{-3}$ in the coarse mode aerosols

(PM_{10-2.5}, Table-4.1 b). The abundance of WSIC in coarse mode is relatively high during summer months ($A_v=10.8 \mu\text{g m}^{-3}$). It is of comparable magnitude in monsoon and relatively low during winter season ($A_v=4.2 \mu\text{g m}^{-3}$) in comparison to the abundance pattern of WSIC in fine mode particles (Tables-4.1 a and b). Such an observation is consistent with the predominance of insoluble mineral dust in the coarse mode during all seasons (Kumar and Sarin, 2009). The temporal data (Tables-4.1 a and b) suggest that the percentage contribution of WSIC to the fine aerosol mass is consistently high during all seasons relative to that in coarse mass fraction. The percentage contribution of an individual water-soluble species to the total WSIC is represented as pie-charts (Fig. 4.2) for the three different seasons (summer, monsoon and winter). In the fine mode, SO_4^{2-} is the most dominant anion followed by minor contribution from HCO_3^- and NO_3^- ions (Fig. 4.2). The dominance of HCO_3^- in the ionic composition of coarse fraction (PM_{10-2.5}; Fig. 4.2), with minor contribution of NO_3^- and SO_4^{2-} , supports the earlier inference on relatively higher abundance of mineral dust. During winter months, the enhanced mass abundances of sulphate, nitrate, and ammonium in the fine-mode, and hence their dominance in the WSIC (Fig. 4.2), are attributable to increase in the source strength of anthropogenic components and transport from the polluted regions of northern India.

4.2.1.1 Sea-salts (Na^+ and Cl^-):

The water-soluble component of Na^+ and Cl^- in atmospheric aerosols is mainly derived from the marine source, more commonly referred as sea-salts; and the abundance of Na^+ is used as a proxy for the sea-salts (Quinn et al, 2004; Kumar et al, 2008a, and b). Also, sea-salt particles are the favoured sites for the uptake of acidic species (SO_4^{2-} and NO_3^-) followed by the release of HCl (gas), a chemical reaction that most commonly occurs over the marine atmospheric boundary layer (MABL). The loss of chloride from sea-salt particles ranges from a few percent to 100% (Keene et al, 1990; McInnes et al, 1994; Kumar et al, 2008a, b). In this study, the abundance of chloride is below the detection limit in PM_{2.5} aerosols and its detectable concentration in the coarse mode makes only a minor contribution to the total anions.

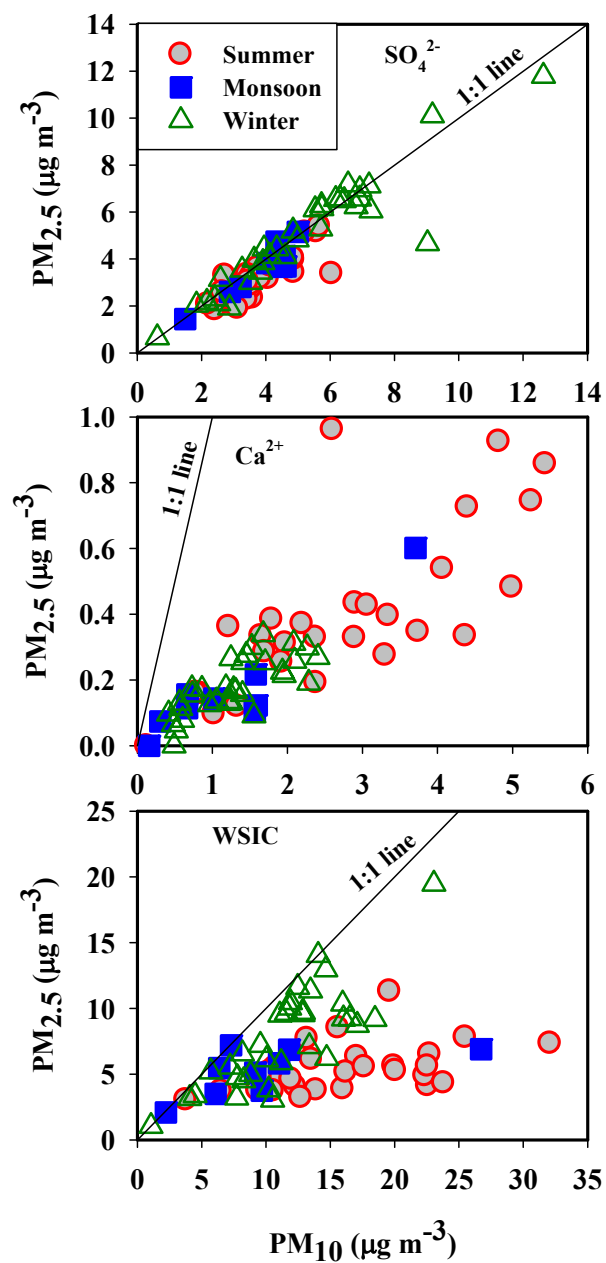


Fig. 4.1 Scatter plot among PM_{10} and $PM_{2.5}$ for water-soluble ionic composition (WSIC), Ca^{2+} and SO_4^{2-} .

Tables 4.1a and b: Minimum, maximum and average concentration ($\mu\text{g m}^{-3}$) of water-soluble ionic constituents in fine ($\text{PM}_{2.5}$) and coarse ($\text{PM}_{10-2.5}$) mode aerosols in Summer (March - June), Monsoon (July – September) and Winter (October –February) seasons.

Components	PM _{2.5}											
	Summer (n = 29)				Monsoon (n = 9)				Winter (n = 34)			
	Min	Max	AM ^a	SD ^b	Min	Max	AM	SD	Min	Max	AM	SD
Mass Load	6.8	34.5	16.2	7.0	9.3	31.7	18.7	6.2	1.6	46.1	16.9	9.0
WSIC*	3.0	11.3	5.4	1.8	2.1	7.2	5.2	1.8	1.0	19.5	7.8	3.8
WSIC (%)[#]	15.8	79.4	39.0	19.4	13.4	73.3	31.4	18.8	22.7	80.0	49.5	13.8
NH₄⁺	0.19	1.94	0.77	0.40	0.29	1.72	0.92	0.44	0.24	4.82	1.83	1.00
Na⁺	0.06	0.92	0.27	0.2	0.06	0.44	0.28	0.1	0.05	0.21	0.09	0.03
K⁺	0.07	0.37	0.14	0.07	0.05	0.25	0.10	0.06	0.07	1.21	0.36	0.30
nss-K⁺	0.06	0.36	0.13	0.07	0.04	0.25	0.09	0.06	0.07	1.21	0.36	0.30
Mg²⁺	0.03	0.15	0.06	0.03	bd	0.08	0.06	0.02	bd	0.05	0.03	0.01
nss-Mg²⁺	bd	0.07	0.03	0.02	bd	0.05	0.02	0.01	bd	0.04	0.02	0.01
Ca²⁺	0.10	0.96	0.41	0.20	0.07	0.60	0.19	0.16	bd	0.34	0.18	0.08
nss-Ca²⁺	0.09	0.95	0.40	0.20	0.07	0.59	0.18	0.16	0.04	0.33	0.18	0.08
Cl⁻	bd	0.13	-	-	bd	bd	-	-	bd	bd	-	-
NO₃⁻	bd	0.76	0.26	0.16	bd	0.21	-	-	bd	1.98	0.34	0.48
SO₄²⁻	1.85	5.40	3.13	0.95	1.44	5.16	3.56	1.10	0.65	11.8	4.98	2.30
nss-SO₄²⁻	1.81	5.30	3.06	0.94	1.42	5.12	3.49	1.10	0.65	11.7	4.96	2.30
HCO₃⁻	bd	2.41	0.62	0.5	bd	0.85	-	-	bd	2.41	-	-

Chapter-4

Components	PM _{10-2.5}											
	Summer				Monsoon				Winter			
	Min	Max	AM	SD	Min	Max	AM	SD	Min	Max	AM	SD
Mass Load	6.88	102	41.8	21.5	13.1	49.7	22.1	11.4	2.31	45.5	23.1	9.25
WSIC	1.31	24.8	10.8	5.53	0.47	19.8	5.52	5.50	0.10	9.29	4.24	2.49
WSIC (%)	14.0	37.3	26.1	5.8	3.5	39.9	21.0	11.5	4.5	37.7	17.9	7.6
NH₄⁺	bd	bd	-	-	bd	bd	-	-	bd	1.94	-	-
Na⁺	0.07	2.56	0.73	0.60	0.12	1.26	0.68	0.37	bd	0.76	0.15	0.14
K⁺	0.02	0.11	0.05	0.02	0.021	0.11	0.05	0.03	bd	0.26	0.04	0.06
nss-K⁺	bd	0.05	0.02	0.01	bd	0.08	0.02	0.03	bd	0.27	0.04	0.06
Mg²⁺	0.05	0.43	0.15	0.10	0.04	0.23	0.13	0.06	0.03	0.14	0.08	0.03
nss-Mg²⁺	bd	0.19	0.07	0.05	0.01	0.12	0.05	0.04	bd	0.11	0.06	0.03
Ca²⁺	0.12	4.58	2.33	1.30	0.16	3.11	1.08	0.91	0.03	2.12	1.08	0.55
nss-Ca²⁺	0.11	4.48	2.30	1.30	0.15	3.08	1.05	0.91	0.04	2.12	1.07	0.55
Cl⁻	bd	3.09	0.79	0.80	bd	1.17	0.48	0.36	bd	0.65	-	-
NO₃⁻	0.19	2.46	1.32	0.51	bd	2.29	0.94	0.84	0.06	2.20	1.10	0.54
SO₄²⁻	0.04	2.66	0.65	0.56	0.05	0.93	0.45	0.32	bd	4.37	0.52	0.95
nss-SO₄²⁻	bd	2.01	0.45	0.48	bd	0.78	0.21	0.30	bd	4.35	0.30	0.77
HCO₃⁻	0.29	11.2	5.20	2.95	bd	11.4	2.21	3.7	bd	4.79	1.64	1.33

bd: below detection limit

*Water-soluble ionic composition

#Percentage of total mass load

^aArithmetic mean

^bStandard deviation

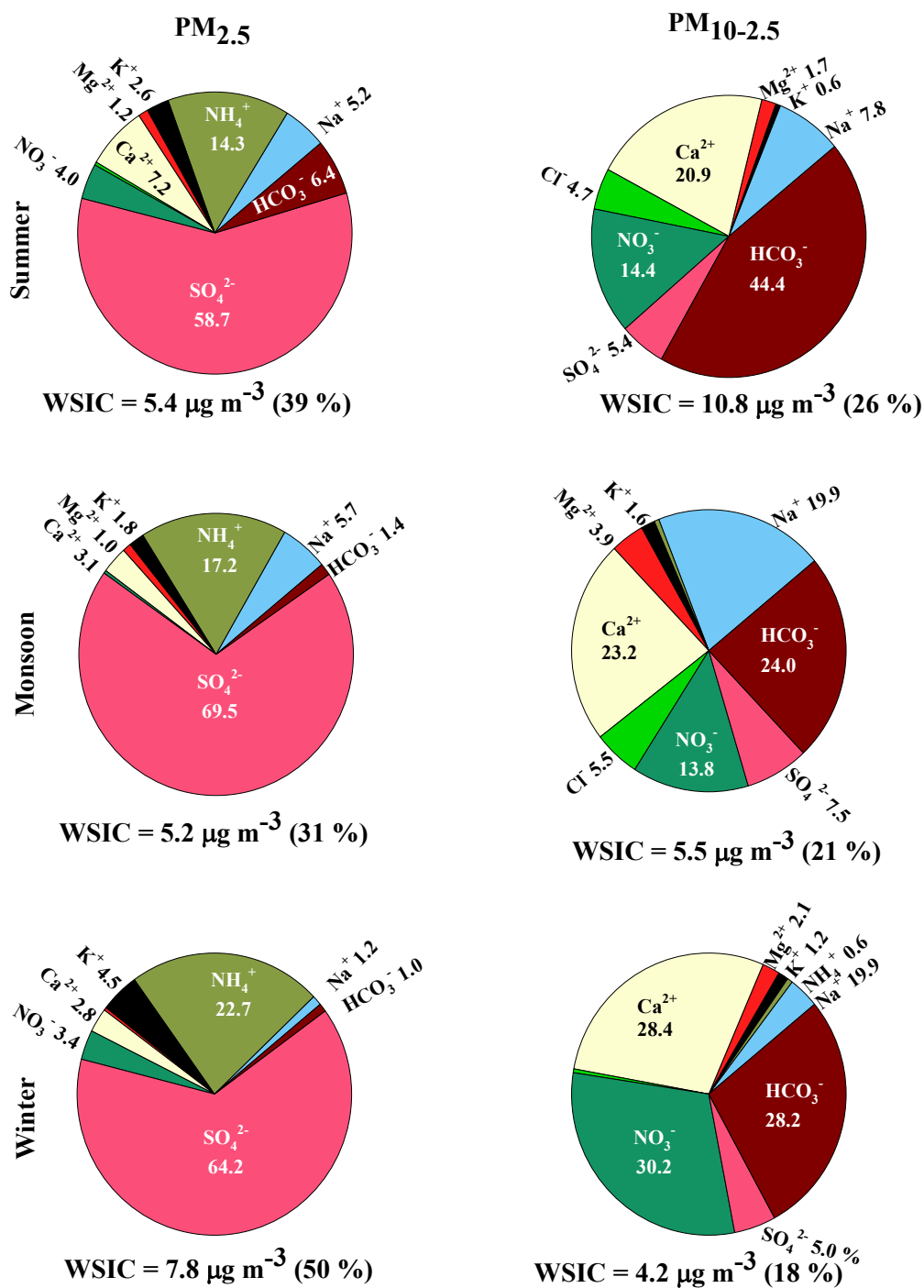


Fig. 4.2 Fractional contribution (%) of individual ionic species to the total WSIC in the coarse and fine mode aerosols during the three seasons. Seasonal average mass abundance of WSIC and its percentage contribution in the fine and coarse aerosols is also indicated. In fine mode, contribution of Cl to WSIC is insignificant during all seasons.

The abundance of Na^+ in the coarse fraction (range: >0.02 to $2.5 \mu\text{g m}^{-3}$, Table-4.1 b) and its conservative transport has been considered to be of marine origin. The conspicuous increase in its contribution to WSIC, during the SW-monsoon (Fig. 4.2), further attests the transport of sea-salts with the prevailing winds from the Arabian Sea. Thus, the sea-salt contribution to the measured species has been corrected based on the abundance of Na^+ in the aerosols and its ionic ratio with the other species in seawater. It may be argued that a finite fraction of Na^+ could originate from soil dust, in particular from the samples collected during summertime (high-dust suspension in the atmosphere). In such a scenario, our approach of using Na^+ as a reference of sea-salt would lead to over correction of sea-salt contribution and hence lower limit on the abundances of water-soluble major ions derived from anthropogenic sources. It is noteworthy that due to lower abundance of Na^+ , during summer and winter season, the sea-salt contribution is no more than 5 % in the fine mode aerosols.

4.2.1.2 Anthropogenic components (NO_3^- , SO_4^{2-} and NH_4^+):

The temporal distribution of nitrate (Fig. 4.3) exhibits relatively high abundance in the coarse size ($\text{PM}_{10-2.5}$) than in fine mode ($\text{PM}_{2.5}$). Furthermore, contribution of NO_3^- to total WSIC in coarse aerosols is relatively high during winter months (Fig. 4.2), attesting to its dominant and seasonal contribution from anthropogenic sources. The neutralization of anthropogenic NO_3^- (HNO_3) by the alkaline dust in the semi-arid region is invoked as a plausible mechanism for dominant occurrence of nitrate in the coarse fraction. It has been also shown that nitrate is the dominant acidic constituents associated with the mineral dust particles rather than nss-SO_4^{2-} (Ooki and Uematsu, 2005). However, aerosol mass concentration of NO_3^- ($\mu\text{g m}^{-3}$) is predominant in coarse mode, during summer months (Table-4.1 b); suggesting its possible source from the regional dust. Based on the chemical data alone, it is difficult to decipher atmospheric abundance of NO_3^- associated with primary mineral dust and/or via uptake of acidic species by mineral aerosols. The mass abundance of SO_4^{2-} varied from 0.65 to 11.8 and <0.02 to $4.4 \mu\text{g m}^{-3}$ in fine and coarse mode aerosols respectively (Tables-4.1 a and b); and its

average contribution to the total WSIC during the three season is summarized in Fig 4.2.

During all seasons significantly high abundance of SO_4^{2-} is observed in the fine fraction compared to that in the coarse aerosols. The accumulation of SO_4^{2-} in the fine mode is attributed to gas-to-particle conversion of SO_2 gas (Hering and Friedlander, 1982; Venkatraman et.al, 2002) and its subsequent growth under humid conditions. The conversion of SO_2 to sulphate, in the presence of oxidizing species (e.g. H_2O_2 or O_3), is the dominant pathway for sulphate formation. The atmospheric abundance of SO_4^{2-} is also derived from sea-salt and regional soils. The contribution of SO_4^{2-} from sea-salts has been estimated based on the abundance of Na^+ measured in aerosols (Tables-4.1 a and b) and found to be less than 5 % in fine aerosols. However its sea-salt contribution in the coarse fraction is significant, increasing up to as much as 50 % during the monsoon season. The temporal variability in the abundance of nss- SO_4^{2-} (non-sea-salt sulphate corrected for sea-salts) in the two size fractions is depicted in Fig 4.3; suggesting that more than 90% of nss- SO_4^{2-} exists in the fine mode and that its contribution in $\text{PM}_{10-2.5}$ (coarse) is insignificant. Furthermore, a two-fold increase in the abundance of nss- SO_4^{2-} during wintertime, relative to that in summer months (Fig. 4.3), is attributable to its dominant contribution from anthropogenic sources in northern India and meteorological conditions favouring the long-range transport under the influence of prevailing NE-winds. In fine mode, contribution of SO_4^{2-} from regional dust is relatively insignificant as inferred from decrease in the nss- Ca^{2+} /nss- SO_4^{2-} ratio of 0.32 in summer to 0.10 during wintertime. However seasonal variability of SO_4^{2-} in coarse mode is nowhere pronounced. The sulphate is one of the non-volatile secondary ions that makes the aerosols acidic in the absence of alkaline species (such as HCO_3^- for efficient neutralization) and further leads to the removal of volatile anions e.g. Cl^- and NO_3^- .

The temporal variation of NH_4^+ mass concentration (in $\mu\text{g m}^{-3}$) in the fine mode is very similar to that of sulphate (Fig 4.3), implying that the formation of NH_4^+ salt is controlled by the SO_4^{2-} abundance. The atmospheric abundance of NH_4^+ is

primarily derived from the decomposition of animal waste as well as from the regional practices of its use in fertilizers (in the form of ammonia/urea). Being volatile in nature, it is emitted from the ground sources, and neutralizes the atmospheric acidic species to form particulate ammonium salt. The water-soluble particulate NH_4^+ is relatively concentrated in the fine mode ($\text{PM}_{2.5}$). Thus, the contribution of ammonia to the total WSIC is relatively high (22.7%) in the fine mode during winter months compared to that in summer season (Fig. 4.2). It is noteworthy that contribution of particulate ammonia in the coarse fraction ($\text{PM}_{10-2.5}$) is insignificant all through the annual seasonal cycle (Table-4.1 b, concentration of NH_4^+ below detection in the coarse fraction implies that all of NH_4^+ occurring in PM_{10} size are contributed by $\text{PM}_{2.5}$).

4.2.1.3 Biomass burning component (K^+):

It has been suggested that abundance of potassium (K^+) in fine mode aerosols can serve as a diagnostic tracer for biomass burning source (Andreae, 1983; Andreae et al, 1998). However, its contribution from sea-salts and dust sources is highly variable for regional case studies with its dominance in the coarse fraction. In this study, the temporal variability of nss- K^+ (0.02 to $1.21 \mu\text{g m}^{-3}$) is significantly pronounced in $\text{PM}_{2.5}$ fraction, with enhanced abundance during wintertime (Fig 4.3). The dominance of regional biomass burning sources and boundary layer dynamics are the possible causes for the large variability over the annual seasonal cycle. As a result, contribution of K^+ to the total WSIC is relatively high in fine mode aerosols compared to that in the coarse mode.

4.2.1.4 Dust components (Ca^{2+} , Mg^{2+} and HCO_3^-):

In coarse mode, significant contribution of Ca^{2+} , Mg^{2+} and HCO_3^- to WSIC (Fig. 4.2) establishes their dominant and uniform contribution from mineral dust. The temporal distribution of non-sea-salt- Ca^{2+} (nss- Ca^{2+} corrected for sea-salts), HCO_3^- and nss- Mg^{2+} in the coarse and fine fractions is shown in Fig 4.4. It is noteworthy that nss-

Ca^{2+} and HCO_3^- abundances in coarse particles, during summer, increases by a factor of two or more than those observed in monsoon and winter season (Table-4.1 b).

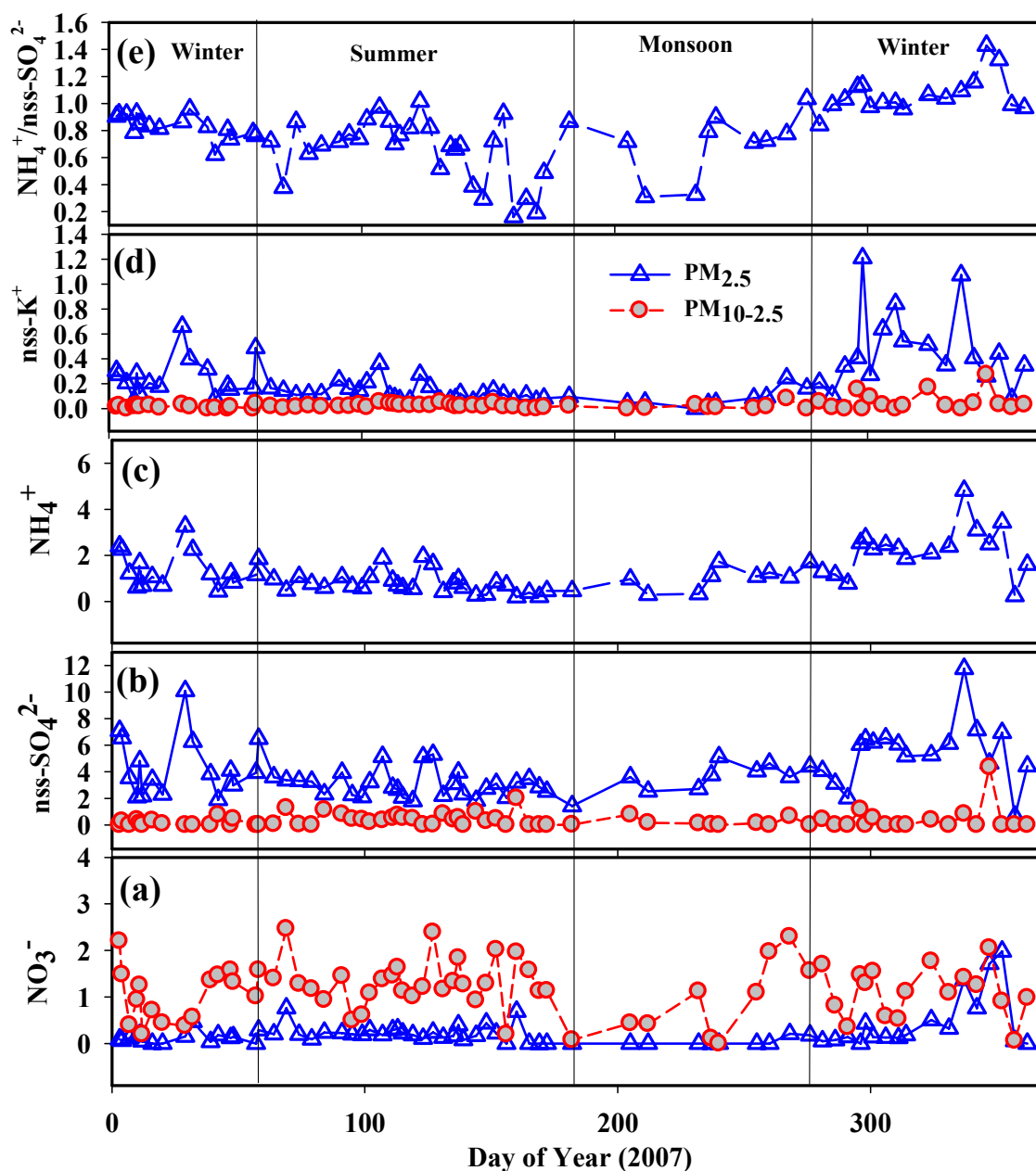


Fig. 4.3 Temporal variation of (a) NO_3^- , (b) nss-SO_4^{2-} , (c) NH_4^+ , (d) nss-K^+ and (e) $\text{NH}_4^+/\text{nss-SO}_4^{2-}$ in the two size fractions (All concentrations are in $\mu\text{g m}^{-3}$).

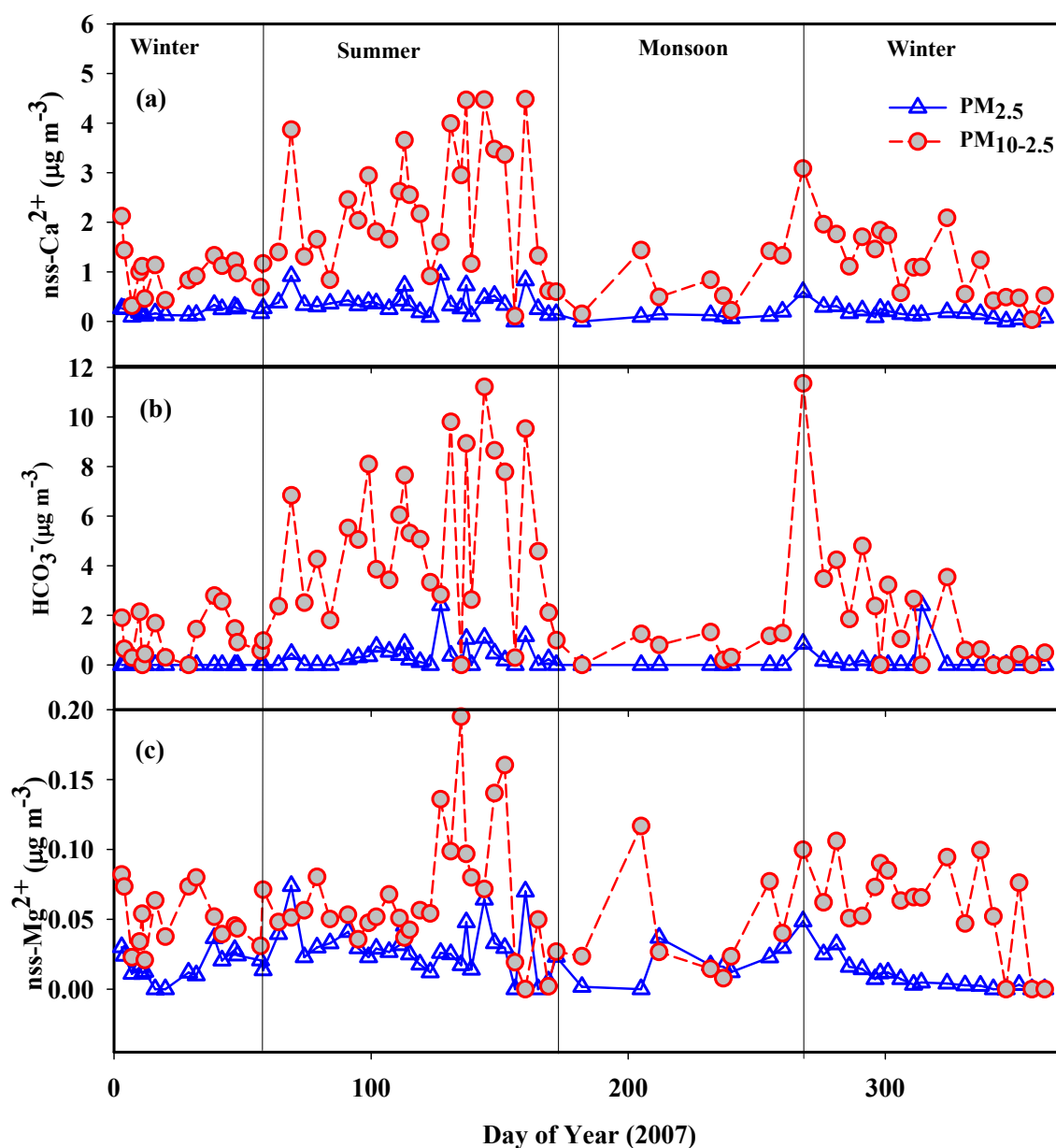


Fig. 4.4 Temporal variation of $nss-Ca^{2+}$, HCO_3^- and $nss-Mg^{2+}$ in the coarse and fine aerosols. Relatively high abundances observed during summer months in both size fractions indicate dominance of dust.

In fine fraction, during summer, $nss-Ca^{2+}$ abundance is also significantly higher (more than two times) than that in monsoon and winter months (Table 4.1 a).

This is also evident from its enhanced contribution to WSIC during summer (Fig. 4.2). A significant co-variation of nss-Ca^{2+} and HCO_3^- in the coarse mode with relatively higher abundances in summer season (Fig. 4.4) is attributed to the regional source region of dust from the Thar Desert under the influence of prevailing strong winds. The abundance of water-soluble Mg^{2+} and its dominant occurrence in coarse fraction is attributed to its source from the mineral dust and sea-salts. The scatter plot between Na^+ and Mg^{2+} (Fig. 4.5) reveals that most of the data points fall away from the sea-water line suggesting dominant contribution of Mg^{2+} from crustal sources; and that the sea-salt contribution of Mg^{2+} is less than 15% and does not exceed more than 25% during the monsoon season.

4.2.2 Inter-relationship among water-soluble ionic constituents

The abundances of nss-SO_4^{2-} and NH_4^+ (equivalent units) in fine mode aerosols exhibit significant linear correlation ($r^2 = 0.92$, Fig 4.6) over the study location, indicating the predominance of nss-SO_4^{2-} as ammonium salt in the fine mode. A similar observation has been reported from the coastal (Zhuang et al, 1999a), urban (Xiaoxiu et al, 2003; Rengarajan et al, 2007), and marine regions (Matsumoto et al, 2004). In contrast, relatively low abundance of nss-SO_4^{2-} in coarse mode is associated with the regional dust transported from the Thar Desert. The $\text{NH}_4^+/\text{nss-SO}_4^{2-}$ ratio (in equivalence units) in $\text{PM}_{2.5}$ shows pronounced temporal variability (varying from 0.19 to 1.5, Fig 4.3), with higher ratios during winter months compared to those in summer and monsoon season. The lower ratios in fine ($\text{PM}_{2.5}$) size range, during summer, are associated with parallel increase of dust enriched in carbonate content (as evident from WSIC; Fig. 4.2) and act as a substrate for efficient neutralization of SO_4^{2-} . For such an inference, it is implicit that nss-SO_4^{2-} is not completely neutralized by NH_4^+ in summer months. This further supports near absence of particulate ammonium nitrate, an observation similar to that made by Matsumoto and Tanaka, (1996). It is, thus, suggested that neutralization of nitrate is favoured by its uptake on the coarse dust particles, leading to relatively high abundance of NO_3^- in the coarse mode (Fig. 4.3).

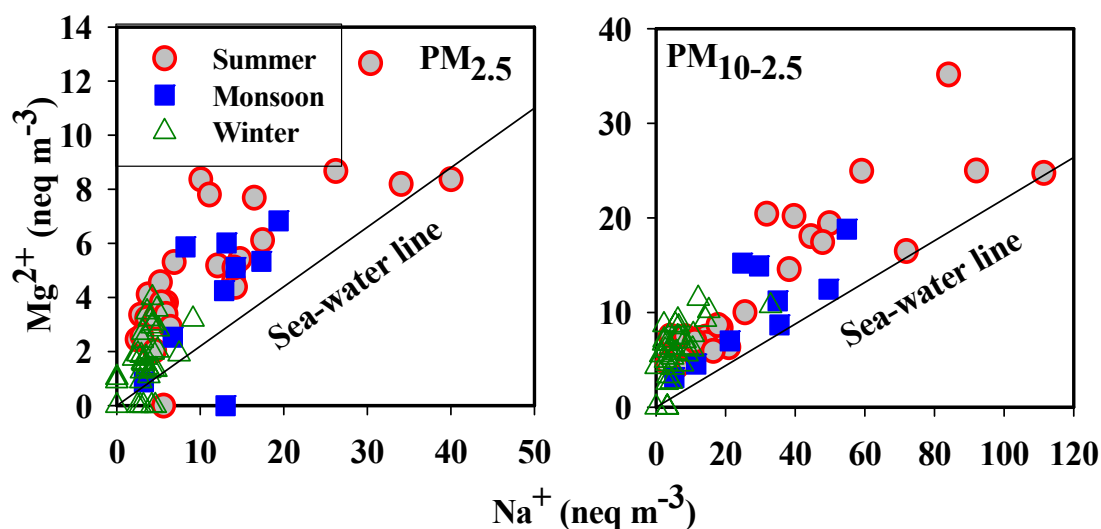


Fig. 4.5 Scatter plot for water-soluble Mg^{2+} and Na^+ to assess the source of Mg^{2+} (sea-salt vs dust). The data points falling away from the sea-water line suggest dominant contribution of Mg^{2+} from the crustal source.

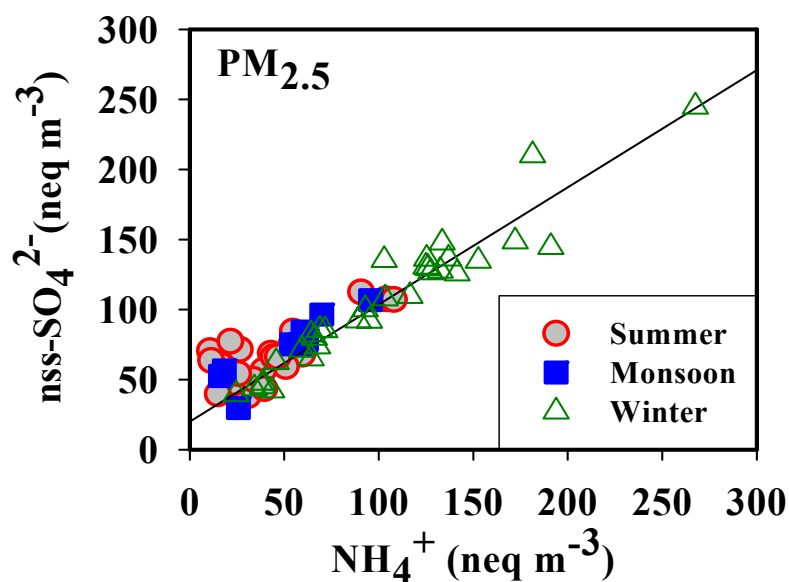


Fig. 4.6 A linear relationship between abundances (in equivalent units) of $nss-SO_4^{2-}$ and NH_4^+ in the fine ($PM_{2.5}$) aerosols during the three seasons suggesting their dominant contribution from anthropogenic sources.

Both NO_3^- and nss-SO_4^{2-} are mainly formed as secondary aerosols during the process of coal combustion, biomass burning and vehicular emissions (Senfield and Pandis, 1998). Therefore, depending upon the abundances of gaseous and particulate phase nitrogen and sulphur from local emissions and long-range transport, a large scatter in the data is expected, especially during the monsoon season when both species are efficiently scavenged from the ambient atmosphere by the wet precipitation. As discussed in section 4.2.1, the abundance of SO_4^{2-} in coarse mode and that of NO_3^- in fine mode is considerably low, resulting in large scatter of data point in the NO_3^- vs nss-SO_4^{2-} plot for both size fractions. Nevertheless, the scatter plot of nss-SO_4^{2-} versus NO_3^- in PM_{10} aerosols (Fig 4.7) shows somewhat meaningful linear relationship for the data from summer and winter seasons compared to a large scatter observed during the monsoon. The linear regression analysis between these two acidic components suggests some degree of similarities in their sources and sinks during a particular season. Within the reasonable degree of scatter, the data set for winter and summer seasons show distinct slope for the linear regression (winter: $m = 0.21$; summer: $m = 0.39$; Fig 4.7). These differences clearly address to the different source regions of atmospheric sulphur and nitrogen as well as their distinct sinks. The $\text{nss-SO}_4^{2-}/\text{NO}_3^-$ weight ratio for PM_{10} varied from 1.5 to 10.5 ($A_v=2.7$, $sd: 0.13$) in the summer and 1.6 to 17.1 ($A_v=4.4$, $sd: 0.12$) during the winter season. Furthermore, the $\text{nss-SO}_4^{2-}/\text{NO}_3^-$ weight ratios have been evaluated in both coarse ($\text{PM}_{10-2.5}$) and fine ($\text{PM}_{2.5}$) mode aerosols during winter months, when regional pollution sources in northern India are predominant. The $\text{nss-SO}_4^{2-}/\text{NO}_3^-$ ratios exhibit extreme variability, with values ranging from 2.7 to 101 in $\text{PM}_{2.5}$ and 0.001 to 2.7 in coarse ($\text{PM}_{10-2.5}$) mode aerosols. Rastogi and Sarin, (2005a), have documented $\text{nss-SO}_4^{2-}/\text{NO}_3^-$ weight ratio varying from 1.2 to 4.4 in samples collected from an urban location (Ahmedabad) in western India. Arimoto et al (1996) had reported that the differences in the $\text{nss-SO}_4^{2-}/\text{NO}_3^-$ ratios at different sites could arise from the regional differences in the pollution component of aerosols. Yao et al (2002) had used $\text{SO}_4^{2-}/\text{NO}_3^-$ ratios as an indicator of the relative dominance of stationary (coal combustion, biomass burning) versus mobile (vehicular emissions) sources of sulphur and nitrogen in the

atmosphere and attributed higher ratios to the dominance of stationary pollutant sources and lower ratios to that of mobile sources. The higher ratios observed over the sampling site can be explained on the basis of long-range transport of sulphate aerosols (associated with ammonia) in the fine mode and that of NO_3^- (associated with dust) in the coarser mode particles.

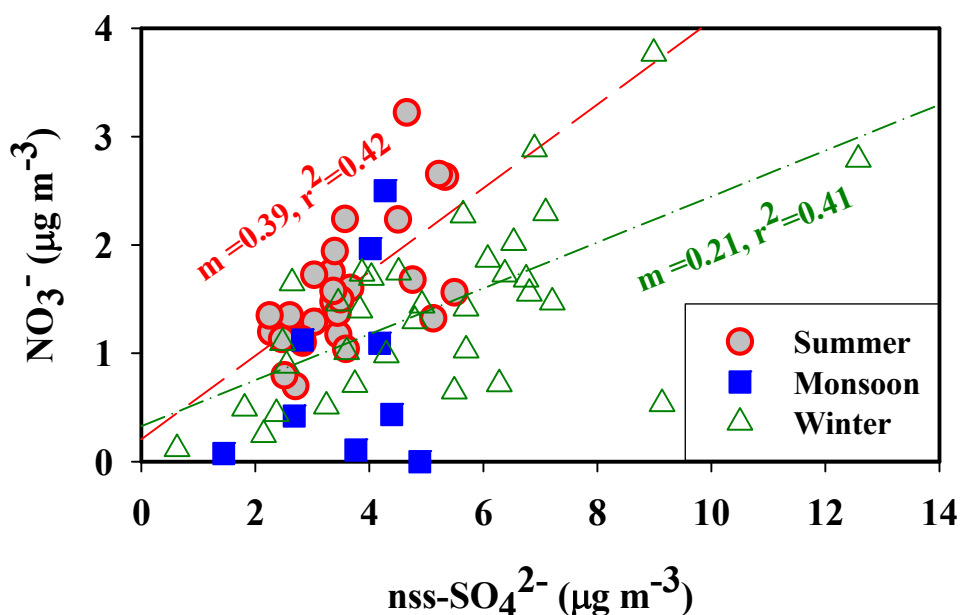


Fig. 4.7 Scatter plot between NO_3^- and SO_4^{2-} in PM_{10} aerosols in the high-dust region.

The coarse fraction is dominated by the mineral dust all through the year in contrast to the fine mode that is enriched in dust during summer months (Fig. 4.2). A scatter plot between HCO_3^- and nss-Ca^{2+} , for the $\text{PM}_{2.5}$ and $\text{PM}_{10-2.5}$ data during summer months, exhibits a significant linear relationship (Fig 4.8, for coarse mode: $r^2=0.92$ and fine mode: $r^2=0.75$). In contrast, relatively large scatter is observed during winter months ($r^2 = 0.63$) in the coarse mode ($\text{PM}_{10-2.5}$). The significant correlation, during summertime, is attributed to the strong source strength and enhanced dust contribution compared to lower abundance of dust during winter, and hence large scatter in Ca^{2+} and HCO_3^- (Fig. 4.8).

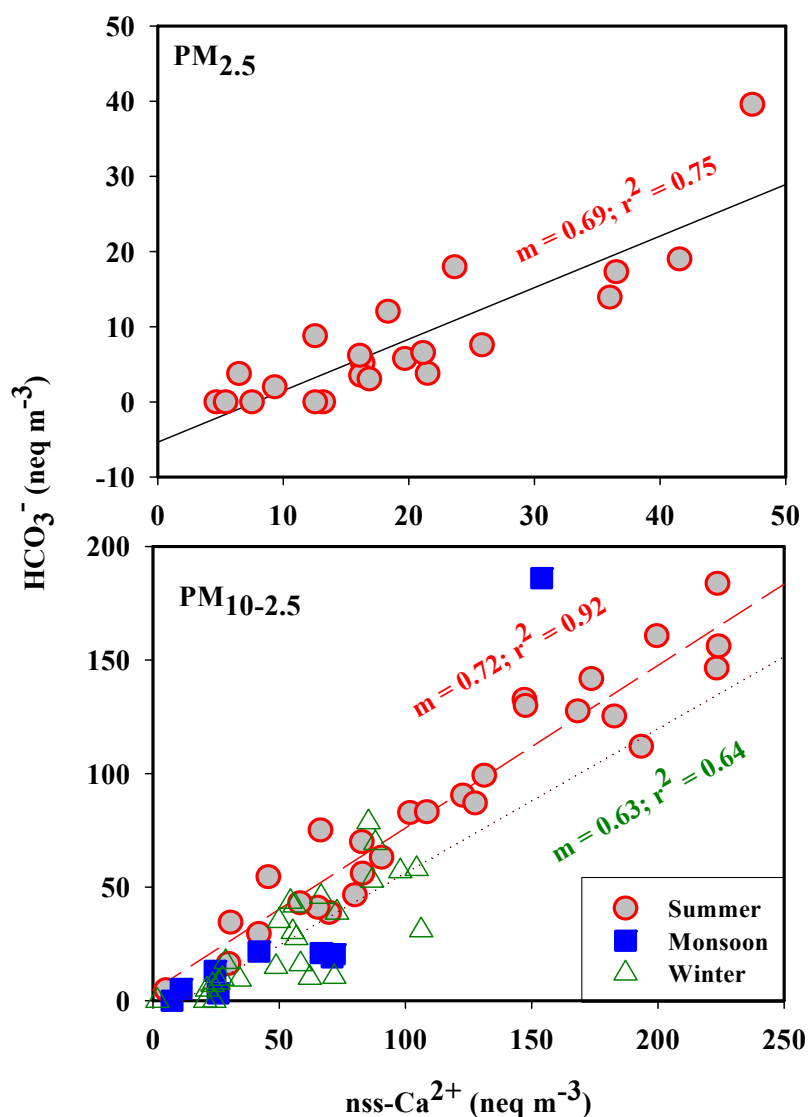


Fig. 4.8 Linear regression plot between nss-Ca^{2+} and HCO_3^- in the fine and coarse mode aerosols suggests their major source from mineral dust. 'm' represents slope of the best-fit lines drawn through summer ($m=0.72$) and winter ($m=0.63$) seasons in the coarse mode ($\text{PM}_{10-2.5}$). In fine mode, data for summer season has been presented (as discussed in the text).

In addition, increased abundances and neutralization of anthropogenic constituents (NO_3^- and nss-SO_4^{2-}) further contribute to large scatter during wintertime. In the fine

mode (PM_{2.5}), HCO₃⁻ abundance in several of the samples collected during winter and monsoon season is close to detection limit (Table 4.1 b, Fig. 4.4 b).

The abundance of nss-Mg²⁺ and its contribution to WSIC is found to be an order of magnitude lower than that of nss-Ca²⁺. A large scatter observed between nss-Ca²⁺ and nss-Mg²⁺ (in equivalence units) for coarse mode ($r^2 = 0.50$) compared to fine mode ($r^2 = 0.64$) is observed (Fig. 4.9), indicates that contribution of water-soluble nss-Mg²⁺ from dust sources is independent of higher abundance of water-soluble nss-Ca²⁺ (dominant in coarse fraction) arising from the enhanced solubility of calcium carbonate through neutralization reaction with the acidic species. The nss-Mg²⁺/nss-Ca²⁺ ratio (in equivalent units) in coarse fraction ranged from 0.02 to 0.14 (Av=0.06, sd: 0.03) in summer and from 0.05 to 0.26 (Av=0.10, sd: 0.04) in winter months. In comparison, their ratio in fine aerosols varied from 0.04 to 0.25 (Av=0.14, sd: 0.04) during summer and from 0.02 to 0.20 (Av = 0.12, sd = 0.05) in winter.

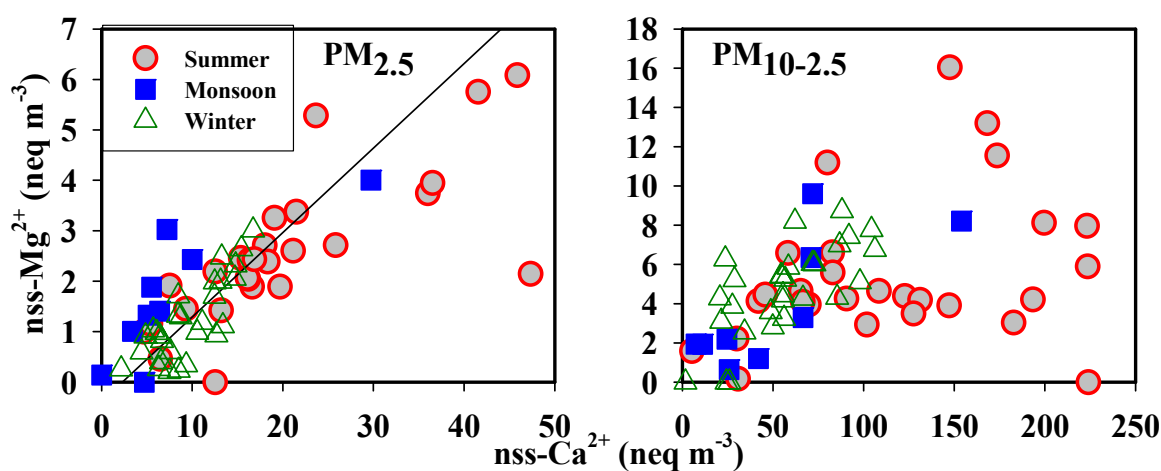


Fig. 4.9 Scatter plot between sea-salt corrected water-soluble Mg²⁺ and Ca²⁺ in equivalence unit.

4.2.3 Inter-annual variability of various ionic ratios

In this section, comprehensive comparisons of weight ratio of different ionic species have been discussed for the PM₁₀ collected during two different years (2006

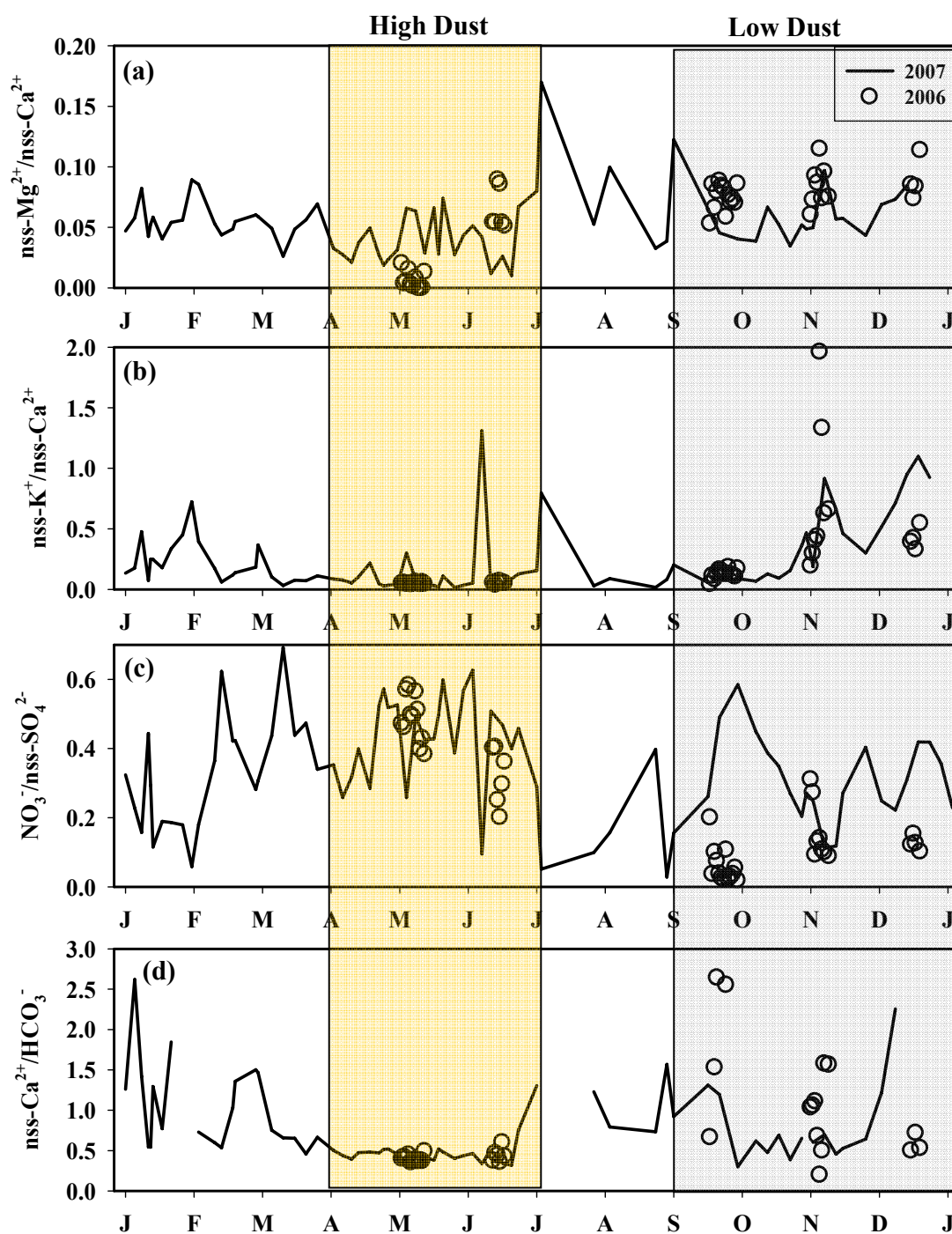


Fig. 4.10 Temporal variability of diagnostic ionic ratios in two subsequent years (2006 and 2007). The two shaded region are representative of high (April-June) and low dust condition (September-December).

and 2007). The sample collection done during 2006 were campaign mode, however, a regular sampling frequency (every 4th or 5th day) have been maintained during 2007. The temporal variability of diagnostic ionic ratios ($\text{nss-Mg}^{2+}/\text{nss-Ca}^{2+}$, $\text{nss-K}^+/\text{nss-Ca}^{2+}$, $\text{NO}_3^-/\text{nss-SO}_4^{2-}$ and $\text{nss-Ca}^{2+}/\text{HCO}_3^-$) have been shown in Fig. 4.10. The annual seasonal cycle has been divided into two different conditions (shown as shaded portion in Fig. 4.10); 1) high dust (April, May and June) and 2) low dust (September – December) based on the dust loading during these two periods. The low dust season is mainly post monsoon period, and lower loading of dust is due to washing out of particles via precipitation. In addition, during wintertime, the winds are from north/north-eastern part of India, which brings air parcel rich in anthropogenic species via long-range transport.

The characteristics $\text{nss-Mg}^{2+}/\text{nss-Ca}^{2+}$ ratios are found to vary from 0.006 to 0.15 with higher values shown during monsoon season (July-August). A large variability is observed during wintertime compared to summer (high dust). This is largely caused by strong source strength in high dust period, when the air parcels are originating from desert region (western India). Similar feature is observed in wintertime of 2006. However, relatively lower ratios were seen in May, 2006. The $\text{nss-K}^+/\text{nss-Ca}^{2+}$ ratio can be used as a tracer for biomass burning. The plot (Fig 4.10b) indicates higher values during winter months (low dust conditions) and lower values in summer period for both years (2006 and 2007). The main source for nss-K^+ is biomass burning products as well as dust. However, the temporal variability of nss-K^+ (shown in Fig. 4.3d) exhibits almost negligible concentration during high dust condition suggesting insignificant contribution of K^+ from regional dust. The lower ratios during high dust period are due to a decrease in nss-K^+ (strength of biomass burning) and subsequent increase in calcium content from dust sources. However, there is a significant enhancement in nss-K^+ (as evident from Fig 4.3d) along with decrease in calcium content resulting in an enhancement of this ratio in low dust condition. As discussed in previous section, the $\text{NO}_3^-/\text{nss-SO}_4^{2-}$ ratio can be used as an indicator of the relative dominance of stationary (coal combustion, biomass burning) versus mobile (vehicular emissions) sources of sulphur and nitrogen in the

atmosphere. The lower ratios (Fig. 4.10c) are attributed to the dominance of stationary pollutant sources and higher ratios to that of mobile sources. However, it is highly unlikely that regional pollution can affect the ambient atmosphere over the sampling location as it is dominated by long-range transport. The ratios are showing large variability in high dust as well as low dust period with values ranging from 0.05 to 0.7. The higher values were observed more frequently during dusty time compared to low dust period. The formation of nitrate on coarser alkaline dust is more favourable than that of sulphate (Ooki and Uematsu, 2005). The sulphate is getting neutralized by the ammonium leading to the higher abundance of nitrate during high dust season. The higher $\text{NO}_3^-/\text{nss-SO}_4^{2-}$ ratios, during May-June are evident in both years as well as lower ratios during wintertime. The ratios were found very low during October-November, 2006, mainly because of the efficient removal of coarser nitrate from atmosphere via precipitation. The $\text{nss-Ca}^{2+}/\text{HCO}_3^-$ ratio can be used as a diagnostic tracer for the degree of chemical interaction of mineral dust with anthropogenic species at this high altitude location. A very low and constant value of this ratio has been seen during high dust period (Fig. 4.10d). However, large variability is observed during low dust conditions. The HCO_3^- content is also found to be below detection limit for some samples, during wintertime, when influence of anthropogenic components (acidic species e.g. SO_4^{2-} and NO_3^-) are dominant. A large variability observed in the ratios during wintertime, is caused due to high abundances and neutralization of anthropogenic constituents (NO_3^- and nss-SO_4^{2-}) by dust particle leading to a decrease in HCO_3^- content. On the contrary, lower and constant ratios are attributed to strong source strength of dust. Thus, it can be interpreted that relatively higher ratio represents chemically un-reacted mineral aerosols, whereas the lower ratios signify chemically aged particles.

4.2.4 Interaction between mineral dust and anthropogenic components

The temporal variability in water-soluble species (Ca^{2+} and HCO_3^-) of atmospheric mineral dust and in particular that of Ca^{2+} follows the abundance of dust in coarse and fine mode aerosols (Fig 4.4 a and b). In fine mode, HCO_3^- abundance is

below detection limit in most of the samples collected during the winter and monsoon as well as in few of the samples in summer month. During wintertime, long-range transport of pollutants from northern India and dominance of SO_4^{2-} in fine mode ($\text{PM}_{2.5}$) provide conducive environmental conditions for the efficient neutralization of SO_4^{2-} by the alkaline dust in semi-arid western India. During summer months, mineral dust (in both coarse and fine mode) transported from the Thar Desert and as far as from the desert regions of Arabia/Oman is enriched in the carbonate content, suggesting that bicarbonate abundance can be used as a diagnostic tracer for the degree of chemical interaction of mineral dust with anthropogenic species at this high altitude location. Relatively high abundance of bicarbonate content would represent nascent mineral aerosols, whereas the lower abundance of HCO_3^- would imply long-range transport of aged aerosols.

In addition to the atmospheric mineral dust, NH_4^+ and K^+ are the dominant species for the neutralization of acidic constituents. The charge balance among ($\text{NH}_4^+ + \text{nss-K}^+$) versus ($\text{nss-SO}_4^{2-} + \text{NO}_3^-$) and ($\text{nss-Ca}^{2+} + \text{nss-Mg}^{2+}$) versus HCO_3^- can be used to investigate the degree of chemical interaction between dust and anthropogenic components (Maxwell-Meier et al, 2004; Rastogi and Sarin, 2005a, b; 2006]. In the absence of dust, complete neutralization of ($\text{nss-SO}_4^{2-} + \text{NO}_3^-$), referred as total acid (TA), is balanced by ($\text{NH}_4^+ + \text{nss-K}^+$). In this study, scatter plots among ($\text{NH}_4^+ + \text{nss-K}^+$) and TA ($\text{nss-SO}_4^{2-} + \text{NO}_3^-$) for the fine and coarse mode (Figs 4.11 a and b, respectively), suggest that the total acid is efficiently neutralized by ($\text{NH}_4^+ + \text{nss-K}^+$) in $\text{PM}_{2.5}$ with data points falling very close to 1:1 line. However, few of the data points with characteristic low concentrations (shown as inset), during summer months, tend to deviate from the equiline indicating lack of availability of NH_4^+ . In contrast, the coarse mode particles show large deviation from 1:1 line (Fig 4.11 b); suggesting that complete neutralization of total acidity is not adequate due to the lower abundances of ($\text{NH}_4^+ + \text{nss-K}^+$) and requires additional neutralizing constituents. The scatter plot between ($\text{nss-Ca}^{2+} + \text{nss-Mg}^{2+}$) and HCO_3^- for both the size fractions has been investigated (Fig. 4.12). For nascent mineral aerosols, in absence of interaction with acidic species, the data points in the scatter-plot should

fall on equiline. However, a significant data points, in both the size fractions, plot towards $(\text{nss-Ca}^{2+} + \text{nss-Mg}^{2+})$ axis (Fig. 4.12) indicating that neutralization of HCO_3^- is predominant during atmospheric transport.

In case of the fine size-fraction, data points for only summer season have been shown; the abundance of HCO_3^- during the monsoon and winter seasons is below the detection limit. These observations bring to focus the role of mineral dust in neutralization of excess acid (EA; units expressed in neq m^{-3}) defined as:

$$\text{EA} = (\text{nss-SO}_4^{2-} + \text{NO}_3^-) - (\text{NH}_4^+ + \text{nss-K}^+) \quad (1)$$

The EA constitutes 65 to 100 % of the total acid in coarse fraction and 10 to 84 % in the fine fraction, with relatively high values occurring during summer months. Furthermore, an overall decreasing trend is observed in the scatter plot (Fig 4.13) between $\text{EA}/(\text{nss-Ca}^{2+} + \text{nss-Mg}^{2+})$ and $\text{HCO}_3^-/(\text{nss-Ca}^{2+} + \text{nss-Mg}^{2+})$; suggesting that the ambient coarse dust plays a dominant role in neutralization of acidic species during the winter and summer seasons. However, neutralization by the fine mode dust is pronounced only during summer (in absence of NH_4^+). A ubiquitous alkaline-nature of wet-precipitation in the semi-arid region (Rastogi and Sarin, 2005c) further supports the chemical data on water-soluble ionic species (Table 4.1 a and b, Fig. 4.2). The amount of bicarbonate neutralized by the excess acid (defined as $\text{nss-Ca}^{2+} + \text{nss-Mg}^{2+} - \text{HCO}_3^-$) divided by total acid (TA) in each size fraction gives the percentage of acid uptake by mineral dust. Based on these calculations, acid uptake by mineral dust in coarse fraction accounts for as much as 95 %, when averaged over the annual seasonal cycle. In fine fraction, acid uptake by mineral dust is evident only during summer season (averaging around 20 %).

4.3 Summary and conclusions:

This study documents large temporal variability in the abundances of water-soluble ionic constituents (Na^+ , NH_4^+ , K^+ , Mg^{2+} , Ca^{2+} , Cl^- , NO_3^- , SO_4^{2-} , and HCO_3^-),

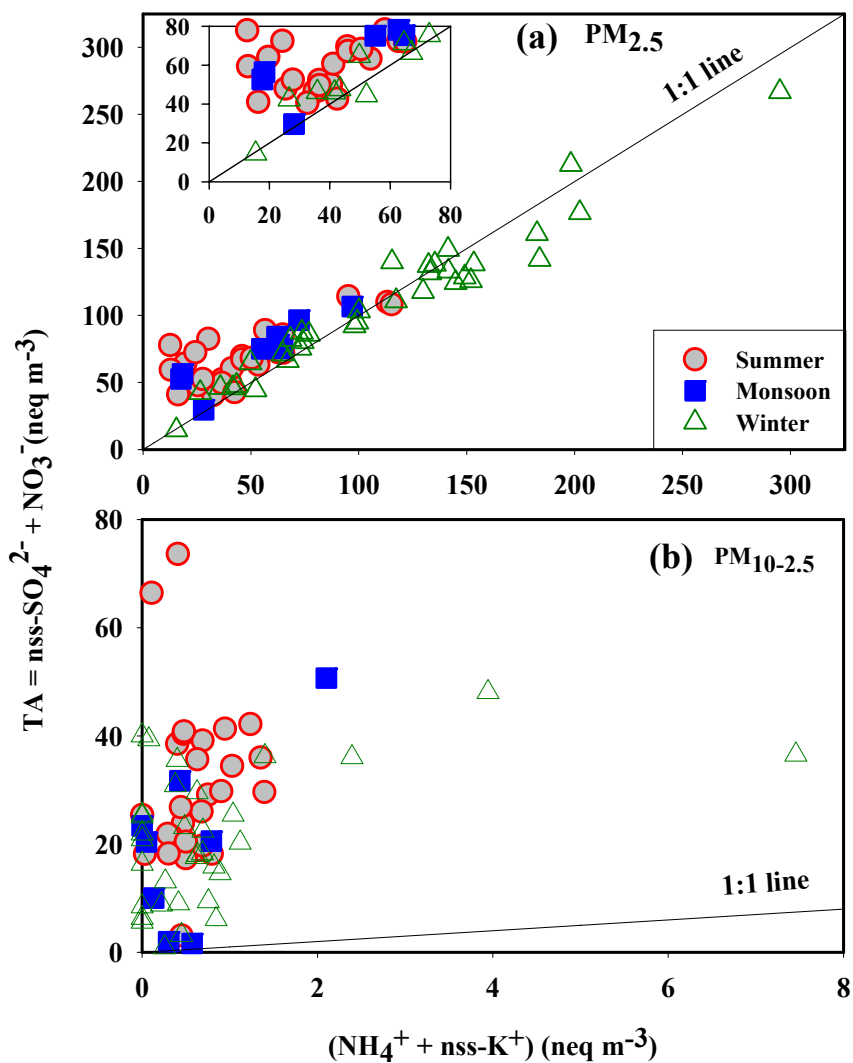


Fig. 4.11 Scatter plot between total acid (TA) and $(\text{NH}_4^+ + \text{nss-K}^+)$ for (a) fine and (b) coarse aerosols. Data points falling along 1:1 line in fine mode suggest the neutralization of TA by $(\text{NH}_4^+ + \text{nss-K}^+)$ with exception of data points during summer seasons (characterized by low concentrations as shown in inset). In coarse mode, large deviation from equiline requires neutralization by the alkaline dust.

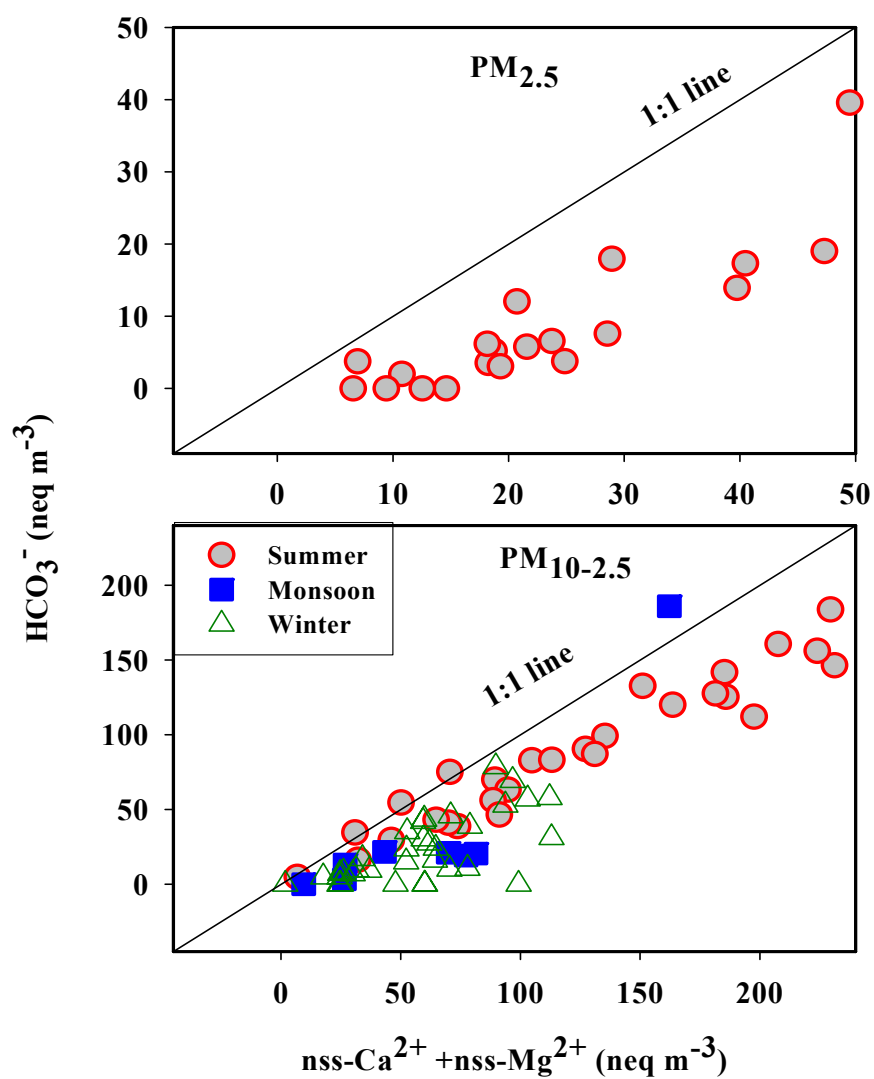


Fig. 4.12 Scatter plot between $(\text{nss-Ca}^{2+} + \text{nss-Mg}^{2+})$ and HCO_3^- ; deviation of data points towards X-axis suggest neutralization of HCO_3^- ion via uptake of acidic species by mineral aerosols.

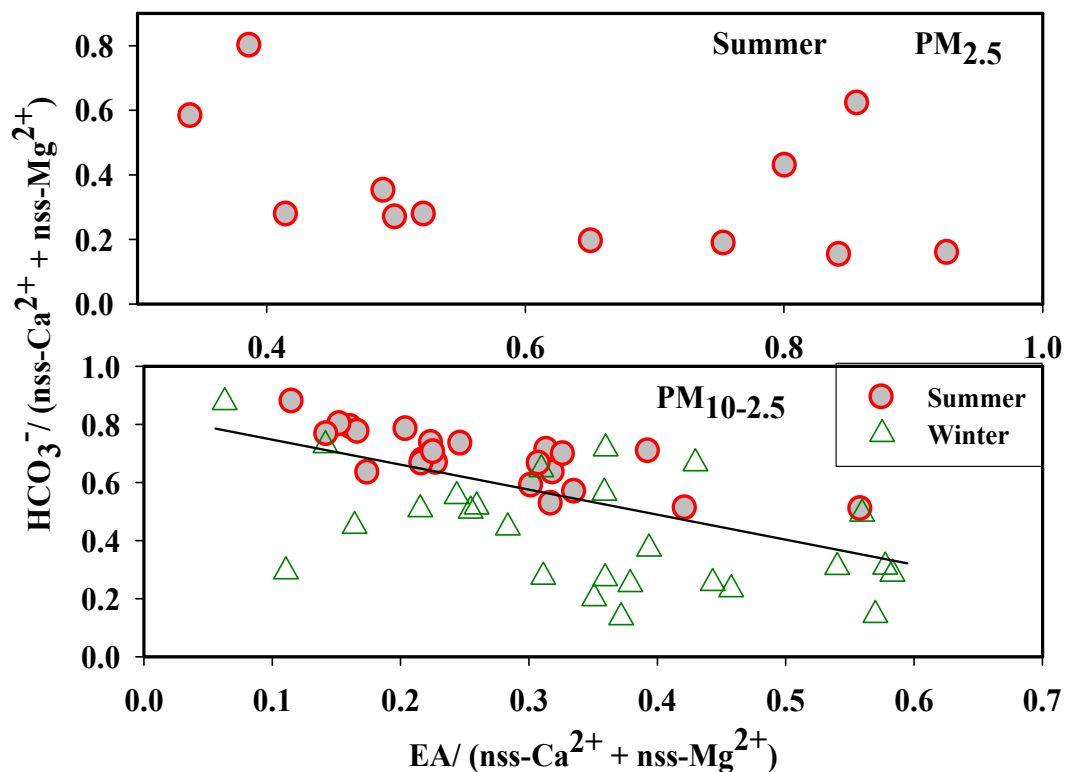


Fig. 4.13 An overall decreasing trend observed in the scatter plot between “excess acid” (EA) and HCO_3^- (normalized to the abundances of Ca^{2+} and Mg^{2+}) provides a direct evidence for the neutralization of acidic species by mineral dust. Although a best-fit line has been drawn through the data points, linear regression parameters are not significant due to large scatter.

as measured in the fine ($\text{PM}_{2.5}$) and coarse ($\text{PM}_{10-2.5}$) mode aerosols from a high-altitude site in high-dust semi-arid region of western India. The major findings are:

- 1) A uniform dominance of nss-Ca^{2+} and HCO_3^- in the coarse mode ($\text{PM}_{10-2.5}$) over the annual seasonal cycle suggests dominant abundance of carbonate rich mineral dust. This is in sharp contrast to the higher abundances of NH_4^+ and nss-SO_4^{2-} in fine ($\text{PM}_{2.5}$) aerosols.

- 2) During wintertime, the relative enrichment of NH_4^+ and nss-SO_4^{2-} and their significant linear relationship in fine aerosols, suggests their predominant anthropogenic source. Significantly lower abundances of these species, during summer months, impart a characteristic seasonal variability in the water-soluble ionic composition. Documentation of such major seasonal shift in aerosol chemical composition is a unique feature of the data from high-dust semi-arid region, hitherto lacking in the literature.
- 3) The mineral dust serves as a dominant neutralizing component for the atmospheric acidic species and on average accounts for as much as 95% of the acid uptake in coarse mode. In fine mode, during summer months, occurrence of dust accounts for nearly 20% of the acid neutralization.

This brings to focus the role of semi-arid regions and atmospheric mineral dust in modifying the abundances of atmospheric acidic species (SO_4^{2-} and NO_3^-) and their size distribution from fine to coarse mode. This in turn changes the surface properties of the mineral aerosols making them active sites for the heterogeneous phase chemical reactions involving SO_x , NO_x and O_3 . The data presented in this study provides a better insight into the relationship between water-soluble ions and mineral dust that requires appropriate parameterization in the current climate models. Also, chemical interaction of dust, near to the source region, with the long-range transport of pollutants is an important process to be accounted for in the regional chemical transport models.

MINERAL AEROSOLS OVER ARABIAN SEA

5.1 Introduction

The long-range transport of continental aerosols from natural (mineral dust) and anthropogenic (SO_4^{2-} , NO_3^-) sources to the remote marine environment has been recognized as a major source for many biogeochemically important trace metals and nutrients to the world oceans (Prospero et al., 1981; Duce, 1986; Martin et al., 1989; Duce et al., 1991; Jickells, 1999; Arimoto et al., 2001; Jickells et al., 2005). Mineral dust is one of the dominant components of aerosol budget, accounts for 36% of the global aerosol emissions and has been increasingly recognized to influence the regional and global atmospheric chemistry (Dentener et al., 1996; Levine et al., 1996; Tegan et al., 1996; Tang et al., 2004a,b; Laskin et al., 2005; Ooki and Uematsu, 2005; Rastogi and Sarin, 2006). These dust particles are not readily soluble in water but mineralogical studies have shown that processed mineral dust in the atmosphere has strong affinity for water (Koretsky et al., 1997) and can act as cloud condensation nuclei (CCN) (Rosenfeld et al., 2001).

The Arabian Sea, one of the most biologically productive oceanic regions and surrounded by the arid (Oman desert on the west) and semi-arid (Thar desert in western India) continental regions, provides an ideal marine environment to study the inflow of both natural and anthropogenic chemical constituents and their impact on the surface ocean biogeochemistry. With its unique geographical setting and well-known annual reversal in the wind regimes, SW-winds at the onset of SW-monsoon (May-onwards) and NE-winds during winter months (December - March), are expected to impart characteristic changes to the aerosol composition in the Arabian Sea-atmospheric boundary layer (AABL). During the

US-JGOFS Arabian Sea study, Tindale and Pease, (1999), had provided an overview of the transport pathways of dust and sea-salts on an annual basis except for inter-monsoon period (April-May). Studies by Johansen et al. (1999), and Siefert et al. (1999), had reported on the major ions and trace metal composition of aerosols over the Arabian Sea. However, in the latter study, aerosol samples were confined only to the western part of Arabian Sea.

In the present study, a cruise was undertaken in the Arabian Sea during 18th April – 11th May 2006 as a part of the Integrated Campaign for Aerosol Trace Gases and Radiation Budget (ICARB) sponsored by ISRO-Geosphere Biosphere Programme. Our specific objective is to characterize the chemical composition of aerosols in the AABL under the influence of the northward progression of ITCZ- a characteristic feature over the tropical region. The ITCZ also acts as a barrier to restrict the transport of continental species (anthropogenic and natural) to the south of ITCZ. In an earlier study, Norman et al., (2003), has shown that, during the NE-monsoon, a sharp gradient occurs across the ITCZ with concentration of nss-SO_4^{2-} , NH_4^+ , and nss-K^+ decreasing by an order of magnitude on the southern side of ITCZ. The entrainment of continental emission products, north of ITCZ (transported via NE/NW-winds), are expected to impact the chemical composition of aerosols in the central and northern Arabian Sea with the northward progression of ITCZ during April-May. This forms the basis for undertaking a cruise during the spring inter-monsoon season. Furthermore, this study (cruise track is shown in Fig. 5.1) provides a comprehensive chemical composition data set consisting of water-soluble constituents, crustal elements and carbonaceous species in the aerosols covering a vast expanse of the Arabian Sea.

5.2 Results and discussion

5.2.1 Air-mass back trajectory analysis:

The seven-day back trajectories of air masses, for five different dates covering the cruise period, were computed using the Hysplit-4 model and FNL-meteorological data set at 50, 100, 500 m altitude (Fig. 5.2) in order to track the origin of air parcels at various sample locations. The selected back trajectories (Fig. 5.2) are representative of the transport pattern observed during the cruise.

The back trajectory on the first day of the cruise (18th April, 06) describes the movement of air parcel originating off the coast of Oman. Subsequently all back trajectories for 19th to 28th April show almost the same trend as represented by the trajectory of 21st April (Fig. 2) for transect: 9.00 °N, 60.19 °E. On 27th April 2006, the high altitude winds (500 m) originated over the western Arabian Sea before arriving at the sampling position 14.18 °N, 72.88 °E (Fig.2). From 29th April onwards, air parcels mainly originated within the AABL except on 8th May when high altitude winds were located over the urban region in western India (Fig. 5.2). Of the total 22 days cruise, the frequency of trajectories originating off the coast of Oman was 9.

In order to describe the spatial distribution of different aerosol components and chemical species, the sampling transects have been grouped into three different latitudinal regions (Fig. 5.1) Region A: 8-12 °N representing south Arabian Sea, Region B: 12-16 °N encompassing central Arabian Sea and Region C: 16-22 °N designating north Arabian Sea. We thus summarize that air parcels in Region A originated mainly from north-western Arabian Sea (off the coast of Oman); whereas air parcels were located within the AABL over the other two Regions (except on 27th April and 8th May). The position of ITCZ, as monitored during the cruise, was located between 3-4 °S on 18th April, 0-1 °N on 30th April and 5-6 °N on 8th May (positions for 30th April and 8th May are shown in Fig. 5.3).

5.2.2 Total suspended particulate (TSP) concentrations:

Overall, the TSP varied considerably from 8.2 to 46.9 $\mu\text{g m}^{-3}$ ($A_v = 24.7 \pm 10.4 \mu\text{g m}^{-3}$) whereas the average abundance pattern in the three different latitude regions (i.e. A, B, C) is summarized in Table-5.1 and Fig. 5.4 a. The TSP abundance in regions A and C are comparable (26.6 and 28.7 $\mu\text{g m}^{-3}$ respectively); whereas central region (Region B) is characterized by relatively lower abundance of TSP (17.2 $\mu\text{g m}^{-3}$, Fig. 5.4 a). The highest TSP (46.9 $\mu\text{g m}^{-3}$) was observed on 8th May in the northern most transect (Region C) when the winds were confined within the AABL (Arabian Sea-atmospheric boundary layer). During the spring inter-monsoon, the winds are predominantly northwesterly pass directly over Oman and Wahiba sand-sea areas before entering the Arabian Sea.

Due to its proximity to desert area, one would expect high abundance of dust in the northern Arabian Sea (and hence high TSP). On the contrary, we observe relatively high mass fraction of dust in the southern transect with a conspicuous northward decreasing trend (Fig. 5.4 b). This conspicuous spatial pattern is also supported by the air-mass back trajectories. In northern section, the winds were localized within the AABL and shifted to south-westerly direction. A simultaneous study on aerosol optical properties has shown dominance of coarse mode fraction (mineral dust and sea-salts) over the Arabian Sea (Kedia and Ramchandran, 2008).

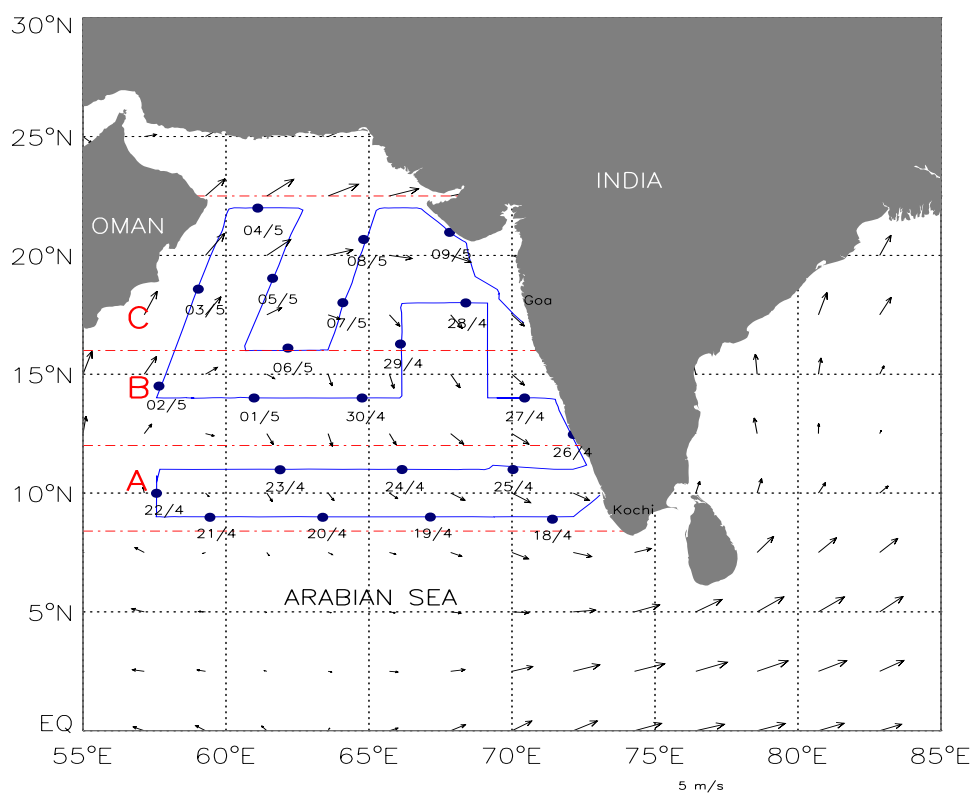


Fig. 5.1 Surface-level average wind vectors along the cruise track (cruise no. SK223B) during 18 April to 10 May 2006 in the Arabian Sea.

5.2.3 Water-Soluble constituents:

Water-soluble species ranged from 2.1 to 33.4 $\mu\text{g m}^{-3}$ and their contribution to TSP varied from 22 to 71%. The cation and anion abundances in

three different latitude regions are summarized in Fig. 5.5; with dominant contribution of Na^+ and Ca^{2+} to the cation balance (Fig. 5.5 a); and Cl^- and SO_4^{2-} among the anions (Fig. 5.5 b). The sea-salt concentration was estimated from the Na^+ and Cl^- abundance based on following relation:

$$\text{Sea-salt } (\mu\text{g m}^{-3}) = \text{Cl}^- (\mu\text{g m}^{-3}) + 1.47 \text{Na}^+ (\mu\text{g m}^{-3}) \quad (1)$$

Where 1.47 is the ratio of $(\text{Na}^+ + \text{K}^+ + \text{Mg}^{2+} + \text{Ca}^{2+} + \text{SO}_4^{2-} + \text{HCO}_3^-) / \text{Na}^+$ in Sea water (Holland, 1978; Quinn et al., 2004). This approach excludes the contribution of non-sea-salt K^+ , Mg^{2+} , Ca^{2+} , SO_4^{2-} , and HCO_3^- in the sea-salt mass and allows for the loss of Cl^- due to its depletion through chemical reaction. It also assumes that all measured Na^+ and Cl^- are derived from sea-salts. In this study, $\text{Mg}^{2+}/\text{Na}^+$ molar ratio is 0.20; nearly same as that in the sea-salts (0.22, Keene et al., 1986). Hence Na^+ has been used as a reference for calculating nss-component of other constituents. The contribution of sea-salts to TSP is relatively low in the southern (Region A) and central Arabian Sea (Region B); whereas it is maximum in the northern region (Fig. 5.4 a). The increase in sea-salt contribution is a manifestation of increased wind speeds (~ 9 m/s) during the later part of the cruise and sampling sites along the coastal region. The scatter plot of Cl^- versus Na^+ (Fig. 5.6) reflects tendency of the data points below the seawater line (slope = 1.16), indicating pronounced deficiency of chloride with respect to Na^+ caused by reaction of sea-salt with acidic species (NO_3^- and SO_4^{2-}) (Savoie & Prospero, 1982; Wu and Okada, 1994; Kerminen et al., 1998; Zhuang et al., 1999). This chemical uptake of NO_3^- and SO_4^{2-} onto sea-salt particles has been suggested to be the major pathway for the formation of coarse mode NO_3^- and nss- SO_4^{2-} in marine boundary layer (Sievering et al., 1991; 1995; Chameides and Stelson, 1992). The Chloride deficit has been calculated as follows:

$$\text{Cl}^- \text{ deficit } (\%) = 100[(1.16 \text{Na}^+) - \text{Cl}^-_m] / (1.16 \text{Na}^+) \quad (2)$$

Table 5.1: Concentrations of chemical species ($\mu\text{g m}^{-3}$) in the Arabian sea-atmospheric boundary layer representing three different regions with average, minimum and maximum values.

Species	Region A 8-12 $^{\circ}\text{N}$ n=11	Region B 12-16 $^{\circ}\text{N}$ n=5	Region C 16-22 $^{\circ}\text{N}$ n=5	Average \pm s.d	Minimum	Maximum
TSP	26.6 \pm 8.5	17.2 \pm 8.0	28.7 \pm 13.5	24.7 \pm 10.4	8.2	46.9
Mineral dust	14.1 \pm 6.6	7.4 \pm 3.4	7.8 \pm 2.6	10.7 \pm 5.9	2.7	23.7
Mineral dust(%)	51.6 \pm 13.6	42.3 \pm 7.7	32.2 \pm 15.1	44.1 \pm 14.7	13.0	77.7
Sea-Salt	2.7 \pm 1.9	2.2 \pm 2.4	12.0 \pm 12.4	5.0 \pm 7.4	0.3	30.4
Sea-Salt(%)	9.7 \pm 6.3	11.1 \pm 8.4	33.0 \pm 23.9	16.2 \pm 16.4	1.9	64.7
nss-SO₄²⁻	3.6 \pm 1.2	2.2 \pm 0.8	2.3 \pm 1.1	2.9 \pm 1.2	1.3	5.7
nss-SO₄²⁻(%)	13.8 \pm 3.7	13.7 \pm 3.7	9.7 \pm 5.1	12.7 \pm 4.3	3.0	20.7
Al	1.13 \pm 0.53	0.59 \pm 0.27	0.63 \pm 0.21	0.85 \pm 0.47	0.21	1.89
Ca	1.30 \pm 0.62	0.48 \pm 0.29	0.58 \pm 0.18	0.89 \pm 0.60	0.13	2.48
Fe	0.61 \pm 0.29	0.28 \pm 0.13	0.30 \pm 0.11	0.44 \pm 0.27	0.09	1.01
Na⁺	1.19 \pm 0.68	0.96 \pm 0.85	1.49 \pm 0.87 ^s	1.92 \pm 2.43	0.22	10.3
K⁺	0.10 \pm 0.03	0.09 \pm 0.04	0.19 \pm 0.14	0.12 \pm 0.08	0.04	0.42
Mg²⁺	0.14 \pm 0.06	0.08 \pm 0.05	0.41 \pm 0.47	0.20 \pm 0.26	0.04	1.13
Ca²⁺	1.21 \pm 0.59	0.43 \pm 0.26	0.62 \pm 0.28	0.85 \pm 0.56	0.12	2.24
Cl⁻	0.95 \pm 0.98	0.75 \pm 1.14	1.44 \pm 1.69 ^s	2.16 \pm 3.88	BDL	15.3
NO₃⁻	0.58 \pm 0.44	0.23 \pm 0.31	0.49 \pm 0.53	0.40 \pm 0.40	BDL	1.34
NH₄⁺	BDL*	BDL	BDL	BDL	BDL	BDL
EC	0.10 \pm 0.04	0.07 \pm 0.02	0.07 \pm 0.02	0.10 \pm 0.08	BDL	0.20
OC	0.24 \pm 0.18	0.11 \pm 0.02	0.27 \pm 0.07	0.27 \pm 0.07	BDL	0.68
POM	0.50 \pm 0.39	0.24 \pm 0.06	0.56 \pm 0.27	0.44 \pm 0.32	0.21	1.42

^sTwo data points with high abundance of Na⁺ (6.2 and 10.3 $\mu\text{g m}^{-3}$) and Cl⁻ (9.7 and 15.3 $\mu\text{g m}^{-3}$) have not been considered.

*Below detection limit

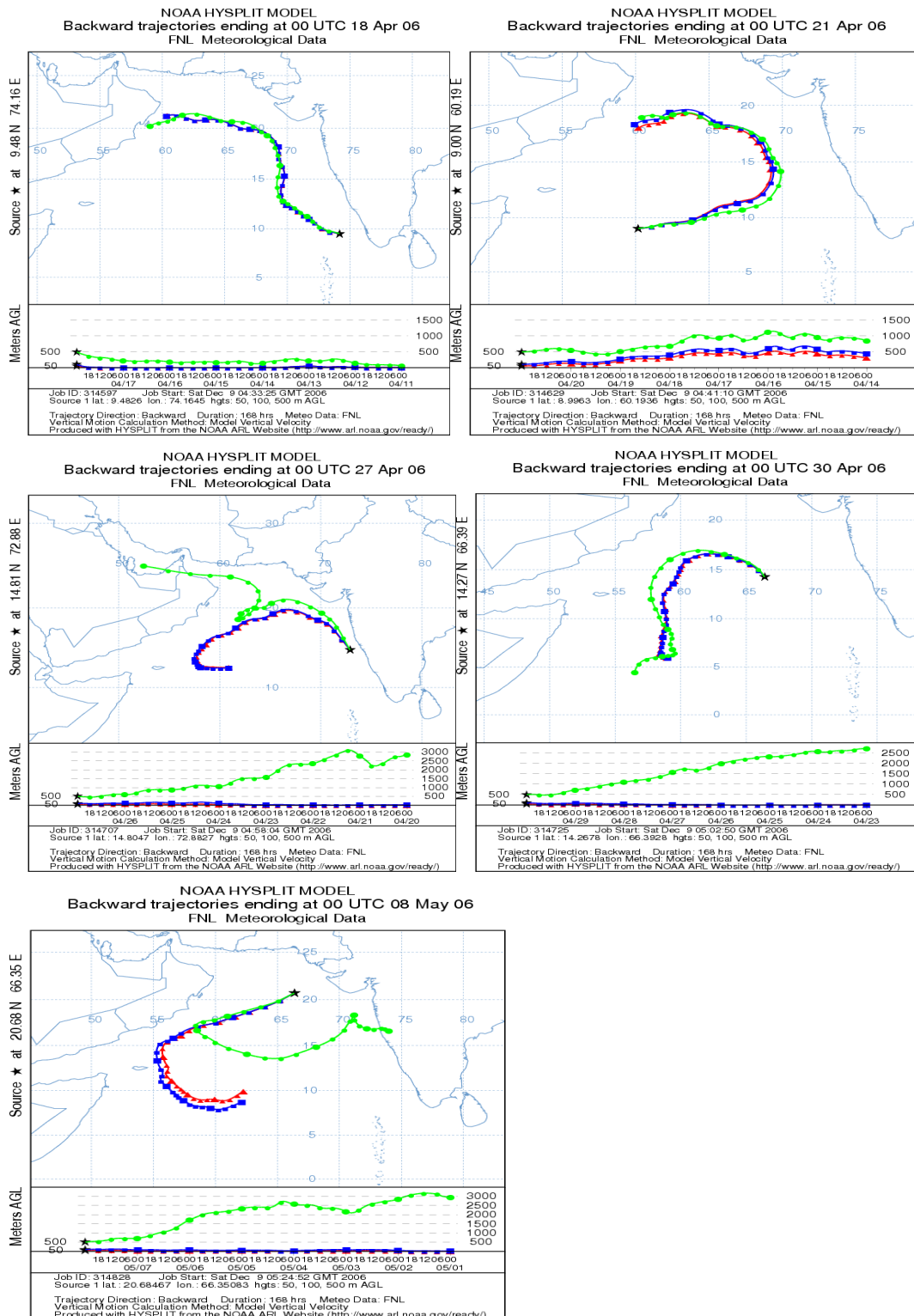


Fig. 5.2 Typical 7-day air-mass back trajectories at three (50, 100, 500 m) arrival heights representing different air-parcels for five different dates during the cruise period.

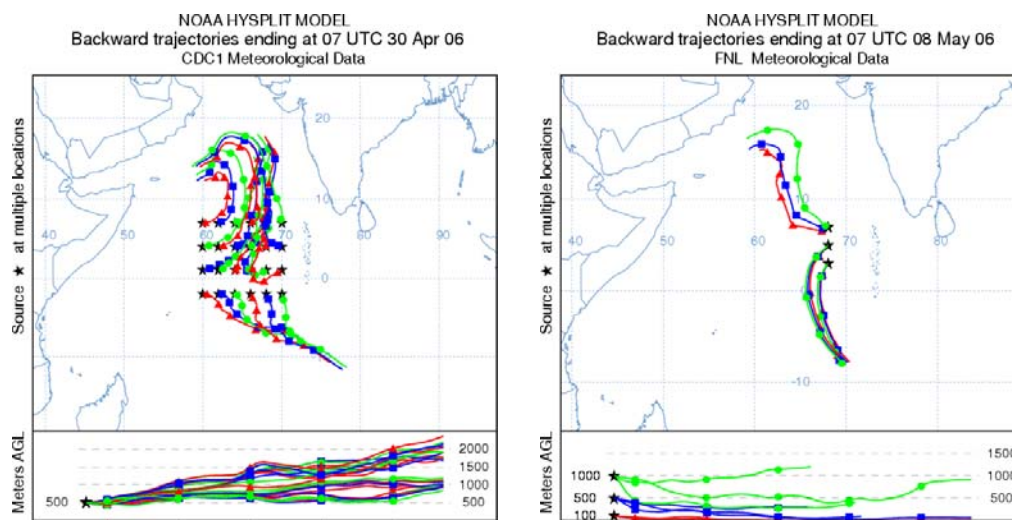


Fig. 5.3 Air-mass back trajectories showing northward progression of ITCZ during the inter-monsoon period.

Where $(Na^+ * 1.16)$ is expected Cl^- concentration from sea-salts, in absence of any loss of Cl^- and all Na^+ in ambient aerosols is of sea-salt origin, Cl^-_m is chloride measured in the sample.

On a spatial scale, aerosol concentration of NO_3^- is 5 to 10 times lower than that of SO_4^{2-} (Table-5.1). Therefore, Cl^- deficit is largely attributed to chemical reaction involving uptake of SO_4^{2-} by sea-salts. The Cl^- deficit (%) varied from 12-100 %, in proportion to the abundance of nss- SO_4^{2-} ($r^2 = 0.67$, for the linear regression), suggesting that sea-salts are one of the potential sink for (anthropogenic) SO_2 in the AABL. This observation is in close agreement with the result obtained from other open ocean regions (Graedel and Keene, 1995). In an urban site (Mumbai, $19^{\circ}23' N$, $72^{\circ}50' E$) on west-coast of India, Venkatraman et al., (2002), had reported Cl^- deficit of 78 ± 11 and 39 ± 24 % in two different sampling periods during January to March and attributed this deficiency to the reaction of HNO_3 with sea-salt particles forming coarse mode nitrates. It is further suggested that depletion would be favoured in fine mode under high humidity conditions (Venkatraman et al., 2002). The contribution of Mg^{2+} and K^+ to the total water-soluble components is insignificant as seen in Fig. 5.5 b.

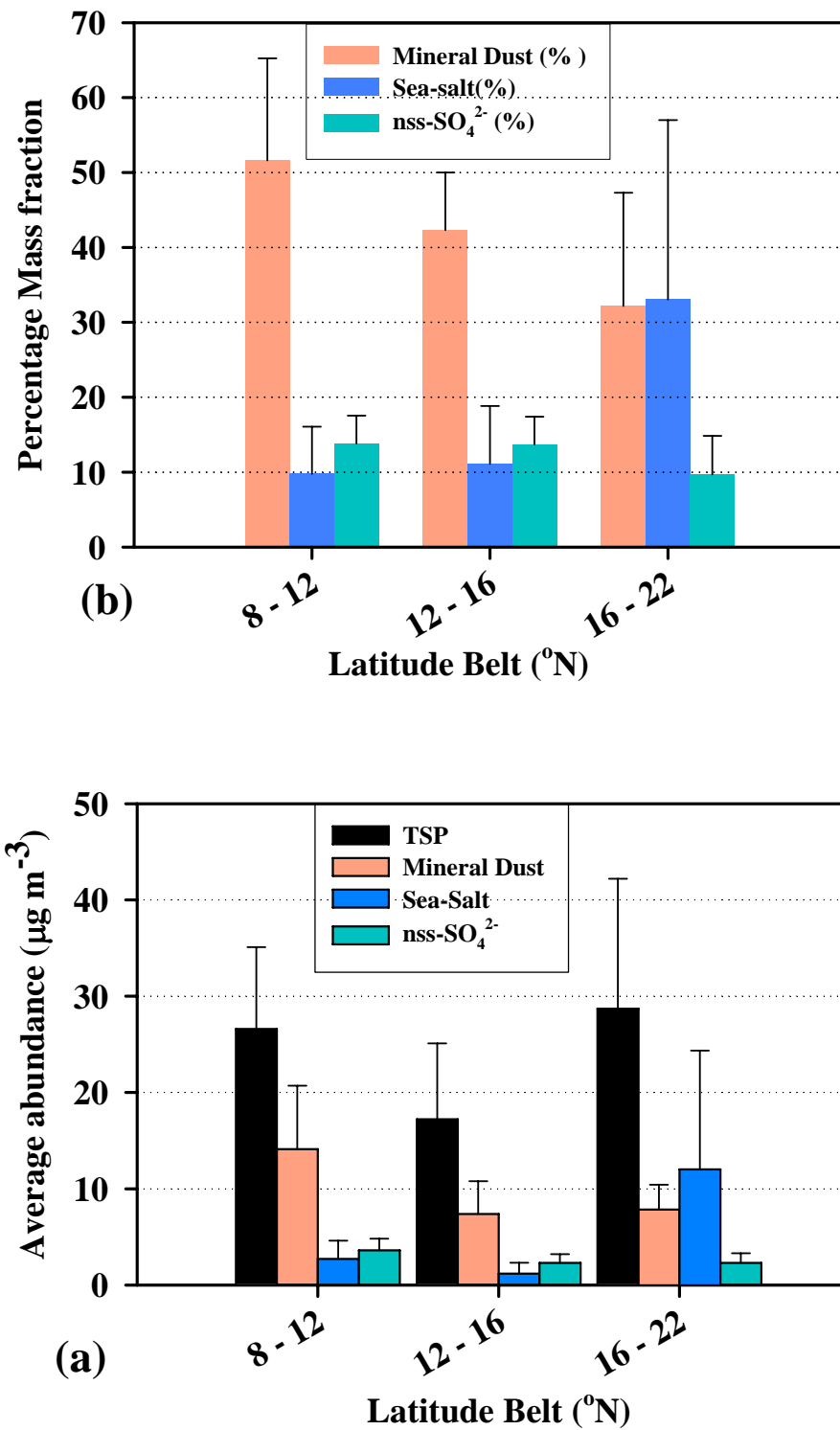


Fig. 5.4 (a) Average abundances and spatial variation of aerosol components ($\mu\text{g m}^{-3}$) in the three Regions (A, B, and C) identified based on wind regimes. (b) Percent mass fraction of mineral dust, sea-salts and nss- SO_4^{2-} to TSP.

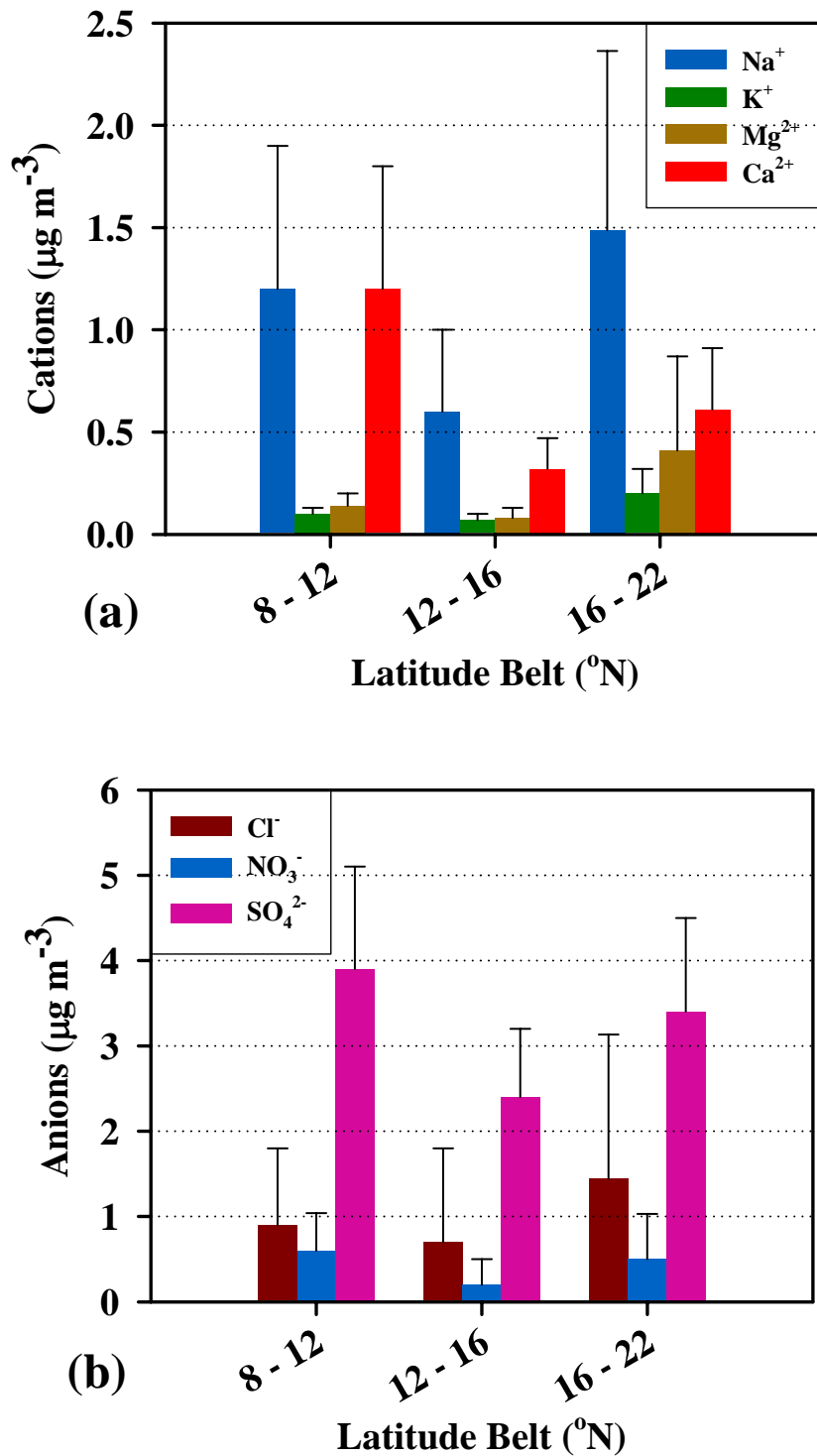


Fig. 5.5 Spatial variations in water-soluble components (a) cations, dominated by Ca^{2+} and Na^+ and (b) anions, dominated by SO_4^{2-} followed by Cl^- . The high data points for Na^+ and Cl^- (Table-1) have not been included in computing mean values.

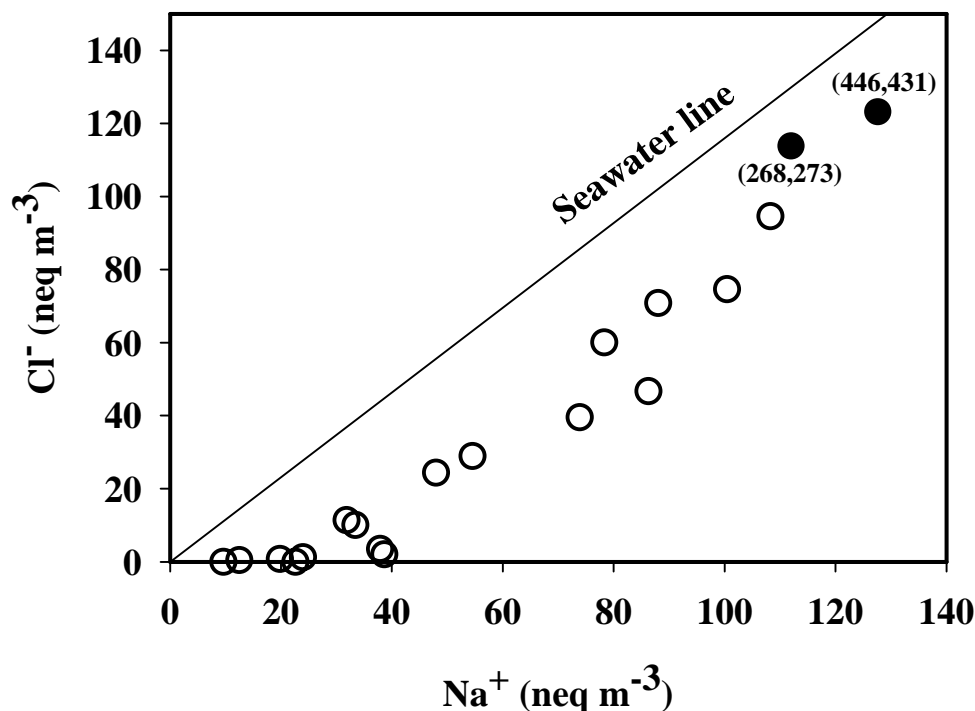


Fig. 5.6 Scatter plot for Na⁺ and Cl⁻; all data points falling below the sea-water line imply large scale depletion of Cl from NaCl occurring in the ABL.

The nss-Mg²⁺ is negligible indicating that sea-salt is the only source for water-soluble Mg²⁺; whereas nss-K⁺ contributes no more than 50% to the soluble K⁺ (Table-5.1). The abundance of nss-SO₄²⁻ is estimated by subtracting sea-salt SO₄²⁻ from the total SO₄²⁻, where sea-salt component is inferred from measured Na⁺ concentration and the constant SO₄²⁻/Na⁺ ocean water ratio of 0.252 (Keene et al., 1986). In this study, abundance of nss-SO₄²⁻ varied from 1.3 – 5.7 μg m⁻³ (Av = 2.9, sd = 1.2) and, on average, accounts for 12.7 % of TSP (Table-5.1). In an earlier study, during the intermonsoon period, Johansen et al., (1999), have reported nss- SO₄²⁻ concentration as 2.1±1.2 μg m⁻³ (constituting 9.2 % of TSP); of which 65% contribution is of anthropogenic nature, 21% biogenic and 14% derived from gypsum. In this study, spatial variation in mass fraction of nss-SO₄²⁻ concentration is not significantly pronounced (Fig. 5.4 b). In southern section (Region A (Fig.5.1)), nss-SO₄²⁻ averages around 13.8±3.7 % of TSP (Table-5.1), compared to its contribution of 9.7±5.1 % observed in northern section (Region C). The higher nss-SO₄²⁻/SO₄²⁻ ratio of 0.86±0.15 suggests dominance of

anthropogenic sulphate during the spring inter-monsoon. Johansen et al. (1999), have demonstrated similar impact of anthropogenic inputs ($\text{nss-SO}_4^{2-}/\text{SO}_4^{2-} = 0.76 \pm 1.04$) during inter-monsoon compared to south-west monsoon season ($\text{nss-SO}_4^{2-}/\text{SO}_4^{2-} = 0.33 \pm 0.13$) over the Arabian Sea. It is noteworthy that during the NE-monsoon this ratio increases up to 0.95 ± 0.28 and 0.91 ± 0.62 in two different sets of sample collection because of continental inflow from surrounding region (Johansen and Hoffmann, 2004).

The scatter plot between nss-SO_4^{2-} and nss-Ca^{2+} with a significant correlation, $r^2 = 0.68$ and slope = 0.73, indicates the neutralization of anthropogenic nss-SO_4^{2-} , produced largely by heterogeneous oxidation of SO_2 by $\text{H}_2\text{O}_2/\text{O}_3$, on alkaline dust (CaCO_3). The ratio of water-soluble calcium (nss-Ca^{2+}) to total Ca approaching close to unity is a further evidence for the enhanced solubility of calcium (CaCO_3) as it undergoes acid uptake reaction. In a recent study, Rastogi and Sarin (2006) have documented uptake of acidic species by mineral dust component (CaCO_3) over an urban area located in a semi-arid region of western India. Similar field observations over the continental sites (Sullivan et al., 2007) and marine environment (Ooki and Uematsu, 2005) have been demonstrated based on correlation among Ca^{2+} and NO_3^- measured in bulk-aerosols. Unlike sulphate, abundance of NO_3^- is dominated by coarser mode as a result of heterogeneous reaction of gaseous HNO_3 with mineral dust particles (Ooki and Uematsu, 2005). The correlation coefficient is further significant ($r^2 = 0.79$) for the scatter plot between ($\text{nss-SO}_4^{2-} + \text{NO}_3^-$) and nss-Ca^{2+} in this study

5.2.4 Mineral aerosols over Arabian Sea:

The abundance of aluminum (Al) is typically used as an indicator of mineral aerosols (Duce and Tindale, 1991). Based on the assumption that the ratio of Al in mineral aerosols to be the same as in UCC (upper-continental crust with Al content of 8%, Taylor and McLennan, 1985), the atmospheric abundance of mineral dust ranged from 2.7 to 23.7 $\mu\text{g m}^{-3}$ in the AABL (Table-5.1). This is in contrast to the high dust concentrations, 12-117 $\mu\text{g m}^{-3}$ (Av: 50 $\mu\text{g m}^{-3}$), reported over the Arabian Sea (Pease et al., 1998).

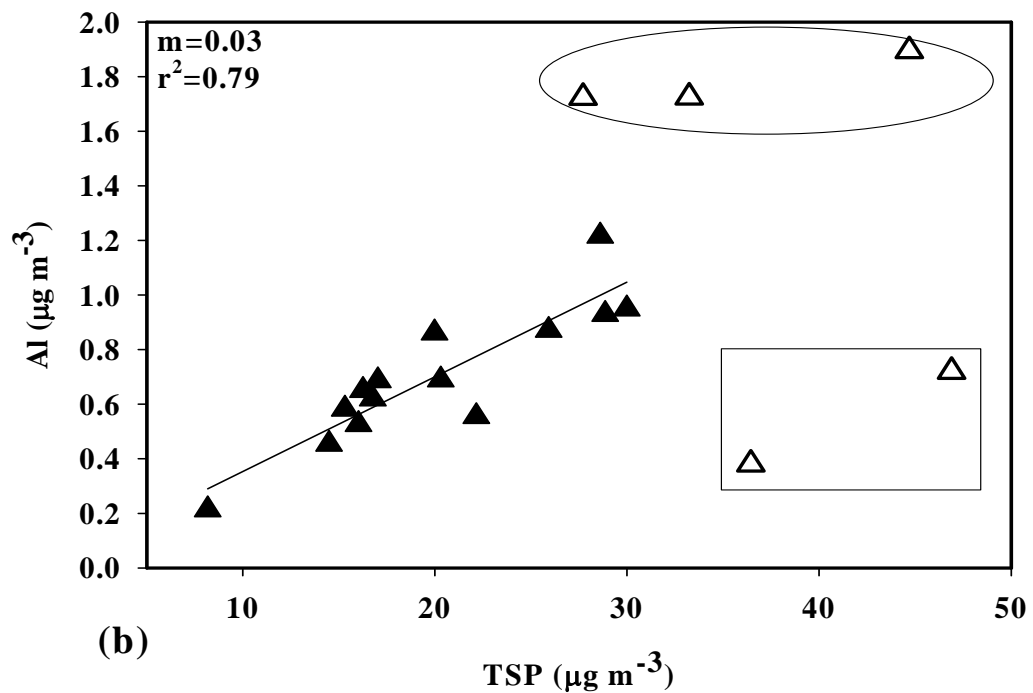
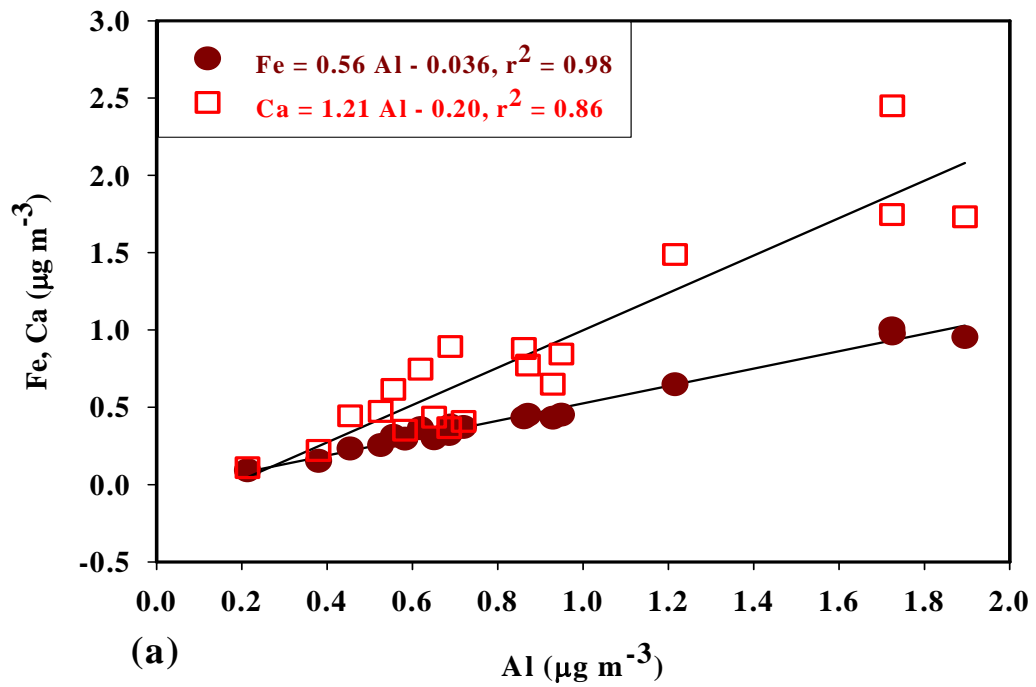


Fig. 5.7 (a) Scatter plot of Al with crustal components (Fe and Ca) showing characteristic ratios (Average Fe/Al = 0.51, and Ca/Al = 0.89) representing the mineral aerosols in the Arabian Sea-atmospheric boundary layer. (b) Linear regression of Al with TSP indicates characteristic feature of high Al/TSP ratio in the sample collected along the west-coast of India.

The mass fraction of dust in the three different latitude Regions (A, B, and C) is shown in Fig. 5.4 b; with conspicuous decreasing trend from southern to northern transect. This decreasing pattern is associated with the changes in wind regimes from north-westerlies (in the southern section) to the south-westerlies prevailing in the north Arabian Sea. The north-westerlies transport dusts from the coast of Oman; whereas high winds (9-10 m/s) prevalent in the northern transect during the cruise period are associated with relatively high abundance of sea-salts. The sources of dust over the Arabian Sea primarily include transport from Oman, Yemen and Rub-Al-Khali sand-sea and, to some extent, the sabkha complexes along the south-eastern coast-line of Arabian Peninsula. The Wahiba sand-sea is an active dune field located on the eastern coast of Oman. Most of the sediments throughout the Wahiba area consist primarily of carbonate, quartz and notable amounts of ultramafic minerals (e.g. olivine and pyroxene) originating from an ophiolite (abducted oceanic crust) sequence (Pease et al., 1998).

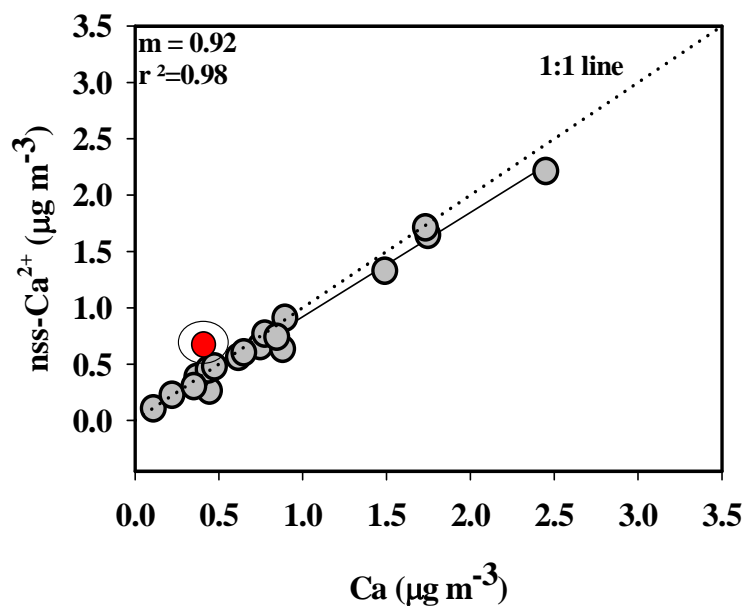


Fig. 5.8 Scatter plot among total Ca and water-soluble Ca²⁺. Almost all data points falling close to 1:1 line imply enhanced solubility of calcium due to acid-uptake (SO₄²⁻) by mineral dust.

In an attempt to characterize the mineral aerosols over the Arabian Sea, we have analyzed other crustal components like Fe and Ca. The concentrations of

these crustal elements vary as Fe: 0.09 to 1.01 and Ca: 0.1 to 2.5 $\mu\text{g m}^{-3}$, respectively. The linear regression analysis performed for these elements with respect to Al (Fig. 5.7 a), yields significant regression coefficients: Fe ($r^2 = 0.98$) and Ca ($r^2 = 0.86$) suggesting that there is no fractionation of mineral dust (silicate grain) and Ca-rich particles (CaCO_3) during their transport to AABL. The Fe/Al ratio varied from 0.40 to 0.58 (Average = 0.51; sd = 0.05), in comparison to Fe/Al ratio in upper continental crust (0.44; Taylor and McLennan, 1985). It is also noteworthy that the scatter plot of Al with TSP (Fig. 5.7 b) exhibit significantly higher Al/TSP ratio for some of data points (encircled data in Fig. 7b). These data points, coincidentally, represent the samples collected along the west-coast of India. On the other hand Ca/Al ratio ranged from 0.51 to 1.42 (Average = 0.89; sd = 0.27), a factor of 2-3 higher than that expected from UCC (0.38; Taylor and McLennan, 1985); indicating that mineral aerosols in the AABL are enriched in calcium carbonate with high capacity to neutralize acidic species. The presence of carbonate rich dust over Arabian Sea and its potential to remove acidic species (nss-SO_4^{2-}) is reflected from the significant linear regression among nss-SO_4^{2-} and nss-Ca^{2+} ; with molar ratio of $\text{Ca}^{2+}/\text{SO}_4^{2-}$ ranging from 0.20 to 1.16, Average = 0.61 and positive intercept ($\text{nss-SO}_4^{2-} = 1.52 \mu\text{g m}^{-3}$); attesting to the fact that major contribution from gypsiferous soils is very unlikely. As stated earlier, a linear plot between water-soluble nss-Ca^{2+} and total calcium with significantly high correlation coefficient ($r^2 = 0.97$) demonstrates that sparingly soluble CaCO_3 undergoes in-situ chemical transformation reaction with nss-SO_4^{2-} to form CaSO_4 and hence increase in solubility of calcium (Fig. 5.8).

5.2.5 Carbonaceous aerosols over Arabian Sea:

The organic carbon (OC) and elemental carbon (EC) concentrations were determined using EC-OC analyzer (Sunset Laboratory, Forest Grove, USA, model 2000) on a 1.5 cm^2 filter punch from the sample filter. Details of analytical protocol on EC–OC measurements used in our lab have been described in a recent article by Rengarajan et al. (2007). The contribution of EC and OC mass to TSP is insignificant in the entire study area during the sampling period. The abundance of EC and OC varied from < 0.05 to $0.20 \mu\text{g m}^{-3}$ (Av: $0.08 \mu\text{g m}^{-3}$) and < 0.1 to

0.68 $\mu\text{g m}^{-3}$ (Av: 0.21 $\mu\text{g m}^{-3}$) respectively. Relatively high concentrations of both EC and OC were observed in the southern transect (Region A) where the continental influence is more predominant (as discussed above). There is no significant correlation observable between EC and OC concentrations suggesting their weak source strength and transport to AABL. The mass of particulate organic matter (POM, Average: 0.44 $\mu\text{g m}^{-3}$) has been calculated by multiplying the measured OC concentration with a factor of 2.1, which is an estimated average of the molecular weight per unit weight of carbon for the organic aerosols in the marine atmospheric boundary layer (Turpin and Lim, 2001; Quinn et al., 2004).

The average composite of aerosols in the Arabian Sea-atmospheric boundary layer is presented in the form of a pie-chart (Fig. 5.9), showing the dominance of mineral dust (44%) followed by contributions from sea-salts (16%), nss- SO_4^{2-} (13%) and POM (2%). The unaccounted component (25% of TSP) of aerosol composition can be attributed to water content of aerosols (Tsai and Kuo, 2005).

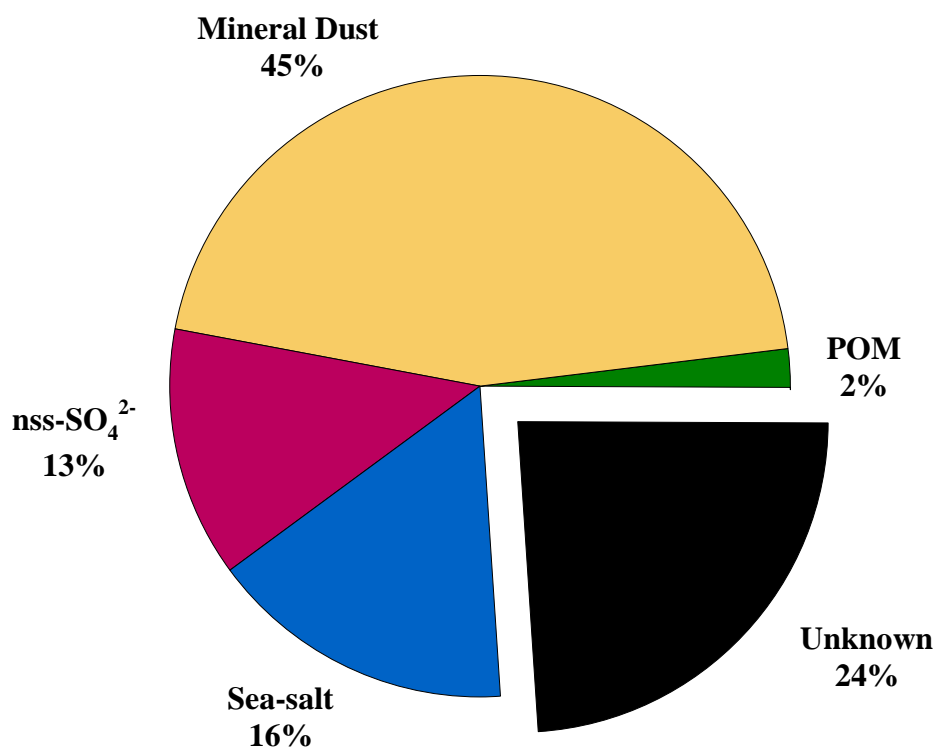


Fig. 5.9 Average compositions of aerosols in the Arabian Sea-atmospheric boundary layer during inter-monsoon season indicating the dominant role of mineral dust in chemical mass closure of aerosols.

5.2.6 Deposition Fluxes:

It has been well recognized that the dissolution of certain crustal elements e.g. Fe, via air-sea deposition of mineral aerosols, is an important (at times dominant) source for the surface water of open ocean (Duce et al., 1991). Trace elements attached to the aerosols can reach the sea surface following different pathways by: 1) dry-deposition in which aerosols reach sea-surface under the influence of gravity, and 2) wet-deposition in which aerosols are scavenged and their subsequent dissolution (Tindale and Pease, 1999). However, the magnitude and significance of the dry-deposition velocities and scavenging ratios used to convert aerosol concentration to deposition flux calculations are poorly documented both on a temporal and spatial scales; and hence represent a major uncertainty in estimates of atmospheric fluxes to ocean (Arimoto and Duce, 1986; Galloway, 1993; Jickells, 1995; Arimoto et al., 2003). The evaluation of wet inputs from rain water concentrations and rainfall intensity are by and large better constrained, but the estimation of dry deposition is more questionable because of large uncertainties of dry deposition velocities used in the calculation model (Duce et al., 1991; Migon et al., 1997). Atmospheric dry flux can be calculated by using dry deposition velocity (V_d) times the aerosol concentration. Earlier studies by Sarin et al., (1999), over Arabian Sea during intermonsoon period, had estimated effective dry-deposition velocity (V_d) of ~ 0.9 cm/sec for bulk aerosols using ^{210}Pb as a tracer. Considering $V_d = 0.9$ cm/sec, the total deposition flux of Al and Fe has been calculated (664 and $395 \mu\text{g m}^{-2} \text{d}^{-1}$) and compared with trace element fluxes over world ocean (Duce et al., 1991, Rastogi, 2005a). A comparative data are presented in Fig. 5.10. However, the fluxes reported in this study are the average for the inter-monsoon season (April and May); whereas data for other oceanic sites are the annual averages. The deposition flux of Iron, one of the most important micronutrients for surface ocean primary productivity, is significantly higher than that over World Ocean. It was pointed out (Zhuang et al., 1992) that high acidity in the aerosol particles, resulting primarily from H_2SO_4 , derived from both anthropogenic and natural (DMS produced) sources, would enhance solubilization of Fe(III) oxides in the mineral aerosols through the photoreduction reaction during the long-range transport of dust. Water soluble Fe,

which can be considered as bio-available iron, can be calculated assuming solubility of Fe as 10% of total Fe (Zhuang et al., 1990; Duce and Tindale, 1991). Using the above assumption and data presented in Table-1, the bioavailable Fe flux (i.e. water soluble Fe) to the Arabian Sea during inter-monsoon season has been derived as $40 \mu\text{g m}^{-2} \text{d}^{-1}$.

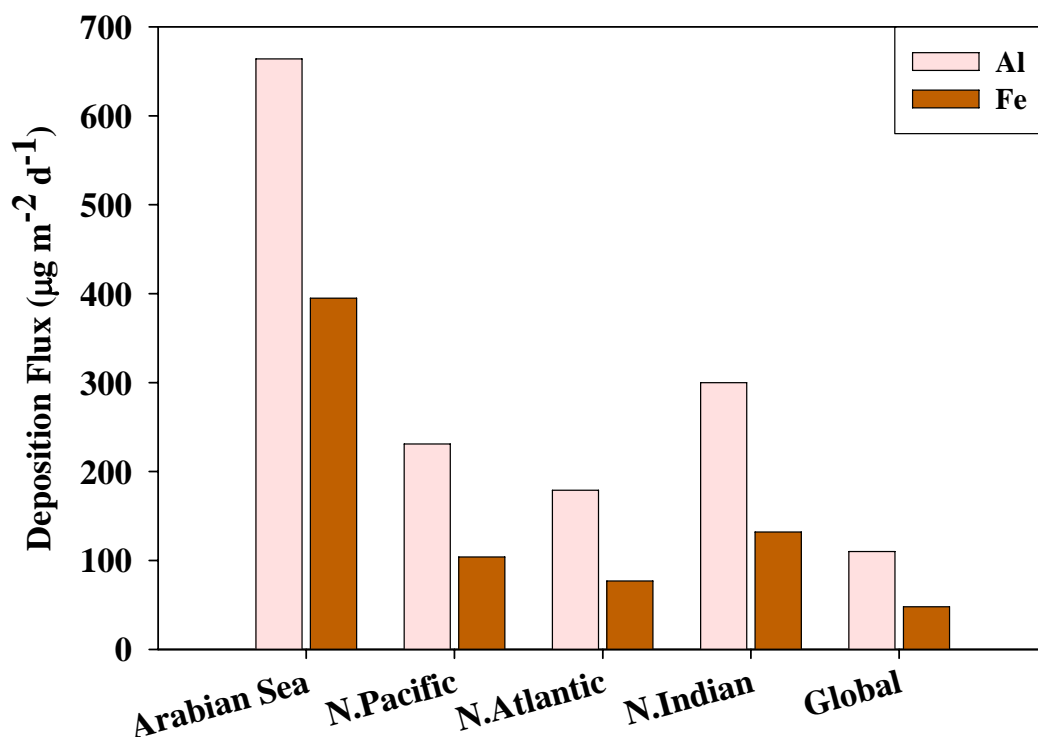


Fig. 5.10 Dry-deposition fluxes of Fe and Al to the Arabian Sea during the inter-monsoon are compared with the corresponding fluxes at other oceanic sites.

5.3. Summary and conclusions:

A comprehensive study involving major ions and crustal elements in the aerosol samples collected during the spring inter-monsoon in the Arabian Sea-atmospheric boundary layer (AABL) is reported here. The nss-SO_4^{2-} and nss-Ca^{2+} account for about 85 and 90%, respectively, to their total water-soluble (WS) concentrations and molar ratio of WS-Ca^{2+} to sulphate centering around 0.61 attest to the dominant impact of anthropogenic sources on the chemistry of aerosols in AABL. This is further supported by the enhanced solubility of Calcium due to large scale uptake of anthropogenic sulphate by alkaline dust. On average, mineral

dust accounts for nearly 45% of the total suspended particulates (Average = $25 \mu\text{g m}^{-3}$), under the influence of rapidly shifting wind regimes from NE-monsoon to spring inter-monsoon. A conspicuous spatial variability is reflected in the south to northward decrease in the abundance pattern of mineral dust, an observation also supported by the air-mass back trajectories. The carbonaceous aerosols do not make a significant contribution to the aerosol loading during the inter-monsoon. The Fe/Al ratios reveal characteristic nature of the dust sources from the surrounding desert region. The relatively larger dry deposition fluxes ($395 \mu\text{g m}^{-2} \text{d}^{-1}$), in comparison to other oceanic regions, has implication to the bioavailability of iron in controlling the surface biogeochemistry of the Arabian Sea.

Chapter 6

AEROSOL IRON SOLUBILITY IN A SEMI-ARID REGION: TEMPORAL TREND AND ANTHROPOGENIC SOURCES

6.1 Introduction:

The atmospheric transport and deposition of mineral dust is considered as one of the major sources by which iron is supplied to the ocean surface (Duce and Tindale, 1991; Fung et al., 2000; Mahowald et al, 2005, 2009; Jickells et al, 2005). Also, iron is hypothesized as a limiting factor in controlling the phytoplankton production in the high nutrient low chlorophyll (HNLC) regions (Martin et al, 1991). These are recognized as potential regions in modulating the CO₂ uptake due to the increase in phytoplankton productivity and thus, affecting the global carbon cycle and climate (Jickell et al, 2005; Meskhidze et al, 2003; Solomon et al, 2009). On average, dust aerosols contain 3.5% of iron mainly existing in the form of aluminosilicate (Duce and Tindale, 1991; Zhu et al, 1997). The aerosol Fe associated with mineral dust remains insoluble at pH conditions typical of sea-water (Stumm and Morgan, 1981; Zhu et al, 1997). However, a finite fraction of the aerosol Fe [referred as dissolved iron], is used by phytoplanktons. Several field based studies, incorporating different analytical techniques, have documented large variability (0.01 to 80 %) in the water-soluble fraction of aerosol iron and continues to remain a major source of uncertainty in assessing the impact of atmospheric supply of iron to the marine ecosystem and the biogeochemical cycle (Hand et al, 2004; Chen and Siefert, 2004; Mahowald et al, 2005; Baker et al, 2006).

One of the proposed mechanisms for the enhanced solubility of iron is the chemical processing of aerosol particles, during long-range transport, mediated by the presence of acidic components (e.g. SO₂ and its oxidation products) and sunlight (Zhuang et al, 1992; Johansen et al, 2000; Meskhidze et al, 2003). On the contrary, some of the field experiments have indicated that the soluble iron can be enriched as a result of direct emission from fossil-fuel combustion and biomass burning (Chuang et al, 2005; Sedwick et al, 2007; Sholkovitz et al, 2009). The mixing state of atmospheric aerosols is also considered as one of the important factors affecting the fractional solubility of aerosol Fe (Baker and Croot, 2008). In the source regions, aerosol particles are represented as a mixture of both externally and/or internally mixed state which acquire internally mixed state during long-range transport. The condensation of gaseous species (on pre-existing particles) as well as in-cloud processing of aerosols is responsible for the increase in internal mixing state which is populated in the fine mode. Baker and Jickells, (2006), have argued that the increase in aerosol iron solubility is influenced by the decrease in particle size (i.e. increase in surface area to volume ratio) during atmospheric transport rather than differences in the composition of aerosols. On the contrary, Buck et al, (2008) have demonstrated that there is no such obvious correlation and that aerosol composition from the source region is a dominant factor in controlling the iron solubility.

It is, thus, imperative to investigate and understand various sources and factors affecting the fractional solubility of aerosol iron at regional scale in order to further constrain its role in the biogeochemical models (Mahowald et al, 2009). In this context, chemical data from high-dust semi-arid regions of south-Asia are lacking in the literature. With this motivation, fine mode (PM_{2.5}) aerosol samples were collected from a high- altitude site located in a semi-arid region of western-India, an important source region for the atmospheric supply of dust to the Arabian Sea. Sampling from a high-altitude site is considered to be advantageous in order to study the long-range transport of mineral dust across western India (Kumar and Sarin, 2009). In this chapter we report on the atmospheric abundance of mineral dust and fractional solubility of iron in the fine mode aerosols (PM_{2.5}).

We have also evaluated the temporal trend and impact of anthropogenic sources affecting the water-soluble fraction of iron.

6.2 Results and discussion:

In the regional context of western India and based on the meteorological parameter, two distinct seasons have been defined (discussed in chapter 2), viz. summer (March – May) characterized by convective mixing and high-dust loading in the atmosphere and winter (October – February) when the advective transport of pollutants from northern India dominates the aerosol composition. Typical monthly average wind pattern for the month of January (representing the winter season) and April (representing the summer season) are shown in Fig. 6.1. The remainder months (June – September) represent the wet phase (monsoonal rain) with efficient washout of the atmosphere.

The water-soluble iron (WS-Fe) was measured on Graphite Furnace-Atomic Absorption Spectrometer (P-E Model AAnalyst 100 coupled to a HGA 800). The selection of Milli-Q water for WS-Fe, instead of seawater, is based on the rationale that Milli-Q water provides a consistent and reproducible leaching solution (Buck et al, 2006; Sedwick et al, 2007). The data on WS-Fe reported in this chapter represent relative amount of soluble Fe (also referred as “operational solubility”) as compared to absolute solubility. Sedwick et al, (2007), have attempted to estimate “effective solubility” of aerosol iron over the Sargasso Sea from the “operational solubility”.

6.2.1 Chemical characteristics of fine mode aerosols and temporal variability:

The temporal variability in the mass concentration of fine mode ($PM_{2.5}$) aerosol (range: 5.5-46.1 $\mu\text{g m}^{-3}$), during the two distinct seasons (summer and winter), is presented in Fig. 6.2 a. A large variability is observed during wintertime compared to that in summer season and is attributed to the down-wind (northeast-winds) advective transport of anthropogenic species from emission sources in northern India. The mass fraction of dust (Fig. 6.2 b) has been calculated using Al abundance in the aerosols, and assuming 8.04 % of Al as composition of upper continental crust (McLennan, 2001; Rastogi and Sarin,

2006; Kumar and Sarin, 2009). The mass fraction of dust, plotted as a function of Julian days (Fig. 6.2 b), makes significant contribution to the PM_{2.5} mass during summer time ($A_v = 56.9 \pm 20.6$ %) compared to winter months ($A_v = 18.1 \pm 12.5$ %), suggesting distinct sources of dust during the two seasons. This is further supported by the air-mass back trajectory analysis depicting the transport of air-masses from the two distinct regions during summer and winter seasons (Fig. 6.1 a and b).

The elemental ratio of Fe/Al has been used to characterize the sources of dust over the study site similar to approach used by Chiapello et al, (1997). The temporal trend in Fe/Al ratio (Fig. 6.2 c) represents a large variability during winter months compared to the summer season. During the high dust season (summertime), Fe/Al ratios are in the narrow range of 0.55 to 0.80 (for ca. 85% of the data points), suggesting a characteristic nature of mineral aerosols derived from desert regions (western India). During wintertime, under the influence of prevailing north-easterlies, significantly higher Fe/Al ratios (range: 0.49-1.58; Fig. 6.2 c) in the fine mode (PM_{2.5}) are attributable to the widespread pollution sources in the Indo-Gangetic Plain (northern India) (Kumar and Sarin, 2009).

Another line of evidence has been drawn based on the Fe/Al ratio ranging from 0.55 to 0.63 in the weathered soils from northern India, as inferred from the composition of river bank sediments (Sarin et al, 1979). It is, thus, proposed that significant contribution of Fe from mineral dust is unlikely and that the enrichment of Fe/Al ratio in PM_{2.5}, during wintertime, may be attributed to anthropogenic sources (fossil-fuel combustion and/or biomass burning). The dominance of biomass burning has been documented based on the OC/EC (organic carbon/elemental carbon) ratios as high as 7-8 in northern India (Rengarajan et al, 2007). The influence of anthropogenic sources on the chemical composition of fine mode aerosols is also well demonstrated by the temporal variability in the chemical constituents (e.g. NH₄⁺, NO₃⁻, and nss-SO₄²⁻) as shown in Figs. 6.2 d, e, and f. The abundances of NH₄⁺ and nss-SO₄²⁻ exhibit parallel increase in proportion with the PM_{2.5} mass during winter months; re-emphasizing the long-range transport of pollutants from northern India (supported by the air-mass back-trajectories; Fig. 6.1 a).

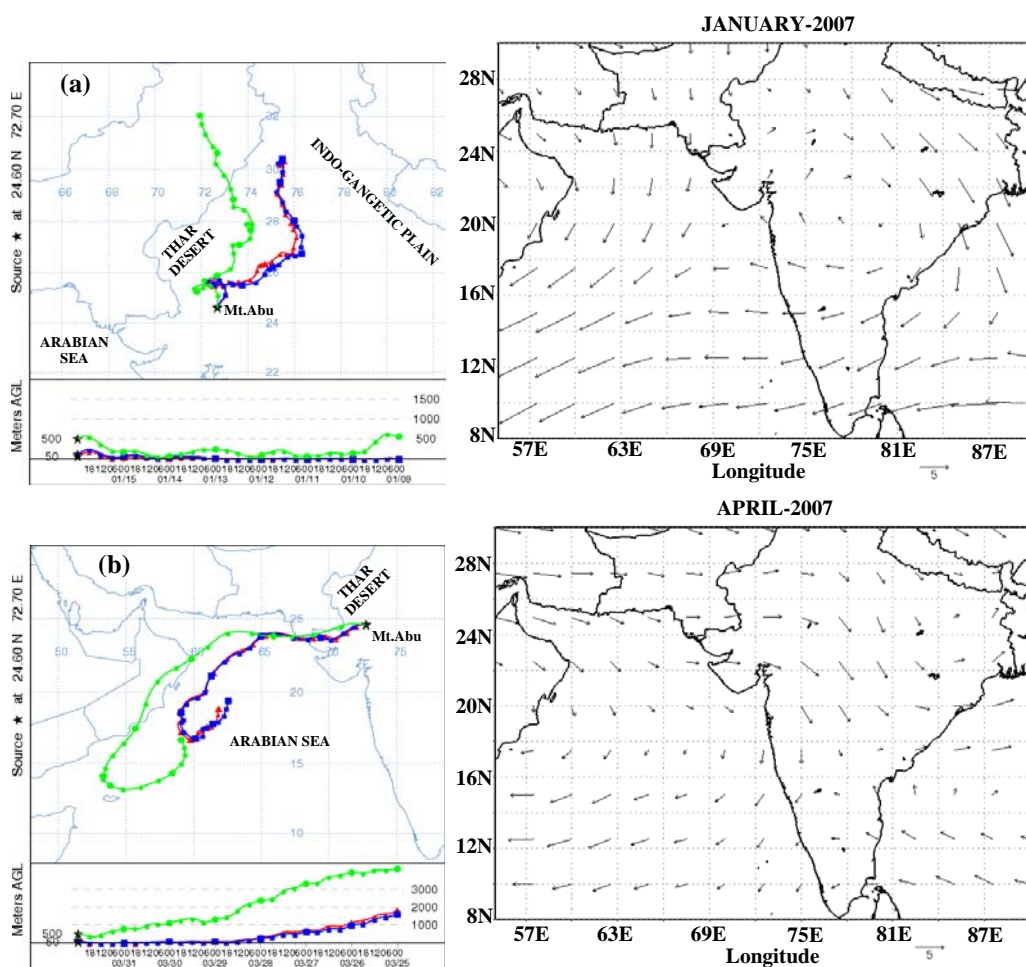


Fig. 6.1 Map showing sampling site (Mt. Abu) and important source regions influencing the transport of aerosols. Typical 7-day air mass back trajectories (using HYSPLIT model; <http://www.arl.noaa.gov/HYSPLIT.php>) at the study site during (a) winter: 16 Jan 2007 and (b) summer: 01 April 2007. Also shown are the monthly average wind regimes during January (representing the winter season) and April (representative of summer season).

On average, NH_4^+ and nss-SO_4^{2-} account for 10 and 30 % of the fine mode ($\text{PM}_{2.5}$) mass during wintertime. It is, however, noteworthy that the concentration of NO_3^- is nearly five times less than that of SO_4^{2-} (Fig. 6.2 e and f).

6.2.2 Temporal variability of aerosol iron (Fe_A) and water-soluble iron (WS-Fe):

During the summer season, contribution of dust to $\text{PM}_{2.5}$ mass is relatively high and steadily decreases in winter months (Fig. 6.2 b). Thus, aerosol Fe (Fe_A) concentration also exhibit similar temporal variability (Fig. 6.3 a), with relatively

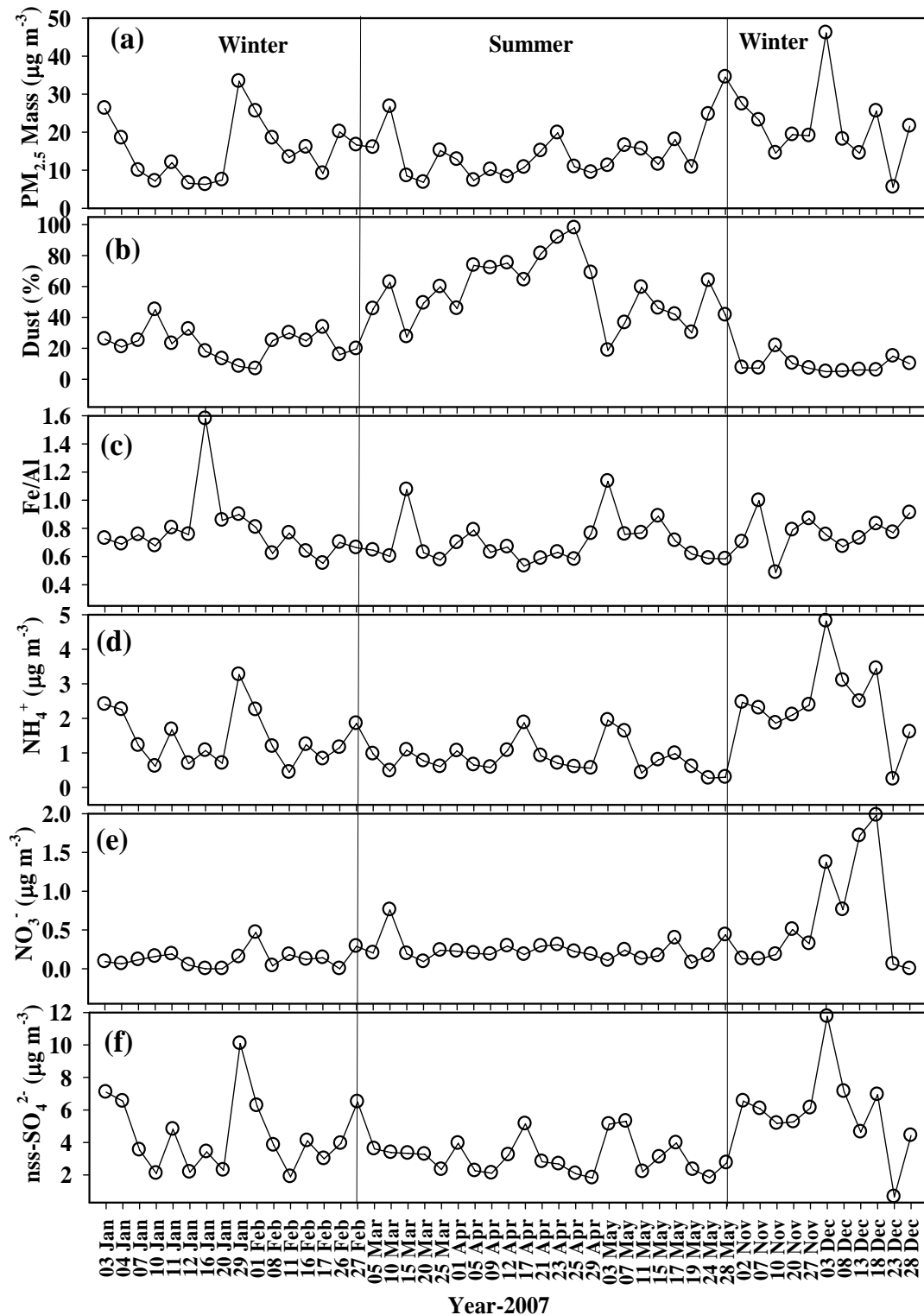


Fig. 6.2 Temporal variability during winter and summer seasons in 2007 at a high altitude station (Mt. Abu), for (a) $PM_{2.5}$ aerosol mass, (b) mass fraction of estimated dust, (c) Fe_A/Al weight ratio (d) concentrations of NH_4^+ , (e) NO_3^- (f) $nss-SO_4^{2-}$.

high values occurring during the summer months (range: 161- 915 ng m⁻³) compared to the winter season (range: 50 to 397 ng m⁻³). In contrast, temporal variability of water-soluble Fe fraction (i.e. [WS-Fe/Fe_A] *100) shows an opposite trend over the annual seasonal cycle (Fig. 6.3 b). The percentage of WS-Fe averages around 8.1 ± 3.5 % (range: 2.5 to 16.1 %) during wintertime and 1.6 ± 1.9 % (range: 0.06 to 6.1 %) during summer months (Fig. 6.3 b). The enhanced fractional solubility of Fe [WS-Fe (%)], during wintertime, is associated with relatively low abundance of dust and Fe_A; whereas lower solubility is a characteristic feature of the high dust season (higher Fe_A). It is noteworthy that the fractional solubility does not show significant correlation with nss-SO₄²⁻ (Fig. 6.4 a). This is unlike the process of enhanced dissolution/leaching of aerosol Fe with the increasing acidity (lower pH) suggested by Meskhidze et al, (2003). The abundances of nss-SO₄²⁻ and NH₄⁺ (expressed in equivalent units) exhibit significant linear correlation (Fig. 6.4 b; r² = 0.90), indicating the predominance of nss-SO₄²⁻ in the fine mode as ammonium salt. A wide range of values for water-soluble Fe fraction have been reported during several field experiments from the oceanic regions (Seifert et al, 1999; Johansen and Hoffmann, 2003; Chen and Siefert, 2004; Baker et al, 2006; Sedwick et al, 2007; Buck et al, 2006). Some of them have also reported on the potential link between acid processing during long-range transport and enhancement in the iron solubility. However, these studies do not firmly conclude acid processing as a primary control for iron fractional solubility. More recently, it has been hypothesized that the increase in fractional iron solubility may vary with the mixing state of aerosols as well as deposition of acid and dust particle simultaneously during atmospheric transport (Baker and Croot, 2008). One of the recent modeling study by Luo et al, (2005), have concluded on the lack of significant correlation between observed sulphate or organic acids and iron solubility. In this study, it is quite reasonable to assume that the long-range transport of fine mode particles sampled from a high-altitude site, during wintertime, are internally mixed. However, based on the observation that the mass fraction of dust significantly decreases during winter months (Fig. 6.2 b), and together with efficient neutralization of nss-SO₄²⁻ by NH₄⁺ it can be inferred that chemical processing of aerosols is of minor significance for the

increased fractional Fe solubility at this study site. In the regional context, it may also be emphasized that the large buffer capacity of the carbonate dust is relevant during the high-dust season.

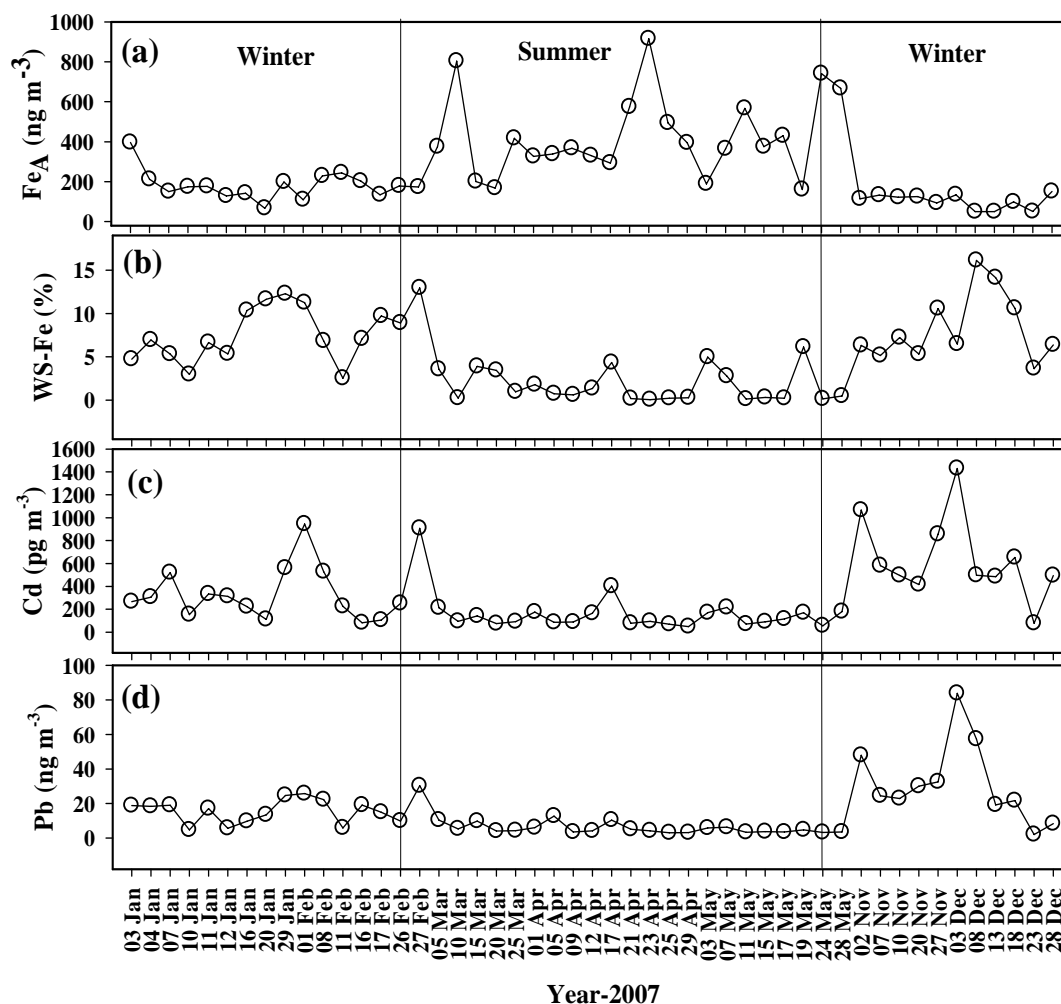


Fig. 6.3 Temporal variability of (a) total aerosol iron (Fe_A) concentration and (b) water-soluble fraction of iron [WS-Fe (%)], (c) concentration of Cd and (d) Pb, in the aerosol samples collected from Mt. Abu.

6.2.3 Solubility of aerosol iron and role of anthropogenic sources

The relatively low abundance of WS-Fe in aerosol samples collected during the high dust season (summertime), and high solubility of aerosol Fe during the winter months (characterized by lower dust abundance) clearly demonstrates that Fe solubility is not dictated by the abundance of the mineral

dust and aerosol Fe. The significantly high Fe_A/Al ratios are characteristic of the $Fe_A < 200 \text{ ng m}^{-3}$ (Fig. 6.5 a). Furthermore, we have evaluated the concentrations of Cd and Pb as a function of total aerosol Fe (Fe_A) concentration (Fig. 6.3 c and d); thus documenting a sharp increase in their abundances at low concentration of Fe_A (less than 200 ng m^{-3}). It is noteworthy that extremely low Fe_A content is characteristic of wintertime when aerosol composition is influenced by the advective transport of pollutants from northern India (Indo-Gangetic Plain) associated with north-easterly winds. The enrichment factors of Cd and Pb (with respect to Al) show exceptionally high values (range: 214-6700 and 85-3650, respectively), during winter months, suggesting dominant impact of anthropogenic sources. The elevated Cd/Al and Pb/Al ratios in the aerosols, compared to the upper continental crust can be used as important indicator of anthropogenic aerosols produced by burning of fossil-fuel (Arimoto et al, 1995; Niragu and Pacyna, 1988). The plot between WS-Fe (%) and Fe_A (Fig. 6.6), shows a similar enhancement shown by Cd/Al and Pb/Al versus Fe_A (Fig. 6.5 b and c), further corroborating that the fractional solubility of Fe is dictated by the contribution from anthropogenic activities (fossil-fuel combustion products) during winter season. In contrast, low solubility of Fe is associated with the high dust conditions and transport from desert and semi-arid region in western India and as far as from Oman desert during summer month. Recently, Buck et al, (2008a), have observed similar type of enrichment of soluble Sb and Pb, over central Atlantic Ocean and suggested the burning of fossil fuel as an important source. Relatively enriched Fe/Al mass ratio has been reported for fuel-oil fly ash and exhaust particle produced by diesel combustion (Desboeufs et al, 2005); where as 77-81 % of water-soluble Fe can be contributed by oil combustion products (Schroth et al, 2009). Chuang et.al, (2005), has demonstrated significant contribution of particulate soluble Fe concentration from anthropogenic activity rather than processing during long-range transport in the East Asian atmospheric outflow over annual timescales.

The “operational solubility” of Fe [WS-Fe (%)] versus total Fe (Fe_A) represents a two component mixing plot (Fig. 6.6). This is also confirmed by plotting WS-Fe (%) and $1/Fe_A$, yielding a best fit linear regression line ($r = 0.82$;

$p < 0.001$). Based on this observation, a conservative mixing line is generated for the two distinct end members (similar to the approach adopted by Sedwick et al, 2007). One end member is characterized by higher Fe_A concentration (915 ng m^{-3}) with fractional solubility of 0.06 % (during the summertime). The other end member is characterized by lowest Fe_A value of 50 ng m^{-3} associated with the soluble fraction of 16.1 % (representing wintertime data).

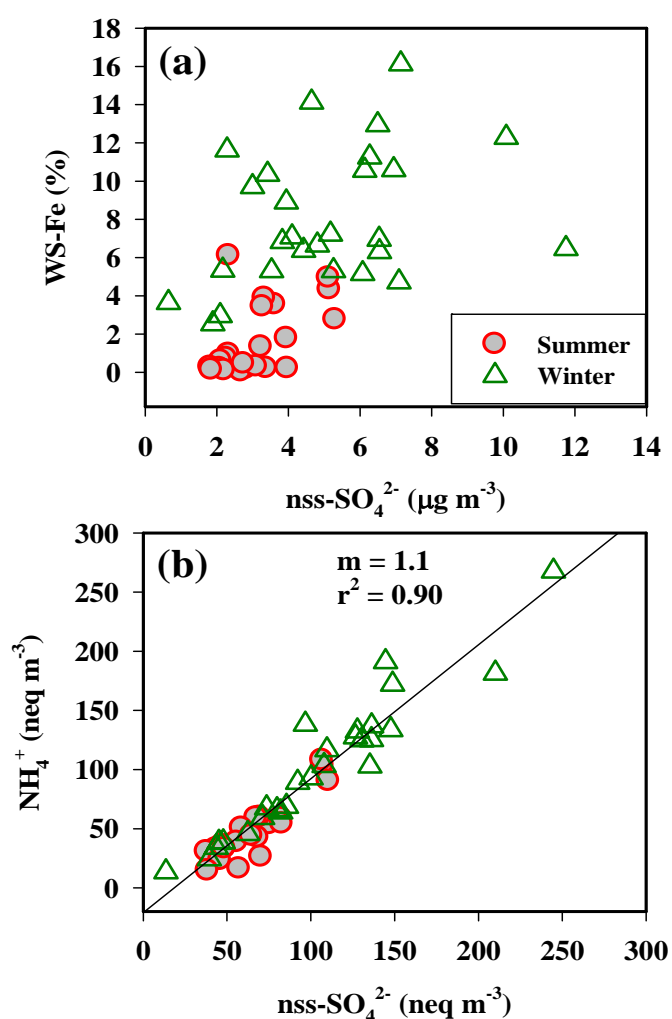


Fig. 6.4 (a) Large scatter between WS-Fe (%) and nss-SO_4^{2-} suggests that chemical processing during aerosol transport is of minor significance for soluble iron fraction at the study site. (b) Linear relationship among abundances (in equivalent units) of nss-SO_4^{2-} and NH_4^+ in the fine ($\text{PM}_{2.5}$) aerosols during summer and winter seasons.

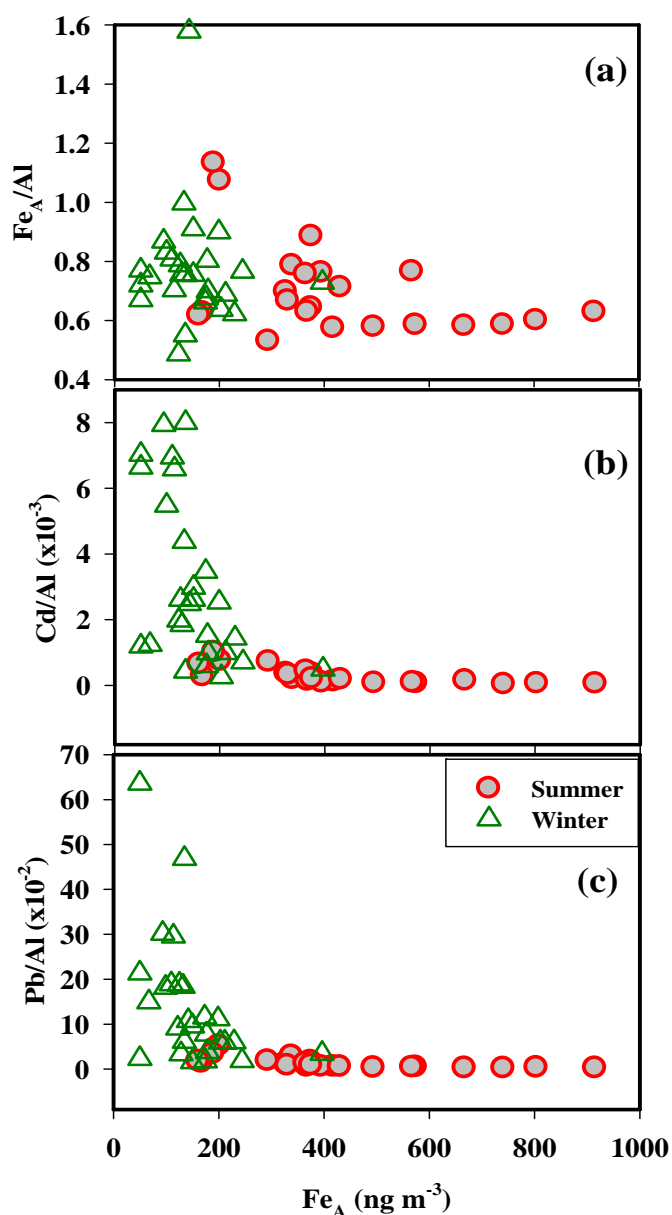


Fig. 6.5 (a) Fe_A/Al (b) Cd/Al , (c) Pb/Al ratios are plotted against total aerosol iron concentration. A sharp increase in Cd/Al and Pb/Al ratio at lower Fe_A concentration is observed for winter month samples.

The modeled curve simulates reasonably well the inverse relationship between WS-Fe (%) and total aerosol Fe, except for the few data points deviating from the mixing line during winter season. The data for the aerosol iron-solubility from Sargasso Sea exhibit similar kind of hyperbolic relationship with the total aerosol iron (Sedwick et al, 2007). For comparison, the FeATMISS (Iron Atmospheric Inputs to the Sargasso Sea; Sedwick et al, 2007) data points

collected over time period ranging from days to months have been plotted on the mixing curve representing this study. This comparison suggests that the contribution of aerosol Fe from anthropogenic sources influences the fractional solubility of Fe nearly to the same degree as over Sargasso Sea. Such an approach provides better insight into operational solubility of aerosol Fe and enforcing our conclusion that Fe solubility in the semi-arid region of western India is primarily controlled by composition and chemical nature of aerosols from the source region rather than chemical processing during their long-range transport.

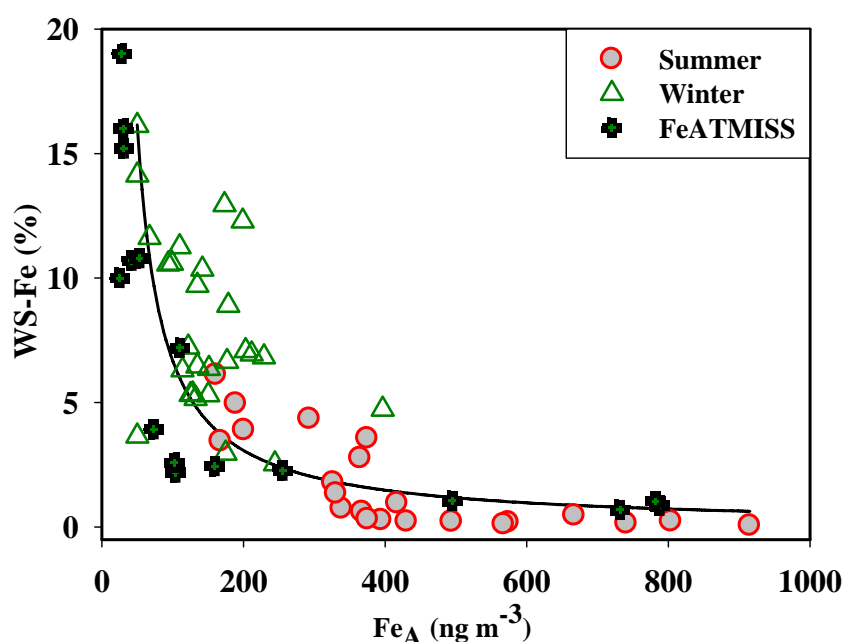


Fig. 6.6 Relationship between WS-Fe (%) and Fe_A for Mt. Abu samples along with the FeATMISS data (Sedwick et al, 2007) from Sargasso Sea. Two of the data points from FeATMISS exceeding $Fe_A > 1000 \text{ ng m}^{-3}$ are not shown in the Figure.

6.3. Conclusions and implications:

The chemical composition of atmospheric particulate matter ($PM_{2.5}$), studied from high-dust semi-arid region of western India, reveals conspicuous temporal variability in the fractional solubility of aerosol iron dominated by the anthropogenic sources. During wintertime, the advective transport of pollutants (derived from fossil-fuel combustion and biomass burning) from the Indo-Gangetic Plain (northern India), with distinctly high Fe_A/Al , Pb/Al and Cd/Al ratios, result in enhanced fractional solubility of Fe ($A_v = 8.1 \pm 3.5 \%$). The

impact of anthropogenic sources is further demonstrated by significant increase in the ambient concentrations of NH_4^+ and SO_4^{2-} in fine mode ($\text{PM}_{2.5}$). In contrast, the high-dust season (summertime) associated with high abundance of aerosol Fe, is characterized by exceedingly low solubility ($A_v = 1.6 \pm 1.9 \%$); suggesting that atmospheric chemical processing is of minor significance.

These results have implications to the atmospheric source of soluble iron associated with large-dust events occurring in the semi-arid regions. In a recent study from the Arabian Sea, the dry-deposition flux of Fe during the period of inter-monsoon (March-April, 2006) was estimated to be $395 \mu\text{g m}^{-2} \text{d}^{-1}$ based on the Fe concentration (range: 90 to 1010 ng m^{-3}) in ambient aerosols (Kumar et. al, 2008). Assuming 10 % as the solubility of aerosol Fe (also commonly referred as bio-available Fe in the literature) would lead to over estimation of the supply of dust related soluble iron to the ocean surface. Such regional scale studies are, thus, important to constrain the existing uncertainties in the atmospheric source and delivery of soluble iron for modeling the impact on surface ocean biogeochemistry.

SYNTHESIS AND FUTURE DIRECTIONS

7.1 SYNTHESIS

The regional scale studies of atmospheric mineral aerosols are important to understand and assess their impact on climate and environmental change. Very limited field measurements of atmospheric mineral dust over Indian region are reported. Real time field observations provide the most direct information about aerosol characteristics. This study provides an expansive and unique data set of size-segregated aerosol samples [fine (PM_{2.5}) and coarse (PM_{10-2.5}) mode] from a high-altitude site located in a semi-arid region (Mt. Abu, 24.6 °N, 72.7 °E, 1680 m asl) during 2006 and 2007 as well as bulk aerosol composition in the MABL of Arabian Sea (April - May 2006). Aerosol samples (in both size fraction) were analyzed for water-soluble ionic species (Na⁺, NH₄⁺, K⁺, Mg²⁺, Ca²⁺, Cl⁻, NO₃⁻, SO₄²⁻ and HCO₃⁻), crustal constituents (Al, Fe, Ca, and Mg). In addition, aerosol iron solubility has also been assessed in fine (PM_{2.5}) fraction based on the water-soluble Fe (WS-Fe) and acid-soluble trace elements (Pb and Cd).

The mass concentrations of fine (PM_{2.5}) and coarse (PM_{10-2.5}) mode aerosols varied from 1.6 to 46.1 and 2.3 to 102 μg m⁻³ respectively over the annual seasonal cycle; with dominant and uniform contribution of mineral dust (60 to 80 %) in the coarse mode relative to large temporal variability (11 to 75 %) observed in the fine mode. The coarse mass fraction shows a characteristic increase with the wind speed during summer months (Mar to Jun); whereas fine aerosol mass and its elemental composition exhibit conspicuous temporal pattern associated with north-easterlies during wintertime (Oct to Feb). The Fe/Al weight ratio in PM_{2.5} ranges from 0.5 to 1.0 during winter months. The relative enrichment of Fe in fine mode, compared to the crustal ratio of 0.44, is attributed

to the down-wind advective transport of combustion products derived from large-scale biomass burning, industrial and automobile emission sources located in the Indo-Gangetic Plain (northern India). In contrast, Ca/Al and Mg/Al weight ratios show relative enrichment of Ca and Mg in the coarse mode; indicating their dominant contribution from carbonate minerals.

The water-soluble ionic composition (WSIC) varied from 1.0 to 19.5 $\mu\text{g m}^{-3}$ in the fine mode and constitutes 50, 39 and 31 % of the aerosol mass during winter, summer and monsoon respectively, with dominant contribution from SO_4^{2-} , NH_4^+ and HCO_3^- . Furthermore, a two fold increase in the abundances of nss- SO_4^{2-} and NH_4^+ and their co-variability during wintertime, relative to high-dust conditions in summer, suggest dominance of anthropogenic sources and long-range transport of combustion products (biomass burning and fossil-fuel emissions) from northern India. In the coarse mode, WSIC ranged from 0.1 to 24.8 $\mu\text{g m}^{-3}$ and its contribution to aerosol mass was consistently low (annual average = 21 %) with predominance of Ca^{2+} and HCO_3^- , indicating contribution from carbonate rich mineral dust. The nss- $\text{SO}_4^{2-}/\text{NO}_3^-$ mass ratio exhibits extreme variability during winter, with values ranging from 2.7 to 101 in $\text{PM}_{2.5}$ and 0.001 to 2.7 in coarse ($\text{PM}_{10-2.5}$) mode. The relatively high abundance of nitrate in the coarse mode, during all seasons, indicates its association with mineral dust. The temporal variability is further evident from significantly lower aerosol mass and WSIC during the SW-monsoon (July – Sept) due to efficient washout. The chemical data set also documents near quantitative neutralization of acidic species (NO_3^- and SO_4^{2-}) by NH_4^+ in $\text{PM}_{2.5}$ and mineral dust in $\text{PM}_{10-2.5}$, thus, representing a dominant atmospheric chemical transformation process occurring in the high-dust semi-arid region. The observed chemical interactions among mineral dust and anthropogenic species (sulphate and nitrate) could significantly alter the size distribution of sulphate and nitrate aerosols (from fine to coarse mode) as well as surface properties of mineral dust (from hydrophobic to hydrophilic). Such observations, if not considered, can introduce significant uncertainties in global and regional scale climate models.

The chemical characteristics of aerosols in the Arabian Sea-Atmospheric Boundary Layer (AABL) have been studied during the spring inter-monsoon

(April-May 2006) based on the analysis of water soluble constituents (Na^+ , NH_4^+ , K^+ , Mg^{2+} , Ca^{2+} , Cl^- , NO_3^- and SO_4^{2-}), crustal elements (Al, Fe, and Ca) and carbonaceous species (EC, OC). The total suspended particulate (TSP) abundance ranged from 8.2 to 46.9 $\mu\text{g m}^{-3}$ (Average (Av) = $24.7 \pm 10.4 \mu\text{g m}^{-3}$) during 22 days cruise covering a latitudinal transect from 9 °N to 22 °N. The water-soluble species account for 35% of TSP; with dominant contribution of Ca^{2+} and SO_4^{2-} followed by Na^+ and minor contributions of K^+ , Mg^{2+} , Cl^- , and NO_3^- . The abundances of Ca^{2+} and SO_4^{2-} do not exhibit any noticeable latitudinal distribution pattern but the non-sea-salt (nss) component constitutes ~85-90% of their total concentration, indicating dominant transport from continental sources. Furthermore, a significant linear positive correlation among nss- Ca^{2+} and nss- SO_4^{2-} , and nss- Ca^{2+} /nss- SO_4^{2-} molar ratio averaging around 0.61 (range: 0.20-1.16) suggests uptake of anthropogenic SO_4^{2-} by mineral dust (CaCO_3). The chemical reaction favouring this neutralization of nss- SO_4^{2-} is also evident from the abundance pattern of water-soluble- Ca^{2+} nearly equal to the total Ca content measured in the aerosols. Using Al as a proxy, the mineral dust in AABL ranged from 2.7 to 23.7 $\mu\text{g m}^{-3}$; with relatively high abundance occurring over the south Arabian Sea. On average, mineral dust accounts for 44% of the TSP and Fe/Al weight-ratio exhibit characteristic narrow range: 0.40 to 0.59. The impact of carbonaceous species (EC, OC) is nowhere pronounced in the AABL. The dry-deposition fluxes of Al, Fe and bioavailable Fe to the surface Arabian Sea are estimated to be 665, 395, and 40 $\mu\text{g m}^{-2} \text{d}^{-1}$ respectively. High deposition flux of Fe over Arabian Sea can significantly affect the surface ocean biogeochemistry which in turn may influence the regional as well as global climate.

The temporal variability in the abundance of mineral dust and fractional solubility of aerosol Fe (referred as water-soluble Fe), in $\text{PM}_{2.5}$, over Mt. Abu, reveal an inverse relationship between aerosol Fe (range: 50-915 ng m^{-3}) and fractional Fe solubility (range: 0.06-16.1 %). A significant increase in the solubility of iron, during wintertime, is also well marked by a uniform decrease in the mass fraction of mineral dust. These observations suggest that the advective transport of Fe derived from anthropogenic combustion emission is one of the possible causes for the enhanced solubility of iron over a semi-arid region in

western India. The impact of anthropogenic sources is further demonstrated by significant increase in the ambient concentrations of NH_4^+ and SO_4^{2-} in fine mode ($\text{PM}_{2.5}$) as well as enrichment of heavy metals in $\text{PM}_{2.5}$ (ascertained from Pb/Al and Cd/Al ratios). In contrast, the high-dust season (summertime) associated with high abundance of aerosol Fe, is characterized by exceedingly low solubility ($A_v = 1.6 \pm 1.9 \%$); suggesting that atmospheric chemical processing is of minor significance. Such regional scale studies are important to constrain the existing uncertainties in the atmospheric source and delivery of soluble iron for modeling the impact on surface ocean biogeochemistry.

7.2 Scope of future research:

This study has provided a very comprehensive data set of the composition of mineral aerosols and discussed its role in atmospheric chemistry by investigating spatial as well as temporal distribution of mineral dust. However, there are issues pertaining to dust chemistry which need further attention for better understanding of the dust-climate interactions.

(a) Heterogeneous phase chemistry of Mineral Dust:

Heterogeneous phase chemistry of mineral aerosols is one of the important issues in changing climate scenario because of several perspectives. The most important is the gas phase perspective, wherein, the chemical interactions between gaseous species and dust particles have potential to alter the chemical balance of atmosphere. Similar issues have been addressed in the present study, based on long term measurement of particulate aerosol (dust) chemical composition in different size fractions. The gas precursors (SO_2 and NO_x) which are mainly responsible for sulphate and nitrate formation via oxidation process are mainly interacting with dust particle. To gain better understanding of the partitioning of these species between gaseous and particulate phase in the atmosphere and the factors/processes control this partitioning, simultaneous measurements of SO_2 and NO_x along with the chemical composition of particulate matter are essential.

One of the powerful oxidizing species present in the atmosphere is Ozone, produced mainly from oxidation of hydrocarbons and anthropogenically emitted products. This is responsible to affect human health (via lung tissue damage) as well as plant health (via leaf damage). It has been also observed that, mineral dust removes ozone during various heterogeneous phase reactions and hence, a most likely inverse relationship exist between ozone and mineral dust concentration. Some of the modeling studies have shown a decrease in ozone level by 10 % in the presence on high dust emissions. However, till date there are no field based observations available to investigate these interactions. It is thus, important to develop large field programmes to asses the impact dust on ozone concentrations.

(b) Aerosol Fe solubility over marine region:

It has been shown in the present study the behaviour of soluble Fe in the atmosphere which is mostly dependent on the source region rather than the alteration (chemical processing) during long-range transport. The enhancement in iron solubility has been linked to chemical processing (in the presence of acidic components, e.g. SO₂ and its oxidation products) of mineral dust particles during long-range atmospheric transport over marine region. This has led several workers to examine the relation between fractional solubility of aerosol iron and concentration of acidic species based on real-time samples collected in the marine region (Atlantic and Pacific Ocean). However, these studies do not provide a firm conclusion in favour of acid processing as a primary control for enhanced fractional solubility of aerosol iron. The recent studies over these oceanic regions have suggested anthropogenic emissions (biomass burning and fossil-fuel combustion) as a significant source of soluble aerosol Fe, in contrast to its supply from mineral aerosols (or processed dust).

In the recent years, there has been substantial interest in the anthropogenic emissions and atmospheric transport from south and south-east Asian regions. The impact of anthropogenic emissions has been observed in the remote marine regions of the Arabian Sea and Bay of Bengal. However, the issues concerning the solubility of aerosol iron have not been addressed over these under-sampled oceanic regions. It is thus pertinent to assess the soluble Fe behaviour in marine

atmosphere (Indian Ocean) which is better representative of the pathway of soluble iron to the surface ocean. More importantly, the newer concept of combustion sources as most likely source for soluble iron can further be assessed in the marine region affected by outflow from Indian subcontinent during winter monsoon, when winds are flowing from Indo-Gangetic Plain to the adjoining marine region (Arabian Sea and Bay of Bengal).

(c) Mineralogical and Isotopic characterization of Dust aerosols:

It is important to highlight the mineralogy of dust aerosols and connect to the soluble Fe fraction which undergoes oceanic deposition, especially for Fe rich aerosols. This will require a complimentary approach that involves both the application of state-of-art characterization techniques to mineral dust aerosols to identify iron-containing components of dust as well as reactivity and dissolution studies to get more insight to the behaviour of these components. In particular, there is a need to understand potential reaction pathways, proposed in the literature [e.g. photochemical reduction of Fe (III) present in dust in the presence of SO_4^{2-} , nonphotochemical nitrate reduction of Fe (III)], based on lab as well as real-time field studies, that may only be encountered in unique atmosphere resulting from the mixing of dust plumes and anthropogenic pollutants.

Furthermore, owing to low solubility and high biological demand for iron, it has a short residence time in ocean water and consequently may have spatial and temporal variability in the isotopic composition. The iron isotope composition can be altered by several low temperature processes, which include redox reactions and partial dissolution. Thus, the study of iron isotopes, in the atmospheric aerosol will provide a better handle to decipher various sources and transformation process of aerosol Fe. It will be a good attempt to asses the variations in isotopic composition of aerosol Fe at different locations in Indian subcontinent (continental as well as marine locations).

(d) Halogen Chemistry:

The study of aerosol chemical composition over Arabian Sea indicates a high degree of chloride-depletion owing to acid displacement of sea-salt by

anthropogenic species, whereby concentration of SO_4^{2-} is crucial in removing chloride compared to the NO_3^- . These chlorine atoms could be a significant active free radical in the troposphere, similar to its action in the stratosphere where high UV flux is available to produce chlorine atoms which is subsequently responsible for ozone depletion. These free radicals will also react with many volatile organic compounds, including the potent greenhouse gas methane, speeding up their removal from the atmosphere. Also, lab studies have suggested to the possibility of enhancement in the ozone levels in troposphere via chloride free radicals. In addition to chloride free radical, there are reactive halogen compounds (X, XO, XY, OXO, HOX, XONO₂, XNO₂; where X, Y = Cl, Br, I) present in various domains, throughout the troposphere. These compounds play an important role in tropospheric chemistry and climate forcing by influencing the oxidative capacity of the atmosphere, the ozone budget as well as in aerosol nucleation and growth. Thus, the study of reactive halogens, at temporal and spatial scale, is of utmost importance in the growing anthropogenic environment. The real time measurement of these species will contribute to numerical models to determine the regional and global role of reactive halogen compounds in a series of physico-chemical processes in the troposphere.

REFERENCES

- Abbatt JPD. (2003), Interactions of atmospheric trace gases with ice surfaces: adsorption and reaction. *Chem. Rev.* 103:4783–800
- Alappattu, D.P., et al., (2007), Spatio-temporal variability of surface-layer turbulent fluxes over the Bay of Bengal and Arabian Sea during the ICARB field experiment, *Boundary Layer Meteorol.*, doi: 10.1007/10546-007-9233-2
- Alfaro, S. C., et al., (2003), Chemical and optical characterization of aerosols measured in spring 2002 at the ACE-Asia supersite, Zhenbeitai, China, *J. Geophys. Res.*, 108(D23), 8641, doi: 10.1029/2002JD003214.
- Alpert, P., and E. Ganor (2001), Sahara mineral dust measurements from TOMS: Comparison to surface observations over the Middle East for the extreme dust storm, March 14–17, 1998, *J. Geophys. Res.*, 106(D16), 18275-18286.
- Andreae, M. O., (1983), Soot carbon and excess fine potassium: Long range transport of combustion –derived aerosols, *Science*, 220, 1148-1151.
- Andreae, M. O., Andreae, T. W., Annegarn, H, Beer, J., Cachier, H., Canut, P., Elbert, W., Maenhaut, W., Salma, I., Wienhold, F. G., Zenker, T., (1998), Airborne studies of aerosol emissions from savanna fires in southern Africa: Aerosol chemical composition; *Journal of Geophysical Research*, 103, 32,119-32,128.
- Arimoto, R., and Duce, R.A., (1986), Dry deposition models and the air/sea exchange of trace elements. *J. Geophys. Res.*, 91, 2787-2792.
- Arimoto R., Duce R. A., Ray B. J., Ellis, Jr., W. G., Cullen J. D. and Merrill J. T.,(1995), Trace elements in the atmosphere over the North Atlantic. *J. Geophys. Res.* 100, 1199–1213.
- Arimoto, R., Duce, R. A., Savoio, D. L., Prospero, J. M., Talbot, R., Cullen, J. D., Tomza, U., Lewis, N. F., Ray, B. J., (1996). Relationships among aerosol constituents from Asia and North Pacific during PEM-West A. *Journal of Geophysical Research* 101, 2011-2023.
- Arimoto, R., (2001), Eolian dust and Climate: Relationship to sources, tropospheric chemistry, transport and deposition, *Earth Science Rev.*, 54, 29-42.

- Arimoto, R., Duce R.A., Ray B.J., and Tomza, U., (2003), Dry deposition of trace elements to the Western North Atlantic. *Global Biogeochem. Cycles*, 17(1), doi: 10.1029/2001GB001406.
- Arimoto, R., Zhang, X. Y., Huebert, B. J., Kang, C. H., Savoie, D. L., Prospero, J. M., Sage, S. K., Schloesslin, C. A., Khaing, H. M., Oh, S. N., (2004), Chemical composition of atmospheric aerosols from Zhenbeitai, China, and Gosan, South Korea, during ACE-Asia. *J. Geophys. Res.*, 109, D19S04, doi: 10.1029/2003JD004323.
- Baker, M.B., (1997), Cloud microphysics and climate, *Science*, 276, 1072-1078.
- Baker, A. R., and T. D. Jickells, (2006), Mineral particle size as a control on aerosol iron solubility, *Geophys. Res. Lett.*, 33, L17608, doi:10.1029/2006GL026557.
- Baker, A. R., T. D. Jickells, M. Witt, and K. L. Linge, (2006), Trends in the solubility of iron, aluminium, manganese and phosphorus in aerosol collected over the Atlantic Ocean, *Mar. Chem.*, 98, 43–58.
- Baker, A.R., and Croot, P.L., (2008), Atmospheric and marine controls on aerosol iron solubility in seawater, *Mar. Chem.*, doi:10.1016/j.marchem.2008.09.003
- Bates, T. S., et al., (2004), Marine boundary layer dust and pollutant transport associated with the passage of a frontal system over eastern Asia. *J. Geophys. Res.*, 109, D19S19, doi:10.1029/2003JD004094.
- Bergametti et.al, (1989), African dust over Canary Island: Source regions identifications and transport pattern for some summer situation, *J. Geophys. Res.*, 95, 14855–14864.
- Birch, M. E., and R. A. Cary, (1996), Elemental carbon-based method for monitoring occupational exposures to particulate diesel exhaust, *Aerosol Sci. Technol.*, 25, 221– 241.
- Buck, C. S., W. M. Landing, J. A. Resing, and G. T. Lebon, (2006), Aerosol iron and aluminum solubility in the northwest Pacific Ocean: Results from the 2002 IOC cruise, *Geochem. Geophys. Geosyst.*, 7, Q04M07, doi:10.1029/2005GC000977.
- Buck, C.S., W. M. Landing, and J. A. Resing, (2008), Particle size and aerosol iron solubility: A high resolution analysis of Atlantic aerosols *Mar. Chem.*, doi:10.1016/j.marchem.2008.11.002
- Buck, C.S., W. M. Landing, J. A. Resing, and C.I. Measures, (2008a), The solubility and deposition of aerosol Fe and other trace elements in the North Atlantic

- Ocean: Observations from the A16N CLIVAR/CO₂ repeat hydrography section, *Mar. Chem.*, doi:10.1016/j.marchem.2008.08.003
- Chameides, W.L., and Stelson, A.W., (1992), Aqueous-phase chemical processes in deliquescent sea-salt aerosols: a mechanism that couples the atmospheric cycles of S and sea-salt, *J. Geophys. Res.*, 97, 20565-20580.
- Charlson, R. J., J. Langner, H. Rodhe, C. B. Leovy, and S. G. Warren, (1991), Perturbation of the Northern Hemisphere radiative balance by backscattering from anthropogenic sulfate aerosols, *Tellus, Ser. A*, 43, 152–163.
- Chen, Y., and R. L. Siefert, (2004), Seasonal and spatial distributions and dry deposition fluxes of atmospheric total and labile iron over the tropical and subtropical North Atlantic Ocean, *J. Geophys. Res.*, 109, D09305, doi:10.1029/2003JD003958.
- Chester, R., Elderfield, J.J., Griffin, J.J., Johnson, L.R., Padgham, R.C., (1972), Eolian dust along the eastern margins of the Atlantic Ocean. *Marine Geology* 13, 91–106.
- Chiapello, I., Bergametti, G., Chatenet, B., Bousquet, P., Dulac, F., Santos Soares, E., (1997), Origins of African dust transported over the Eastern Tropical Atlantic. *J. Geophys. Res.* 102, 13701–13709.
- Chuang, P. Y., R. M. Duvall, M. M. Shafer, and J. J. Schauer (2005), The origin of water soluble particulate iron in the Asian atmospheric outflow, *Geophys. Res. Lett.*, 32, L07813, doi:10.1029/2004GL021946.
- Claquin, T., M. Schulz, and Y. Balkanski (1999), Modeling the mineralogy of atmospheric dust sources, *J. Geophys. Res.*, 104, 22,243–22,256.
- Cwiertyny D. M., Young, M.A., Grassian, V.H., Chemistry and photochemistry of mineral dust aerosols, (2009), *Annu. Rev. Phys. Chem.* 2008. 59:27–51, doi:10.1146/annurev.physchem.59.032607.093630113:
- Dentener, F.J., Carmichael, G. R., Zhang, Y., Lelieveld, J., Crutzen, P. J., (1996), Role of mineral aerosol as a reactive surface in the global troposphere. *Journal of Geophysical Research* 101, 22869-22889.
- Desboeufs, K. V., A. Sofikitis, R. Losno, J. L. Colin, and P. Ausset, (2005), Dissolution and solubility of trace metals from natural and anthropogenic aerosol particulate matter, *Chemosphere*, 58, 195–203.
- Duce R.A., (1986), The impact of atmospheric nitrogen, phosphorous, and iron species on marine biological productivity. In: Buat-Menard, P., (Ed.), *The*

- Role of Air-sea Exchange in Geochemical Cycling. D. Reidel, Dordrecht, PP 497-529.
- Duce, R. A., et al., (1991), The atmospheric input of trace species to the world ocean, *Global Biogeochem. Cycles*, 5(3), 193– 259.
- Duce, R. A., and N. W. Tindale, (1991), Atmospheric transport of iron and its deposition in the ocean, *Limnol. Oceanogr.*, 36, 1715–1726.
- Duce, R. A. (1995), In *Aerosol Forcing of Climate*; Charlson, R. J., Heintzenberg, J., Eds.; Wiley: Chichester, U.K., 1995
- Fan, S.-M., W. J. Moxim, and H. Levy II (2006), Aeolian input of bioavailable iron to the ocean, *Geophys. Res. Lett.*, 33, L07602, doi: 10.1029/ 2005GL024852.
- Formenti, P., M. Andreae, L. Lange, G. Roberts, J. Cafmeyer, I. Rajta, W. Maenhaut, B. Holben, P. Artaxo, and J. Lelieveld (2001), Saharan dust in Brazil and Suriname during the Large - Scale Biosphere - Atmosphere Experiment in Amazonia (LBA) - Cooperative LBA Regional Experiment (CLAIRE) in March 1998, *J. Geophys. Res.*, 106(D14), 14919-14934
- Franzen, L. G.; Hjelmroos, M.; Kallberg, P.; Brorstrom-Lunden, E.; Juntto, S.; Savolainen, A.-L.,(1994), The ‘yellow snowepisode’ of northern Fennoscandia, march 1991—A case study of long-distance transport of soil, pollen and stable organic compounds, *Atmos. Environ*, 28, 3587
- Fung, I., S. K. Meyn, I. Tegen, S. C. Doney, J. G. John, and J. K. B. Bishop,(2000), Iron supply and demand in the upper ocean, *Global Biogeochem. Cycles*, 14, 281–295.
- Galloway, J.N., et al, (1993), The temporal and spatial variability of scavenging ratios for NSS-sulphate, nitrate, methanesulfonate and sodium in atmosphere over the North Atlantic Ocean, *Atmos. Environment, Part A, General Topic*, 27(2), 235-250.
- George, S. K., P. R. Nair, K. Parameswaran, S. Jacob, and A. Abraham (2008), Seasonal trends in chemical composition of aerosols at a tropical coastal site of India, *J. Geophys. Res.*, 113, D16209, doi:10.1029/2007JD009507.
- Goudie, A.S., and Middleton, N.J., (2001), Saharan dust storm: Nature and consequences, *Earth Sci. Rev.*, 56, 179-204, doi:10.1016/S0012-8252(01)00067-8

- Graedel, T.E., and Keene, W.C., (1995), Tropospheric budget of reactive chlorine, *Global Biogeochem. Cycles*, 9(1), 47-77.
- Grassian VH. (2001), Heterogeneous uptake and reaction of nitrogen oxides and volatile organic compounds on the surface of atmospheric particles including oxides, carbonates, soot and mineral dust: implications for the chemical balance of the troposphere. *Int. Rev. Phys. Chem.* 20:467–548
- Guieu, C., S. Bonnet, T. Wagener, and M.-D. Loyer-Pilot (2005), Biomass burning as a source of dissolved iron to the open ocean?, *Geophys. Res. Lett.*, 22, L19608, doi:10.1029/2005GL022962.
- Hand, J. L., N. M. Mahowald, Y. Chen, R. L. Siefert, C. Luo, A. Subramaniam, and I. Fung, (2004), Estimates of atmospheric- processed soluble iron from observations and a global mineral aerosol model: Biogeochemical implications, *J. Geophys. Res.*, 109, D17205, doi:10.1029/2004JD004574.
- Haywood, J., Boucher, O., (2000), Estimates of the direct and indirect radiative forcing due to tropospheric aerosols: a review. *Reviews of Geophysics* 38 (4), 513–543.
- Haywood, J.M., Francis, P.N., Glew, M.D., Taylor, J.P., (2001), Optical properties and direct radiative effect of Saharan dust: a case study of two Saharan dust outbreaks using aircraft data. *Journal of Geophysical Research* 106 (D16), 18,417 (2000JD900319).
- Haywood, J., Francis, P., Osborne, S., Glew, M., Loeb, N., Highwood, E., Tanre´, D., Myhre, G., Formenti, P., Hirst, E., (2003), Radiative properties and direct radiative effect of Saharan dust measured by the C-130 aircraft during SHADE. 1. Solar spectrum. *Journal of Geophysical Research* 108 (D18), 8577.
- Hering, S. V., and S. K. Friedlander (1982), Origins of aerosol sulphur size distributions in the Los Angeles basin, *Atmos. Environ.*, 16, 2647–2656.
- Holland, H. D., (1978), *The Chemistry of the Atmosphere and Oceans*, 154 pp., John Wiley, Hoboken, N. J.
- Holmes, J., and W. Zoller, (1996) "The Elemental Signature of Transported Asian Dust at Mauna Loa Observatory," *Tellus*, 48B, 83-92.
- Husar, R. B.; Tratt, D. M.; Schichtel, B. A.; Falke, S. R.; Li, F.; Jaffe, D.; Gasso, S.; Gill, T.; Laulainen, N. S.; Lu, F.; Reheis, M. C.; Chun, Y.; Westphal, D.; Holben, B. N.; Gueymard, C.; McKendry, I.; Kuring, N.; Feldman, G. C.;

REFERENCES

- McClain, C.; Frouin, R. J.; Merrill, J.; DuBois, D.; Vignola, F.; Murayama, T.; Nickovic, S.; Wilson, W. E.; Sassen, K.; Sugimoto, N.; Malm, W. C. (2001), Asian dust events of April 1998, *J. Geophys. Res.*, 106(D16), 18317-18330
- Intergovernmental Panel on Climate Change, (IPCC) (2001), *Climate Change 2001: The Scientific Basis*, edited by J.T. Houghton et al, Cambridge University Press, New York, 2001.
- Intergovernmental Panel on Climate Change, (IPCC) (2007), *Climate Change 2007: The Physical Science Basis*, edited by S.D. Solomon et al, Cambridge University Press, New York, 2007.
- Jaffe, D., et al. (1999), Transport of Asian air pollution to North America, *Geophys. Res. Lett.*, 26(6), 711-714.
- Jaffe, D., et al., (2003): Increasing background ozone during spring on the west coast of North America. *Geophys. Res. Lett.*, 30, 1613, doi:10.1029/2003GL017024.
- Jickells, T.D., (1995), Atmospheric input of metals and nutrients to the Oceans: Their magnitudes and effects, *Mar. Chem.*, 48, 199-214.
- Jickells, T. D., Z. S. An, K. K. Andersen, A. R. Baker, G. Bergametti, and co-authors (2005), Global iron connections between desert dust, ocean biogeochemistry and climate, *Science*, 308, 67–71.
- Jickells, T.D., (1999), The inputs of dust derived elements to the Sargasso Sea.: A synthesis, *Mar. Chem.*, 68, 5-14.
- Jickells, T. and L. Spokes (2001), Atmospheric iron inputs to the oceans, in *Biogeochemistry of Iron in Seawater*, IUPAC Ser. on Anal. and Phys. Chem., vol. 7, edited by D. R. Turner and K. A. Hunter, pp. 85– 121, John Wiley, Chichester.
- Johansen, A.M., Siefert, R.L., Hoffmann, R., et.al, (1999), Chemical Characterization of ambient aerosol collected during southwest monsoon and intermonsoon season over the Arabian Sea: Anions and cations, *J. Geophys. Res.*, 104, 26325-26347.
- Johansen, A. M., R. L. Siefert, and M. R. Hoffmann, (2000), Chemical composition of aerosols collected over the tropical North Atlantic Ocean, *J. Geophys. Res.*, 105(D12), 15,277–15,312.
- Johansen, A. M., and M. R. Hoffmann, (2003), Chemical characterization of ambient aerosol collected during the northeast monsoon season over the Arabian Sea:

- Labile-Fe (II) and other trace metals, *J. Geophys. Res.*, 108(D14), 4408, doi:10.1029/2002JD003280
- Johansen, A.M., and Hoffmann, R., (2004), Chemical Characterization of ambient aerosol collected during northeast monsoon season over the Arabian Sea: Anions and cations, *J. Geophys. Res.*, 109, D05305, doi: 10.1029/2003JD004111.
- Jordan, C.E., Dibb, J. E., Anderson, B. E., Fuelberg, H. E., (2003), Uptake of nitrate and sulfate on dust aerosols during TRACE-P. *J. Geophys. Res.*, 108, 8817, doi: 10.1029/2002JD003101.
- Kedia, S., and Ramchandran, S., (2008), Features of aerosol optical depths over the Bay of Bengal and the Arabian Sea during premonsoon season: variabilities and anthropogenic influence, *J. Geophys. Res.*, doi: 10.1029/2007JD009070 (in press)
- Keene, W.C., Pszenny, A. P., Galloway, J. N., Hawley, M. E., (1986), Sea salt correction and interpretation of constituent ratios in marine precipitation. *J. Geophys. Res.*, 91, 6647-6658.
- Keene, W.C., et al, (1990), The geochemical cycling of reactive chlorine through the marine boundary troposphere. *Global Biogeochem. Cycles*, 4, 407-430
- Kerminen, V.M., Teinila, K., Hillamo, R., and Pakkanen, T., (1998), Substitution of chloride in sea-salt particles by inorganic and organic anions. *J. Aerosol Sci.*, 29(8), 929-942.
- Koretsky, C., D. Sverjensky, J. Salisbury, and D. D'Aria (1997), Detection of surface hydroxyl species on quartz, gamma-alumina and feldspar using diffuse reflectance infrared spectroscopy, *Geochim. Cosmochim. Acta*, 61, 2193–2210.
- Krueger, B.J., Grassian, V.H., Laskin, A., Cowin, J.P., (2003), The transformation of solid atmospheric particles into liquid droplets through heterogeneous chemistry: Laboratory insight into the processing of calcium containing mineral dust aerosol in the troposphere. *Geophys. Res. Lett.*, 30, 1148, doi: 10.1029/2002GL016563.
- Kulshrestha, U.C., Saxena, A., Kumar, N., Kumari, K. M., Srivastava, S. S., (1998), Chemical composition and association of size differentiated aerosols at a suburban site in a semi-arid tract of India. *J. Atmos. Chem.*, 29, 109-118.

- Kumar, A., Sudheer, A. K., and Sarin, M. M., (2008a), Chemical characteristics of aerosols in MABL of Bay of Bengal and Arabian Sea during spring inter-monsoon: A comparative study, *J. Earth Syst. Sci.* 117, S1, July 2008, pp. 325–332.
- Kumar, A., Sarin, M. M. and Sudheer, A. K., (2008b), Mineral and Anthropogenic Aerosols in Arabian Sea-Atmospheric Boundary Layer during Inter-monsoon: Sources and Spatial Variability; *Atmos. Env.*, 42, 5169–5181, doi: 10.1016/j.atmosenv.2008.03.004.
- Kumar, A., and Sarin, M.M., (2009), Mineral aerosols from western India: Temporal variability of coarse and fine atmospheric dust and elemental characteristics, *Atmos. Env.*, 43, 4005-4013, doi:10.1016/j.atmosenv.2009.05.014.
- Kurtz, A. C.; Derry, L. A.; Chadwick, O. A., (2001), Accretion of Asian dust to Hawaiian soils: isotopic, elemental, and mineral mass balances, *Geochim. Cosmochim. Acta* , 65, 1971-1983.
- Laskin, A., T. W. Wietsma, B. J. Krueger, and V. H. Grassian (2005), Heterogeneous chemistry of individual mineral dust particles with nitric acid: A combined CCSEM/EDX, ESEM, and ICP-MS study, *J. Geophys. Res.*, 110, D10208, doi: 10.1029/2004JD005206.
- Laskin, A., (2005), Direct observation of completely processed calcium carbonate dust particles, *Faraday Disc.*, 130, 453.
- Levin, Z., E. Ganor, and V. Gladstein, (1996), The effects of desert particles coated with sulfate on rain formation in the eastern Mediterranean, *J. Appl. Meteorol.*, 35, 1511 – 1523.
- Li, S.-M. (1994), Equilibrium of particle nitrite with gas phase HONO: Tropospheric measurements in the high Arctic during polar sunrise, *J. Geophys. Res.*, 99(D12), 25,469–25,478.
- Luo, C., N. M. Mahowald, N. Meskhidze, Y. Chen, R. L. Siefert, A. R. Baker, and A. M. Johansen (2005), Estimation of iron solubility from observations and a global aerosol model, *J. Geophys. Res.*, 110, D23307, doi: 10.1029/2005JD006059.
- Luo, C., N. Mahowald, T. Bond, P. Y. Chuang, P. Artaxo, R. Siefert, Y. Chen, and J. Schauer, (2008), Combustion iron distribution and deposition, *Global Biogeochem. Cycles*, 22, GB1012, doi: 10.1029/2007GB002964.

REFERENCES

- Mahowald, N. M., A. R. Baker, G. Bergametti, N. Brooks, R. A. Duce, T. D. Jickells, N. Kubilay, J. M. Prospero, and I. Tegen (2005a), Atmospheric global dust cycle and iron inputs to the ocean, *Global Biogeochem. Cycles*, 19, GB4025, doi: 10.1029/2004GB002402.
- Mahowald, N.M., S. Engelstaedter, C. Luo, A. Sealy, P. Artaxo, and co-authors, (2009), Atmospheric Iron Deposition: Global Distribution, Variability, and Human Perturbations, *Annu. Rev. Mar. Sci.*, 1, 245-278, doi: 10.1146/annurev.marine.010908.163727.
- Majestic et al, (2006), Developing of a Wet-Chemical Method for the Speciation of Iron in Atmospheric Aerosols, *Environ. Sci. Technol.*, 40, 2346-2351
- Martin, J. H., R. M. Gordon, and S. E. Fitzwater, (1991), The case for iron, *Limnol. Oceanogr.*, 36, 1793– 1802.
- Martin, J.M., et al, (1989), River versus atmospheric input of material to the Mediterranean Sea: An overview, *Mar. Chem.*, 28, 159-182.
- Matsumoto, K., and H. Tanaka (1996), Formation and dissociation of atmospheric particulate nitrate and chloride: An approach based on phase equilibrium, *Atmos. Environ.*, 30, 639– 648.
- Matsumoto, K., Y. Uyama, T. Hayano, and M. Uematsu (2004), Transport and chemical transformation of anthropogenic and mineral aerosol in the marine boundary layer over the western North Pacific Ocean, *J. Geophys. Res.*, 109, D21206, doi:10.1029/2004JD004696.
- Maxwell-Meier, K., Weber, R., Song, C., Orsini, D., Ma, Y., Carmichael, G. R., Streets, D.G., (2004), Inorganic composition of fine particles in mixed mineral dust-pollution plumes observed from airborne measurements during ACE-Asia. *J. Geophys. Res.*, 109, D19S07, doi: 10.1029/2003JD004464.
- McInnes, L.M., D.S. Covert, P.K. Quinn, and M.S. Germani, (1994), Measurement of chloride depletion and sulphur enrichment in individual sea-salt particles collected from remote marine boundary layer, *J. Geophys. Res.*, 99, 8257-8268.
- McLennan, S. (2001), Relationships between the trace element composition of sedimentary rocks and upper continental crust, *Geochem. Geophys. Geosyst.*, 2(4), doi:10.1029/2000GC000109.

REFERENCES

- McKendry, I., J. Hacker, R. Stull, S. Sakiyama, D. Mignacca, and K. Reid (2001), Long - range transport of Asian dust to the Lower Fraser Valley, British Columbia, Canada, *J. Geophys. Res.*, 106(D16), 18361-18370
- Meskhidze, N., W. L. Chameides, A. Nenes, and G. Chen, (2003), Iron mobilization in mineral dust: Can anthropogenic SO₂ emissions affect ocean productivity?, *Geophys. Res.Lett.*, 30(21), 2085, doi:10.1029/2003GL018035.
- Migon, C., Journel, B., and Nicolas, E., (1997), Measurement of trace metal wet, dry and total atmospheric fluxes over the Ligurian Sea. *Atmos. Environment*, 31, 889-896.
- Miller, R.L., Tegen, I., (1999). Radiative forcing of a tropical direct circulation by soil dust aerosols. *Journal of Atmospheric Science* 56 (14), 2403–2433.
- Mohalfi, S., et al., (1998), Impact of short wave radiative effects of dust aerosols on the summer season heat low over Saudi Arabia. *Monthly Weather Review* 126, 3153–3168.
- Molina MJ, Molina LT, Kolb CE. (1996), Gas-phase and heterogeneous chemical kinetics of the troposphere and stratosphere. *Annu. Rev. Phys. Chem.* 47:327–67
- Momin, G.A., Rao, P. S. P., Safai, P. D., Ali, K., Naik, M. S., Pillai, A. G., (1999), Atmospheric aerosol characteristics studies at Pune and Thiruvananthapuram during INDOEX programme-1998. *Curr. Sci.*, 76, 985-989.
- Norman, M., Leck, C., and Rodhe, H., (2003), Differences across the ITCZ in the chemical characteristics of the Indian Ocean MBL aerosols during INDOEX., *Atmos. Chem. Phys.*, 3, 563-579.
- Nriagu J. O. and Pacyna J. M., (1988), Quantitative assessment of worldwide contamination of air, water and soils by trace metals. *Nature*, 333, 134–139.
- Ooki, A., Uematsu, M., (2005). Chemical interactions between mineral dust particles and acid gases during Asian dust events. *J. Geophys. Res.*, 110, D03201, doi:10.1029/2004JD004737.
- Parrington, J. R.; Zoller, W. H.; Aras, N. K., (1983), Seasonal transport to Hawaiian island, *Science*, 220, 195-197.
- Pease, P.P., Tchakerian, V.P., Tindale, N.W., (1998), Aerosols over the Arabian Sea: geochemistry and source areas for Aeolian desert dust, *J. Arid Environment*, 39, 477-496.

REFERENCES

- Perry, K.D., Cahill, T.A., Eldred, R.A., Dutcher, D.D., (1997), Long-range transport of North African dust to the eastern United States. *Journal of Geophysical Research* 102, 11225– 11238.
- Perry, K., T. Cahill, R. Schnell, and J. Harris (1999), Long-range transport of anthropogenic aerosols to the National Oceanic and Atmospheric Administration baseline station at Mauna Loa Observatory, Hawaii, *J. Geophys. Res.*, 104(D15), 18521-18533
- Potts, P.J., (1992), *A handbook of Silicate rock analysis*, Blackie & Sons, Glasgow and London
- Prospero, J.M., Glaccum, R.A., and Nees, R.T., (1981), Atmospheric transport from Africa to South America, *Nature*, 289, 570-572.
- Prospero, J. M., Charlson, R. J., Mohnen, V., Jaenicke, R., Delany, A. C., Moyers, J., Zoller, W., and Rahn, K., (1983), The atmospheric aerosol system – an overview, *Rev. Geophys. Space Phys.*, 21, 1607–1629,
- Prospero, J.M., (1999), Long-term measurements of the transport of African mineral dust to the south-eastern United States: implications for regional air quality. *Journal of Geophysical Research D* 104 \check{Z} 13., 15917–15927.
- Prospero, J. M.; Olmez, I.; Ames, M., (2001), Al and Fe in PM_{2.5} and PM₁₀ suspended particles in south-central florida: The impact of long-range transport of African mineral dust, *Water, Air, Soil Pollut.* 125, 291-317.
- Prospero, J.M., et al., (2002). Environmental characterization of global sources of atmospheric soil dust identified with the Nimbus 7 Total Ozone Mapping Spectrometer (TOMS) absorbing aerosol product. *Reviews of Geophysics* (1): Art. No. 1002.
- Prospero, J.M., and Lamb, P.J., (2003), African droughts and dust transport to the Caribbean: Climate change implications: *Science*, 302, 1024–1027, doi: 10.1126/science.1089915
- Quinn, P.K., et.al, (2004), Aerosol optical properties measured on board the Ronald H. Brown during ACE-Asia as a function of aerosol chemical composition and source region, *J. Geophys. Res.*, 109, D19S01, doi: 10.1029/2003JD004010.
- Ramanathan, V., Crutzen, P.J., Kiehl, J.T., and Rosenfeld, D., (2001a), Aerosols, climate and the hydrological cycle, *Science*, 294, 2119-2124

- Ramanathan, V., et al., (2001b), Indian Ocean Experiment: An integrated analysis of climate forcing and effects of the great Indo-Asian haze, *J. Geophys. Res.*, 106, 28371-28398.
- Rastogi, N., (2005a), Environmental radionuclide and chemical constituents in rain and aerosols: Biogeochemical sources and temporal variations, Ph. D. Thesis, Mohanlal Sukhadia University, Udaipur, India.
- Rastogi, N. and M. M. Sarin (2005b), Long-term characterization of ionic species in aerosols from urban and high altitude sites in western India: Role of mineral dust and anthropogenic sources, *Atmos. Environ.* 39, 5541-5554.
- Rastogi, N. and M. M. Sarin (2005c), Chemical characteristics of individual rain events from a semi-arid region in India: Three-year study, *Atmos. Environ.*, 39, 3313-3323.
- Rastogi, N., and Sarin, M.M., (2006), Chemistry of aerosols over a semi-arid region: Evidence for acid neutralization by mineral dust, *Geophys. Res. Lett.*, 33, L23815, doi: 10.1029/2006GL027708.
- Rastogi and Sarin.(2006a), Atmospheric Abundances of Nitrogen Species in Rain and Aerosols Over a Semi-Arid Region: Sources and Deposition Fluxes, *Aerosol and Air Quality Research*, Vol. 6, No. 4, pp. 406-417, 2006
- Ravishankara AR. (1997), Heterogeneous and multiphase chemistry in the troposphere. *Science* 276:1058–65
- Rengarajan, R., Sarin, M.M., and Sudheer, A.K., (2007), Carbonaceous and inorganic species in atmospheric aerosols during wintertime over urban and high-altitude sites in North India, *J. Geophys. Res.*, 112, D21307, doi:10.1029/2006JD008150.
- Rosenfeld, D., Y. Rudich, and R. Lahav (2001), Desert dust suppressing precipitation: A possible desertification feedback loop, *Proc. Natl. Acad. Sci. U. S. A.*, 98, 5979– 5980.
- Sarin, M.M., D.V.Borole, and S. Krishnaswami, (1979), Geochemistry and geochronology of sediments from the Bay of Bengal and the equatorial Indian Ocean, *Proc. Indian Acad. Sci.*, 88A (Part II), 2, 131-154.
- Sarin, M.M., Rengarajan, R., and Krishnaswami, S., (1999), Aerosol NO_3^- and ^{210}Pb distribution over the central eastern Arabian Sea and their air-sea deposition fluxes, *Tellus*, 51B, 749-758.

- Satheesh, S.K., Ramanathan, V., (2000), Large differences in tropical aerosol forcing at the top of the atmosphere and earth's surface. *Nature* 405, 60–63.
- Satheesh, S.K., KrishnaMoorthy, K., (2005) Radiative effects of natural aerosols: A review, *Atmos. Environ.*, 39, 2089–2110.
- Savoie, D.L., and Prospero, J.M., (1982), Particle size distribution of nitrate and sulphate in marine atmosphere. *Geophys. Res. Lett.*, 9(10), 1207-1210.
- Schroth A. W., Crusius J., Sholkovitz E. R. and Bostick B. C. , (2009), Iron solubility driven by speciation in dust sources to the ocean. *Nat. Geosci.* doi:10.1038/NGE0501.
- Schauer, J. J., et al. (2003), ACE-Asia intercomparison of a thermal-optical method for the determination of particle phase organic and elemental carbon, *Environ. Sci. Technol.*, 37, 993–1001.
- Sedwick, P. N., E. R. Sholkovitz, and T. M. Church, (2007), Impact of anthropogenic combustion emissions on the fractional solubility of aerosol iron: Evidence from the Sargasso Sea, *Geochim. Geophys. Geosyst.*, 8, Q10Q06, doi:10.1029/2007GC001586.
- Seinfeld, J.H. and S. N. Pandis, (1998), *Atmospheric Chemistry and Physics*, First Edition, John Wiley, New York.
- Sholkovitz, E.R., Sedwick, P.N., Church, T.M., (2009), Influence of anthropogenic combustion emissions on the deposition of soluble aerosol iron to the ocean: Empirical estimates for island sites in the North Atlantic, *Geochim. Cosmochim. Acta*, 73, 3981–4003, doi: 10.1016/j.gca.2009.04.029
- Siefert, R.L., Johansen, A.M., and Hoffmann, M.R., (1999), Chemical Characterization of ambient aerosol collected during southwest monsoon and intermonsoon season over the Arabian Sea: Labile- Fe(II) and other trace metals. *J. Geophys. Res.*, 104, 3511-3526.
- Sievering, H., Gorman, E., Ley, T., Pszenny, A., Spring-Young, M., Boatmann, J., Kim, Y., Nagamoto, C., and Wellman, D., (1995), Ozone oxidation of sulfur in sea-salt aerosol particles during the Azores marine aerosol and gas exchange experiment. *J. Geophys. Res.*, 100, 23075-23081.
- Sievering, H., Boatmann, J., Galloway, J., Keene, W., Kim, Y., Luria, M., and Ray, J., (1991), Heterogeneous sulfur conversion in sea-salt aerosol particles: The role of aerosol water content and size distribution. *Atmos. Environment*, 25 A (8), 1479-1487.

- Sokolik, I.N. and O.B. Toon. (1996), Direct radiative forcing by anthropogenic airborne mineral aerosols. *Nature* 381, 681- 683, 1996
- Sokolik, I., and O. Toon (1999), Incorporation of mineralogical composition into models of the radiative properties of mineral aerosol from UV to IR wavelengths, *J. Geophys. Res.*, 104(D8), 9423-9444.
- Sokolik, I., D. Winker, G. Bergametti, D. Gillette, G. Carmichael, Y. Kaufman, L. Gomes, L. Schuetz, and J. Penner (2001), Introduction to special section: Outstanding problems in quantifying the radiative impacts of mineral dust, *J. Geophys. Res.*, 106(D16), 18015-18027.
- Solmon, F., P. Y. Chuang, N. Meskhidze, and Y. Chen, (2009), Acidic processing of mineral dust iron by anthropogenic compounds over the north Pacific Ocean, *J. Geophys. Res.*, 114, D02305, doi:10.1029/2008JD010417.
- Song, C. H., Carmichael, G. R., (2001), A three-dimensional modeling investigation of the evolution processes of dust and sea-salts particles in east Asia. *J. Geophys. Res.*, 106, 18131-18154.
- Streets, D. G., et al., (2003), An inventory of gaseous and primary aerosol emissions in Asia in the year 2000. *J. Geophys. Res.*, 108, 8809, doi:10.1029/2002JD003093.
- Stumm, W., and J. J. Morgan (Eds.), (1981), *Aquatic Chemistry: An Introduction Emphasizing Chemical Equilibria in Natural Waters*, 780 pp., John Wiley, Hoboken, N. J.
- Sullivan, R.C., Guazzotti, S.A., Sodeman, D.A., and Prather, K.A., (2007), Direct observation of the atmospheric processing of Asian mineral dust, *Atmos. Chem. Phys.*, 7, 1213-1236.
- Tang, Y. H., et.al, (2004a), Impacts of dust on regional tropospheric chemistry during the ACE-Asia experiment: A model study with observations, *J. Geophys. Res.*, 109(D19), D19S21, doi: 10.1029/2003JD003806.
- Tang, Y. H., et.al, (2004b), Three dimensional simulations of inorganic aerosol distributions in east Asia during spring 2001, *J. Geophys. Res.*, 109(D19), D19S23, doi: 10.1029/2003JD004201.
- Tanre', D., Haywood, J., Pelon, J., Le'on, J.F., Chatenet, B., Formenti, P., Francis, P., Goloub, P., Highwood, E.J., Myhre, G., (2003). Measurement and modeling of the Saharan dust radiative impact: overview of the Saharan Dust Experiment (SHADE). *Journal of Geophysical Research* 108 (D18), 8574.

- Taylor, S.R., and McLennan, S.M., (1985), *The Continental Crust: its composition and evolution*. Blackwell, Oxford, pp-312.
- Tegen, I., and I. Fung (1994), Modeling of mineral dust in the atmosphere: Sources, transport, and optical thickness, *J. Geophys. Res.*, 99(D11), 22897-22914
- Tegen, I., A. A. Lacis, and I. Fung (1996), The influence of climate forcing of mineral aerosols from disturbed soils, *Nature*, 380(4), 419–422.
- Tegen, I., Miller, R., (1998), A general circulation model study on the interannual variability of soil dust aerosol. *Journal of Geophysical Research–Atmospheres* 103 (D20), 25,975–25,995.
- Tindale, N.W., and Pease, P.P., (1999), Aerosols over the Arabian Sea: atmospheric transport pathways and concentrations of dust and sea-salt. *Deep-Sea Res. II*, 46, 1577-1595.
- Tsai, Y.I., and Kuo, S.C., (2005), PM_{2.5} aerosol water content and chemical composition in a metropolitan and a coastal area in southern Taiwan, *Atom. Environ.*, 39, 4827-4839.
- Turpin, B. J., and H. Lim (2001), Species contribution to PM_{2.5} concentrations: Revisiting common assumptions for estimating organic mass, *Aerosol Sci. Technol.*, 35, 602– 610.
- Twomey, S., (1977), *Atmospheric Aerosols*, 302 pp, Elsevier Sci., New York.
- Wedepohl, K. H., (1995), The composition of the continental crust, *Geochim. Cosmochim. Acta*, 59, 1217-1232.
- Usher, R.C., Amy E. Michel, Vicki H. Grassian, (2003), Reactions on Mineral Dust, *Chem. Rev.*, 103, 4883-4939
- Venkatraman, C., Reddy, C., K., Josson, S., Reddy, M.S., (2002), Aerosol size and chemical characteristics at Mumbai, India, during the INDOEX-IFP (1999), *Atmos. Environ.*, 36, 1979-1991
- Wu, P.M., and Okada, K., (1994), Nature of coarse nitrate particles in the atmosphere – a single particle approach, *Atmos. Environ.*, 28, 2053-2060.
- Xiaoxiu, L., Z. Xiaoshan, M. Yujing, N. Anpu, J. Guibin, (2003), Size fractionated speciation of sulfate and nitrate in airborne particulates in Beijing, China, *Atmos. Environ.*, 37, 2581-2588.
- Yao, X., Chan, C. K., Fang, M., Cadle, S., Chan, T., Mulawa, P., He, K., Ye, B., (2002), The water-soluble ionic composition of PM 2.5 in Shanghai and Beijing, China. *Atmospheric Environment*, 36, 4223-4234.

- Yin, Y., Wurzler, S., Levin, Z., Reisin, T.G., (2002). Interactions of mineral dust particles and clouds: effects on precipitation and cloud optical properties. *J. Geophys. Res.*, 107 (D23) 4724, doi: 10.1029/ 2001JD001544.
- Zender, C.S., (2004), Quantifying mineral dust mass budgets: terminology, constraints, and current estimates. *Eos*, 85, 509–512.
- Zhang, X., Zhang, G., Zhu, G., Zhang, D., An, Z., Chen, T., Huang, X., (1996), Elemental tracers for Chinese source dust. *Sci. China, Ser. D: Earth Sci.* 39, 512–521.
- Zhang, J., and S. Christopher, (2003): Longwave radiative forcing of Saharan dust aerosols estimated from MODIS, MISR and CERES observations on Terra. *Geophys. Res. Lett.*, 30(23), doi:10.1029/2003GL018479.
- Zhu, X. R., J. M. Prospero, and F. J. Millero, (1997), Diel variability of soluble Fe (II) and soluble Fe in North African dust in the trade winds at Barbados, *J. Geophys. Res.*, 102, 21,297–21,305.
- Zhuang, H., Chan, C.K., Fang, M., Wexler, A.S., (1999), formation of nitrate and non-sea-salt sulfate on coarse particles. *Atmos. Environ.*, 33, 4223-4233.
- Zhuang, H., Chan, C.K., Fang, M., Wexler, A.S., (1999a), Size distribution of particulate sulfate, nitrate, and ammonium at a coastal site in Hong Kong, *Atmos. Environ.*, 33, 843-853.
- Zhuang, G., Duce, R.A., and Kester, D.R., (1990), The dissolution of atmospheric iron in surface sea-water of open ocean, *J. Geophys. Res.*, 95, 16,207-16,216.
- Zhuang, G. S., Z. Yi, R. A. Duce, and P. R. Brown, (1992), Link between iron and sulfur cycles suggested by detection of Fe (II) in remote marine aerosols, *Nature*, 355, 537–539.

List of Publications:

Published: (In Peer-reviewed Journals)

- 1) Ashwini Kumar, M.M.Sarin, A.K.Sudheer, (2008) “*Mineral and Anthropogenic Aerosols in Arabian Sea-Atmospheric Boundary Layer during Inter-monsoon: Sources and Spatial Variability*”, **Atmospheric Environment**, 42, 5169-5181, doi:10.1016/j.atmosenv.2008.03.004.
- 2) Ashwini Kumar, A.K.Sudheer, M.M.Sarin, (2008) “*Chemical characteristics of aerosols in MABL of Bay of Bengal and Arabian Sea during spring inter-monsoon: A comparative study*”, **J. Earth Syst. Sci.**, 117, S1, 325-332.
- 3) Ashwini Kumar and M.M.Sarin, (2009) “*Mineral aerosols from western India: Temporal variability of coarse and fine atmospheric dust and elemental characteristics*”, **Atmospheric Environment**, 43, 4005-4013, doi:10.1016/j.atmosenv.2009.05.014.
- 4) Ashwini Kumar and M.M.Sarin, (2010) “*Aerosol iron solubility in semi-arid region: Temporal trend and impact of anthropogenic sources*”, **Tellus**, 62B, 125 – 132 doi: 10.1111/j.1600-0889.2009.00448.x.
- 5) Ashwini Kumar and M.M.Sarin, (2010) “*Water-soluble ionic composition of coarse and fine mode aerosols from high-dust region in western India: Seasonal characteristics*”, **Atmospheric Environment**, 44, 1245-1254, 10.1016/j.atmosenv.2009.12.035.
- 6) Kedia S., S. Ramchandran, Ashwini Kumar and M.M. Sarin, (2010), “*Spatiotemporal gradients in aerosol radiative forcing and heating rate over Bay of Bengal and Arabian Sea derived on the basis of optical, physical and Chemical properties*”, **J. Geophys. Res.**, 115, D07205, doi:10.1029/2009JD013136.
- 7) Ashwini Kumar, M.M.Sarin, Bikkina Srinivas, (2010)“ *Aerosol iron solubility in MABL of Bay of Bengal: Contribution from chemical processing vis-à-vis combustion sources*”, **Marine Chemistry**, (Available Online) 10.1016/j.marchem.2010.04.005

Communicated / Under Review:

- 8) Cherian, R., Venkataraman, C., **Ashwini Kumar**, Sudheer, A.K., Sarin, M.M., and Ramachandran, S., “*Source identification of aerosols influencing atmospheric extinction: Integrating PMF and PSCF with emission inventories and satellite observations*” **J. Geophys. Res.**, (Revised Submission), June, 2010.

Other Publications:

- 9) **Ashwini Kumar**, M.M.Sarin, Bikkina Srinivas, A.K.Sudheer, and N. Rastogi, (2010) “*Mineral dust and anthropogenic trace element inputs to the Bay of Bengal*”, SOLAS-News Letter, Issue-10, winter, 2010.

Manuscripts under preparation:

- 1) B.Srinivas, M.M. Sarin and **Ashwini Kumar** “*Impact of anthropogenic aerosols over MABL of Bay of Bengal: Results from ICARB-W Campaign*” (to be submitted to **J. Geophys. Res.-Atmosphere**)
- 2) **Ashwini Kumar**, M.M. Sarin, B. Srinivas, N. Rastogi and A.K. Sudheer “*Wide spread Chloride-depletion in sea-salt aerosols over Bay of Bengal: Implication to climate forcing*” (to be submitted to **Geophys. Res. Lett.**)
- 3) **Ashwini Kumar** and M.M.Sarin “*Spatio-temporal variability of atmospheric NH_4^+ , NO_3^- , and SO_4^{2-} concentrations over Indian region*” (to be submitted to **Atmospheric Environment**)

Publications: (In Proceedings)

- 1) M.M.Sarin, A.K.Sudheer, **Ashwini Kumar** and R.Rengarajan, “*Wintertime concentration of water-soluble organic compounds in atmospheric aerosols over urban site in northern India.*” National Space Science Symposium - 2006, India.

- 2) B. Srinivas, M.M. Sarin and **Ashwini Kumar**, “*Impact of anthropogenic sources on chemical composition of aerosols over Bay of Bengal*”, Indian Aerosol Science and Technology Association-2010, 24-26 July ‘2010, Darjeeling, India.

Abstracts (Conference/Symposia)

- 1) **Ashwini Kumar** and M.M.Sarin, “*Role of anthropogenic sulphate in the MABL over Bay of Bengal and Arabian Sea* ”International Symposium on Aerosol-Chemistry-Climate Interactions – 2007, Ahmedabad, India
- 2) **Ashwini Kumar** and M.M.Sarin, “*Atmospheric mineral dust and anthropogenic constituents over high altitude site in semi-arid regions of Western India*” 10th International Global Atmospheric Chemistry Conference, 07-12 Sep ‘2008, Annecy, France.
- 3) **Ashwini Kumar** and M.M.Sarin, “*Atmospheric mineral dust in western India: Temporal variability of coarse and fine size fractions and elemental characteristic*” CACGP-MOCA-2009, 19-29 July ‘2009, Montreal, Canada
- 4) **Ashwini Kumar**, M.M.Sarin, B. Srinivas, A.K. Sudheer, and N. Rastogi, “*Large-scale chloride-depletion in sea-salt aerosols over Bay of Bengal: Implications to climate forcing*” Asia Oceania Geosciences Society-2010, 5-9 ‘July, Hyderabad, India.
- 5) **Ashwini Kumar** and M.M.Sarin, “*Atmospheric mineral dust, chemistry and temporal variability in Western India*” Asia Oceania Geosciences Society-2010, 5-9 ‘July, Hyderabad, India.
- 6) B.Srinivas, M.M. Sarin, **Ashwini Kumar** and R. Rengarajan, “*Atmospheric dry deposition of N, P, and Fe to the Bay of Bengal*”, Asia Oceania Geosciences Society-2010, 5-9 ‘July, Hyderabad, India.
- 7) M.M. Sarin, B. Srinivas and **Ashwini Kumar**, “*Atmospheric chemistry in MABL of tropical Bay of Bengal: Impact of continental outflow*”, 11th International Global Atmospheric Chemistry Conference, 11-16 July ‘2010, Halifax, Canada.
- 8) **Ashwini Kumar**, M.M. Sarin, A.K. Sudheer and R. Rengarajan, “*Spatio-temporal variability of atmospheric NH_4^+ , NO_3^- and SO_4^{2-} concentrations over Indian region*” 11th International Global Atmospheric Chemistry Conference, 11-16 July ‘2010, Halifax, Canada.